Haematopoietic clonality in Common Variable Immunodeficiency

by

Gabriel K Wong

University of Birmingham

A thesis submitted for the degree of Doctor of Philosophy

Institute of Immunology and Immunotherapy

Medical School

College of Medical and Dental Sciences

January 2016

I, Gabriel Wong, confirm that the work presented in this thesis is my own. Where information has been derived from external sources, I confirm that this has been specified in the thesis.

Abstract

The aetiology of Common Variable Immunodeficiency (CVID) has fascinated immunologists since Dr. Janeway reported the first case in 1953. While the advances in molecular biology have enlightened us on the aetiology in some patients, the majority is not caused by inherited genetic disorders. A convincing mechanism accounting for the intrinsic variable and partial nature of the condition has yet been proposed. CVID separates itself from other primary antibody deficiencies by the procurement of an abnormal T-cell compartment. Data from this study support that both T-cells and B-cells are subjected to similar deficiency. Investigation of the T-cell receptor repertoire by next-generation sequencing and multi-parametric flow cytometry suggests a severe reduction in naïve T-cell output from the thymus. Similarly, the study of long-lived plasma cell generation and survival highlighted the greatest functional deficits in the naïve B-cell pool, altogether supporting an acquired arrest in lymphogenesis. Using DNA methylation as a surrogate marker for pre-VDJ clonality, this study further shows that some CVID patients exhibited clonal haematopoiesis, adjoining CVID to other clonal haematopoiesis related acquired haematological disorders. Further work is being focused on using high resolution techniques to confirm this association and mechanistically define the development of antibody deficiency in adulthood.

Acknowledgements

I would like to express my deepest gratitude to all those who have supported me through my PhD and this work would not be possible without their inputs. Special thanks to all patients from the West Midlands Primary Immunodeficiency Centre, Birmingham Heartlands Hospital and healthy donors who had unconditionally donated samples on numerous occasions to this project. Their generosity and contribution to clinical research are crucial to advancing our understanding of Common Variable Immunodeficiency and our next generation will be indebted to them.

My supervisors, Professor Mark Cobbold and Professor Peter Lane have helped me grow as a scientist with their candid constructive advices, getting the best out of me. Mark's creativity and courage in science are truly admiring and I am delighted to have the opportunity to learn from him. I also thank Mark for unreservedly supported me through difficult times during my PhD. Thank you to all members of the Cobbold laboratory who have helped me on a regular basis and supported my transition from a clinician into a scientist.

I was fortunate to have excellent collaborators such as Dr. Aarn Huissoon, Julie Jones, Hayley Clifford to provide an excellent clinical research environment at the West Midlands Primary Immunodeficiency Centre. I am also grateful to have the opportunities to work with and learn from Dr. Reuben Tooze (University of Leeds) and Dr. Malek Faham (Adaptive Biotechnologies), who both contributed to this project with their expertise in plasma cell culture and antigen receptor sequencing. The project would not be possible without the general support from the Clinical Immunology service, University of Birmingham and Birmingham Women's Hospital.

For all those evenings and weekends that I spent in tissue culture or in front of my laptop, I would like to thank my family and all my friends for their patience with me.

Finally, I would like to thank the Wellcome Trust for funding this project and my personal development in the past 3 years. This work is supported by the Wellcome Trust and was completed as part of a clinical training research fellowship for Gabriel K Wong at the University of Birmingham [grant number 099908/Z/12/Z].

Table of contents

Glossary

AID	Activation induced cytosine deaminase
AIDS	Acquired Immunodeficiency syndrome
AML	Acute myeloid leukaemia
APRIL	A proliferation-inducing ligand
ATP2A1	Sacroplasmic/endoplasmic reticulum calcium ATPase 1
BAFF	B-cell activating factor
BAFF-R	B-cell activating factor receptor
BCL6	B-cell lymphoma 6 protein
BCMA	B-cell maturation antigen
BCR	B-cell receptor
BLIMP1	PR domain zinc finger protein 1
BMT	Bone marrow transplantation
BTK	Bruton's tyrosine kinase
C3d	Complement component 3 fragment d
CAML	Calcium-modulating cyclophilin ligand
cAMP	Cyclic adenosine monophosphate
CDR3	Complementarity determining region 3
CLEC16A	C-type lectin domain family 16, member A
CMV	Cytomegalovirus
CpG	CpG oligodeoxynucleotides
CSR	Immunoglobulin class-switching
CTLA4	Cytotoxic T-lymphocyte-associated protein 4
CVID	Common Variable Immunodeficiency
EBV	Epstein-Barr virus
ER	Endoplasmic reticulum

ESID	European Society for Immunodeficiencies
FAS	Apoptosis antigen 1
FCS	Fetal calf serum
FOXP3	Forkhead box P3 transcription factor
GWAS	Genome wide association study
HHV	Human herpes virus
HIV	Human Immunodeficiency Virus
HLA	Human leukocyte antigen
ICOS	Inducible T-cell costimulator
ICOSL	Inducible T-cell costimulator ligand
IFIH1	Interferon induced with helicase C domain 1 protein
IgκREHMA	Ig kappa restriction enzyme hot-spot mutation assay
iNKT-cell	invariant natural killer T-cells
IRF4	Interferon regulatory factor 4
ITP	Immune thrombocytopenic purpura
KREC	Kappa-deleting recombinantion excision circle
LCMV	Lymphocytic choriomeningitis virus
LLPC	Long-lived plasma cell
LRBA	LPS-responsive vesicle trafficking, beach and anchor containing gene
MALT	Mucosal associated lymphoid tissue
MDS	Myelodysplastic syndrome
MGUS	Monoclonal gammaopathy of uncertain significance
MHC	Major Histocompatibility Complex
MZB	Splenic marginal zone B-cells
NFAT	Nuclear factor of activated T-cells
NFATC2IP	Nuclear factor of activated T-cells, cytoplasmic, calcineurin-dependent 2 interacting protein

NFκB1	Nuclear factor of kappa light polypeptide gene enhancer in B-cells 1
NFκB2	Nuclear factor of kappa light polypeptide gene enhancer in B-cells 2
NHL	Non-Hodgkin's lymphoma
NK cell	Nature killer cell
P/S	Penicillin and streptomycin
PAGID	Pan-American group for immunodeficiency
PAX5	Paired box 5 gene
PBMC	Peripheral blood mononuclear cell
PCR	Polymerase chain reaction
PD-1	Programmed cell death 1
PID	Primary Immunodeficiency
PKAI	Cyclic AMP and protein kinase A type 1
PLCγ2	Phospholipase C, gamma 2 enzyme
SDI	Simpson's diversity index
SE	Shannon Entropy
SHM	Somatic hypermutation
sIgAD	Selective IgA deficiency
SIR	Standardised incidence ratio
SLE	Systemic lupus erythematosus
smB	Class-switched memory B-cells
SNP	Single nucleotide polymorphism
SNV	Single nucleotide variant
SPAD	Specific polysaccharide antibody deficiency
SRC	Proto-oncogene tyrosine-protein kinase
STR	Short tandem repeats
TACI	Transmembrane activator and calcium modulator and cyclophilin ligand interactor
TCR	T-cell receptor

TLR	Toll-like receptor
TNF	Tumour necrosis factor
TRAF	TNR receptor associating factor
Treg	Regulatory T-cells
TWEAK	TNF-related weak inducer of apoptosis
TWE-PRIL	Fusion protein of TWEAK and APRIL
XBP1	X-box binding protein 1
XLA	X-linked agammaglobulinaemia
XLP	X-linked lymphoproliferative disorder

List of figures

List of tables

Chapter 1

1. Introduction

1.1 Primary immunodeficiency

The immune system plays a key role in maintaining equilibrium between its host and the environment, constantly interacting with billions of commensal microbes and any potential pathogens. Its importance is clearly demonstrated in haematological malignancies and human immunodeficiency virus (HIV), where its elimination, either by iatrogenic or natural means, predisposes the host to life threatening opportunistic infections and death. Inborn or intrinsic factors that result in attenuation or complete failure of the immune system are known as Primary Immunodeficiency Disorders (PID).

Prior to the era of modern hygiene, vaccination and antibiotics, large infection outbreaks regularly occurred in urban and sub-urban areas, killing significant proportion of the population. Smallpox and the European plague were two of the most extreme examples. It was estimated that smallpox wiped out up to 90% of Native American during the 16th to 18th centuries [1] and the "Black death", which was caused by the enterobacteria *Yersinia pestis*, was responsible for almost half of the population in Europe at the time, with Southern Europe reporting a mortality rate of 80-85% at the end of 1353 [2].

The introduction of modern hygiene and large scale vaccination programmes as well as the availability of penicillin in the 20th century resulted in drastic reduction in infectious disease related mortality and eventually the elimination of small pox in 1979 [3, 4]. However, this has unmasked a

new frontier of medicine where some individuals and families continued to demonstrate susceptibility to well-defined patterns of infections due to inherited factors.

The first primary immunodeficiency was described by Dr. Ogden Bruton in 1952, when he reported an eight year old boy with recurrent and severe pneumonia and the lack of γ-globulin in his serum; X-linked agammaglobulinaemia (XLA) [5]. XLA developed as a result of a single gene mutation of a protein tyrosine kinase within the SRC family on the X-chromosomes; Bruton's tyrosine kinase (*BTK*) [6, 7]. Since the first description of XLA, hundreds of genetic mutations, virtually involving every compartment of the immune system, have now been mapped to an immunodeficiency disorder [8].

1.2 Common Variable Immunodeficiency

Common Variable Immunodeficiency (CVID) represents a group of unknown immunodeficiency disorders marked by the intrinsic failure of humoral immunity and immune dysregulation. A year after Dr. Bruton reported the first case of XLA, Dr. Charles Janeway reported a 39-year-old woman with bronchiectasis, recurrent upper and lower respiratory tract infections and the absence of isohaemaglutinin who was successfully treated with gammaglobulin replacement therapy [9]. It is now known that the gammaglobulin proportion of serum protein is largely comprised of immunoglobulins; antibodies. Recurrent and severe respiratory tract infections despite routine vaccinations and adequate antibiotics are the central features of CVID. Large cohort studies showed that the majority of patients will present in adulthood with many demonstrating residual immunoglobulin production; hypogammaglobulinaemia [10].

Defining CVID has been an incredibly difficult task, mostly due to its overlapping clinical and laboratory presentations with other well-characterised immunodeficiency disorders. Hypogammaglobulinaemia and immune dysregulation are frequent bystanders of other immune

disorders; hence CVID can only be considered when other PIDs have been excluded. The definition of CVID has evolved multiple times over the past 60 years [11, 12]. In 1999, the Pan-American Group for immunodeficiency (PAGID) and European society for Immunodeficiencies (ESID) defined the criteria for "probable" and "possible" CVID (Appendix 1). However, the inclusion criteria were very broad and needing refinement. The revised ESID registry (2014) version has since tightened the diagnostic criteria by increasing the minimum diagnostic age to 4, necessitating the presence of relating clinical findings and emphasised on the exclusion of a profound T-cell immunodeficiency. In addition, it also promotes the reduction of class-switched memory B-cells as an additional laboratory marker. Most importantly, marked reduction in both IgG and IgA are now required (Table 1) [12]. However, the benchmark for vaccine response remains difficult to define due to variation in local practices, vaccine availabilities as well as assay inconsistencies.

ESID/PAGID 1999	*Revised ESID 2014*
Key criteria	
	1) At least one of the following: · Increased susceptibility to infection · Autoimmune manifestations · Granulomatous disease · Unexplained polyclonal lymphoproliferation · Affected family member with antibody deficiency
1) Male or female patient who has a marked decrease of IgG (at least 2 SD below the mean for age) and a marked decrease in at least one of the isotypes IgM or IgA	2) AND marked decrease of IgG and marked decrease of IgA with or without low IgM levels (measured at least twice; <2 SD of the normal levels for their age);
2) Onset of immunodeficiency at greater than 2 years of age	3) AND diagnosis is established after the fourth year of life (but symptoms may be present before)
3) Absent isohemagglutinins and/or poor response to vaccines	4) AND at least one of the following: · Poor antibody response to vaccines (and/or absent isohemagglutinins); i.e., absence of protective levels despite vaccination where defined · Low switched memory B cells (<70% of age-related normal value)
4) Defined causes of hypogammaglobulinemia have been excluded	5) AND secondary causes of hypogammaglobulinemia have been excluded
	6) AND no evidence of profound T-cell deficiency, defined as two out of the following (y = year of life): o CD4 numbers/microliter: 2–6 y < 300, 6–12 y < 250, >12 y < 200 o % Naive CD4: 2–6 y < 25%, 6–16 y < 20%, >16 y < 10% o T-cell proliferation absent
Additional factors for consideration:	
o **Most patients with CVI are recognized to have immunodeficiency in the second, third or fourth decade of life, after they have had several pneumonias; however children and older adults may be affected.** o **The serum concentration of IgM is normal in about half of the patients.** o **Viral, fungal and parasitic infections as well as bacterial infections may be problematic.** o **Abnormalities in T cell numbers or function are common.** o **The majority of patients have normal numbers of B cells; however, some have low or absent B cells.** o **Approximately 50% of patients have autoimmune manifestations.** o **There is an increased risk of malignancy.**	

Table 1. Comparison of ESID/PAGID 1999 criteria and Revised ESID 2014 criteria for the diagnosis of CVID.

Please note that criteria for "possible" CVID - 1999 ESID/PAGID are not shown [12].

1.3 Clinical presentation of CVID

According to the US immunodeficiency network in 2012, CVID accounts for up to 28.2% of all primary immunodeficiencies [13] and has an estimated prevalence of 1 in 10,000-50,000 with the majority of patients being Caucasians [14-16]. The up to date ESID registry database, however, has a more conservative estimation of 11.8% of all PIDs. Nevertheless, these figures advocate CVID as the most prevalent PID.

A number of national or international clinical cohort studies demonstrated significant heterogeneity amongst CVID patients [10, 14, 17-22]. In addition to recurrent and severe infections, other pathological features and disease complications such as splenomegaly, non-malignant lymphadenopathy, granulomas, autoimmune cytopenia, enteropathy, liver disease and other autoimmune diseases affect 25-40% of patients. Although the cause is not known, splenomegaly was reported to occur in 30-40% of CVID patients and was closely associated with lymphadenopathy, granulomata and autoimmune cytopenia [10, 19, 21, 23]. Although these non-infectious complications had historically attracted a huge amount of interests, "infection only" CVID without disease complications is by far the most dominant CVID subgroup according to a recent multi-centred international survey; 60-75% of all CVID patients [24]. Sub-classifying CVID patients according to their precise clinical presentations can be difficult as many non-infectious complications may overlap with each other. Sub-classifying patients into either "infection only" or "with inflammatory complication/s" has gained popularity in recent years due to its simplicity.

Upper and lower respiratory tract infections such as otitis media, sinusitis, bronchitis, pneumonia and bronchiectasis account for up to 90% of all reported infections in CVID. Streptococcal pneumoniae and haemophilus influenza are most frequently isolated. Both organisms are known to utilise their polysaccharide capsules as an immune-evasion mechanism, a mechanism that is countered

by opsonisation by immunoglobulins [25]. Hence, the infection pattern of CVID is perfectly consistent hypogammaglobulinaemia. Other infections such as conjunctivitis, cellulitis, skin abscesses, meningitis, viral and fungal infections account for the remaining 10% of infections [22, 26, 27].

The majority of CVID patients have reduced serum IgG and undetectable IgA whilst some will retain a normal IgM level. Specific IgG toward pneumococcus, haemophilus influenzae type B and tetanus are suboptimal and do not increase following vaccine challenges. However, peripheral B-cell counts were often reported as normal to low normal, highlighting a functional failure in the humoral immune system.

1.4 From B-cell to plasma cell to long term antibody production

The humoral immune system is an integral part of our adaptive immune response. B-cells, generated from the bone marrow, are key cellular components of the humoral immune system, occupying various parts of the secondary and tertiary lymphoid architecture. However, they represent only an intermediary of the entire antibody producing machinery [28]. Plasma cells are considered to be the true antibody producing cells, and are responsible for maintaining baseline antibody levels. While the transformation from B-cell into plasma cell may occur under a number of stimulatory conditions, the T-dependent follicular antibody response, via CD40:CD40L interactions between a B-cell and its cognate T-cell, marks the most central and potent mechanism for antibody production (Figure 1).

Activated B-cells ($CD20^+CD38^-$) that have met their cognate T-cells migrate into a primary follicle, where they become centroblasts ($Bcl\text{-}6^+$) and proliferate vigorously, converting the primary follicle into a germinal centre. Within the germinal centre, somatic hypermutation and immunoglobulin class switching are triggered by activation induced cytosine deaminase (AID), resulting in the eventual production of high affinity, class-switched memory B-cells ($CD20^+IgM^-IgD^-$

$CD27^{+}$) and plasma cells ($CD20^{-}CD27^{+}CD38^{++}$). In contrast to other humoral responses, a high proportion of germinal centre derived plasma cells will migrate to the lamina propria of the bowel or back to the bone marrow to undergo final differentiation into long-lived plasma cells (LLPC: $CD20^{-}CD27^{+}CD38^{++}CD138^{+}$), expressing a typical transcriptome signature by up-regulating *BLIMP1*, *XBP1* and *IRF4* and down-regulating *PAX5* and *BCL6* [29, 30]. The bone marrow niche has been shown to be crucial for this final differentiation stage and provides support for the long term survival of these cell, allowing them to contribute to the baseline antibody level in the absence of any infections [31]. The longevity of a newly generated plasma cell is dependent on its ability to compete for the limited niche environment with existing LLPCs and it is estimated that less than 10% of all antibody secreting cells will become long-lived plasma cells [31-33].

Plasma cell niche is made up of a complex network of cytokine and stromal cell signalling. Studies on human myeloma (malignant plasma cell) and human myeloma cell line suggested that IL-6, secreted by bone marrow milieu, plays a major role in their survival [34, 35]. In keeping with this, IL-6R is overexpressed on myeloma to allow enhance interaction with bone marrow milieu [34]. Furthermore, IL-6 was shown to work synergistically with IFN-α to promote survival in myeloma [36]. BAFF and APRIL can improve plasma cell survival by signally via BCMA in both bone marrow and the lamina propria of the bowel [37, 38]. Finally, chemokines and adhesion molecules such as CXCL12 and CD44 home plasma cells toward bone marrow niche [39].

Other less dominant mechanisms also contribute to the overall immunoglobulin output. For example, under the influence of IL-21, B-cell activating factor (BAFF) and a proliferation induced ligand (APRIL), marginal zone B-cells in the spleen can class-switch and differentiate into plasma cells; T-independent responses. However their longevity are not well understood [40]. B-cells may also activate in the absence of T-cell help if an adequate signal is received through the B-cell co-receptor complex (CD19/CD21/CD81) by complement fragments such as C3d [41]. The full spectrum of humoral immune responses is beyond the scope of this thesis. Nevertheless, the observed state of hypogammaglobulinaemia in the absence of infection in CVID patients is likely to reflect the disappearance of long-lived plasma cells regardless of upstream B-cell functions.

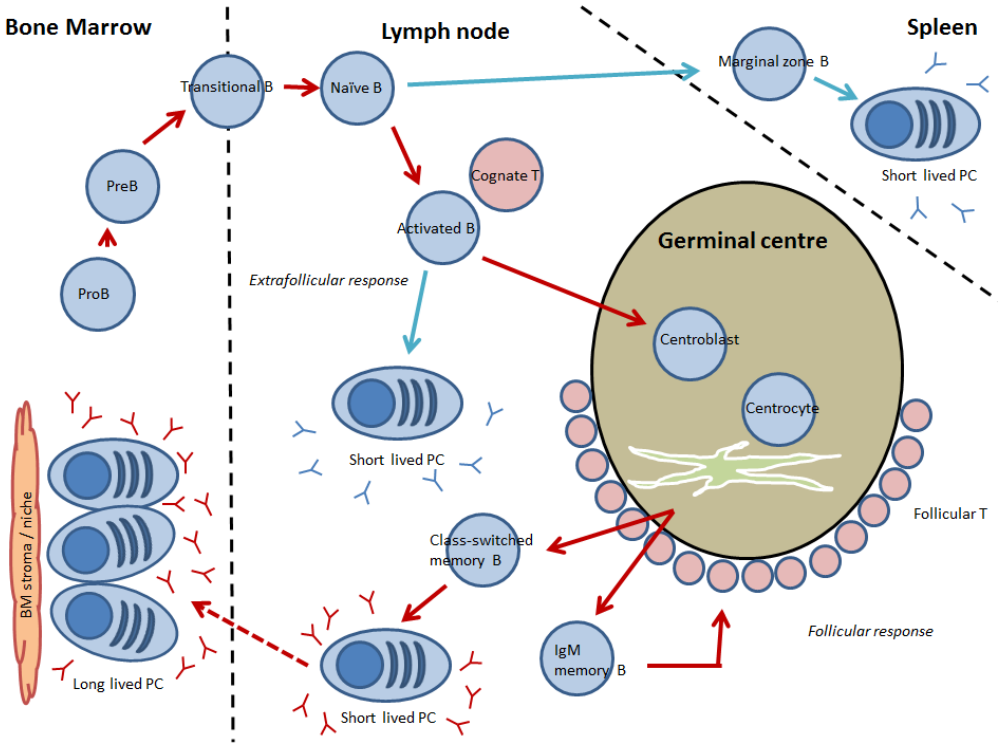

Figure 1. Schema of B-cell ontology and development from Pro B-cell to long-lived plasma cells.

B-cells underwent the process of antigen receptor rearrangement during the ProB-cell to PreB-cell stage in the bone marrow and emerge as naïve B-cells to populate the secondary lymphoid tissues where they encounter antigens and differentiate into plasma cells in the presence or absence of T-cell help, and eventually return to the bone marrow as long-lived plasma cell to contribute to baseline antibody production. The pathway for T-dependent follicular response is illustrated by red arrows. Other accessory pathways are illustrated by blue arrows. Low affinity antibodies (blue) and high affinity antibodies (red) are shown.

1.5 Selective IgA deficiency and CVID

While CVID represents a global failure of antibody production, other more specific antibody deficiencies have been described. Selective IgA deficiency (sIgAD) is characterised by the absence of serum IgA with normal IgM and IgG levels [42]. Protein reference units across the world estimate that sIgAD occurs in 1 in 600 Caucasians but is less common amongst other ethnic groups [42-45]. Immunophenotypic data showed that surface IgA bearing B-cells are readily detectable in individuals with sIgAD, indicating a defect in the terminal activation or secretory pathway of IgA B-cells [46]. The majority of these individuals are, however, asymptomatic and are only identified incidentally. Increase in serum IgG may be seen in patients with sIgAD. Although IgA is secreted in the luminal space of our intestinal and respiratory tract to protect our mucosal surfaces, amply evidence supports that IgG, IgM and even IgD can also be found in these locations; compensating for the loss of IgA [47]. Despite most patients are symptomatic, a subtle form of immunodeficiency has been reported. Blood bank data showed that individuals with low serum IgA were more prone to severe infections and required antibodies more often even if in the absence of a formal clinical diagnosis [48]. Some individuals might be known to their local immunology department due to recurrent and severe infections or a family history of antibody deficiency. A survey of a US cohort suggests that 50% of individuals with sIgAD suffer from recurrent upper respiratory infections. Moreover, autoimmunity, asthma/allergy, cancer and gastrointestinal disorders were all reported in higher prevalence [49].

The cause of sIgAD is not known but it is believed to be part of an extended spectrum of antibody deficiencies. Closer associations with IgG2 deficiency and specific antibody deficiency were previously demonstrated [50]. Importantly, sIgAD and CVID are known to occur in family clusters with up to 10-20% of CVID patients, mostly of Caucasian background, may have a family member affected by sIgAD or CVID, suggesting a common susceptible genetic background [44, 51-53]. Despite this family clustering, the inheritance is non-Mendelian and appears to have incomplete penetrance. Intermediate family members may be unaffected despite the development of disease in the

previous and subsequent generations. Whether sIgAD evolves into CVID overtime is subjected to vigorous debate and concrete supportive longitudinal evidence is lacking. Twenty-eight patients with sIgAD patients were reported by Aghamohammadi *et al* to have progressed into a more severe form of humoral immunodeficiency such as IgG subclasses deficiency and CVID [54]. Nonetheless, the prevalence of sIgAD (1 in 600) and CVID (1 in 25,000) would suggest that transformation is relatively uncommon and is likely to concentrate in those with a history of familial CVID.

An association between sIgAD and CVID was further suggested by immunogenetics data. A number of studies showed that the HLA haplotype - HLA-A1, Cw7, B8, C4AQO, C4B1, BfS and DR3 can be found in higher prevalence amongst CVID and sIgAD patients, indicating a susceptible allele (*IGAD1* gene) located within the MHC region [55-57]. However, linkage disequilibrium studies and more sophisticated mapping strategies with well-designed single nucleotide polymorphisms (SNP) and short tandem repeats (STR) were less conclusive. While these studies continue to highlight the MHC class II region, for both familial and sporadic cases of sIgAD and CVID, the susceptibility gene remained unknown [58, 59]. In addition, no mutations in the HLA genes were found despite strong linkage to the HLA-DQ/DR loci [59]. Other studies concentrating on familial cases of CVID/sIgAD showed linkage to chromosome 4q, 5p and 16q. However, these findings were not supported by replicate studies and exon sequencing of candidate genes did not reveal any responsible mutations [60-62].

Given the major of role of MHC class II in antigen presentation and T-cell activation, some authors hypothesised an autoimmune process behind of aetiology of sIgAD and CVID. In keeping with that, a recent genome wide association study on 772 sIgAD patients highlighted polymorphism in *IFIH1* and *CLEC16A* as risk alleles in addition to *HLA-DR3(DRB1*0301)* [63], with the result of *CLEC16A* being replicated by another study [64]. Both *IFIH1* and *CLEC16A* have been reported to be associated with autoimmune diseases such as type 1 diabetes and systemic lupus erythematosus [65, 66]. Unlike *HLA-DR3* (2.53), the odd ratios for these two genes were however relatively subtle (*IFIH1*:0.67, *CLEC16A*:0.66), indicating they would only play a small role in the overall pathogenesis of sIgAD and CVID [63].

In animal studies, Transmembrane activator and CAML interactor (TACI) was shown to regulate IgA production via APRIL [67] and single nucleotide polymorphism/variant in TACI may be found in both patients with sIgAD and CVID. By studying 27 multiplex families and 135 sporadic cases of CVID, Salzer *et al* identified 18 CVID patients and 1 sIgAD patient with mutations in TACI [68]. The result was supported a parallel study, for which mutations were detected in 4 CVID patients and 1 sIgAD patient [69]. The discovery supported their close relationship, although the same polymorphism may be found in the general population in lower frequency [70-72].

Both sIgAD and CVID increase the susceptibility to gastrointestinal diseases. Coeliac disease is estimated to be 10 to 15 times more common in sIgADs [73], while uncharacterised chronic diarrhoea, colitis and coeliac like sprue occur in 10-15% of CVID patients [74]. Several linkage studies have highlighted the association of Coeliac disease with the chromosome 2q33 locus [75]. Interestingly, this at risk locus, containing the coding regions for CD28, CTLA4 and inducible T-cell costimulator (ICOS), can also be identified in CVID and IgAD [76] and monogenetic mutations in *ICOS* and *CTLA4* were later found to be causal in some in CVID patients [77, 78].

Altogether, family screening, HLA-typing and genome wide association studies demonstrated common clinical and molecular features between sIgAD and CVID patients. Despite the uncertainty if sIgAD would progress into CVID, the two may represent a continuum varying in severity.

1.6 Cancer and CVID

Research in the last decade has revealed the importance of immune surveillance for solid and haematological malignancies, with higher incidence of cancers observed in the absence of a functional immune system such as HIV and AIDS [79, 80]. By elucidating and modifying the mechanisms of the immune system targeting cancer cells, a new generation immunotherapies has emerged to transform oncology practise [81]. Patients with CVID also have increased incidence of both solid and

haematological cancers. According to a recent Australian study (CVID, n=416) the global standardised incidence ratio (SIR) for all cancer in CVID was calculated at 1.94. The increased risk of non-Hodgkin lymphoma (NHL) was noted to be the greatest (SIR=12.1) closely followed by stomach cancer (SIR=7.23) [82]. Although these estimations vary between studies, many had confirmed that the increased incidence is greatest in B-cell NHL [83-86]. The presence of lymphoma in CVID also leads to unfavourable outcome [14, 86]. According to a US-led retrospective study, only 50% of patients with lymphoma survived over a 40-year follow up period [14]. However, sIgAD patients did not appear to be associated with an increase SIR for NHL but a non-significant increase in stomach cancer SIR may be appreciated in patients with sIgAD patients [85, 87].

The biological mechanism for the increasing incidence for lymphoma is not clear. Chapel *et al* suggested that lymphoid malignancy in CVID is a late manifestation and were almost always preceded by polyclonal lymphocytic infiltration with raising serum IgM level [10]. Although lymph node biopsies and splenectomies are regularly carried out for suspected lymphoma in CVID, histological examinations have yet to provide any pathological insights into the connection between lymphoma and CVID. The baseline lymph node architectures of CVID may be disrupted in numerous ways, making them extremely hard to interpret. Changes similar to those of EBV or HHV-8 infections such as, reactive hyperplasia, ill-defined germinal centres and sub-clinical clonality have been reported, suggesting an infective aetiology [88-91]. However, *in situ* hybridisation and PCR for EBV and HHV-8 were negative for the majority of patients [88]. Regardless of the drivers of these reactive changes, transcriptome and surface marker analyses of normal AID activated germinal centre light zone closely resemble that of B-cell malignancies, with high expression of *MYC*, *LMO2* and *EGR1* [92, 93], which could facilitate lymphomagenesis in CVID.

More recently, a number of cases of mucosal associated lymphoid tissue (MALT) lymphoma were reported in CVID patients [94, 95]. MALT lymphoma is a low-grade B-cell lymphoma histologically similar to marginal zone lymphoma. In the gastrointestinal tract, chronic antigen activation by H. pylori is thought to be the major driver of the disease. Regression is observed with treatment of H. pylori providing a strong causal relationship between H. pylori and MALT lymphoma [96, 97].

However MALT lymphoma remains a rare phenomenon in CVID and it is not clear if patients are at higher risk in comparison to the general population.

Members of the TNF superfamily and their receptors such as TACI, BAFF-R and APRIL play crucial roles in the activation and differentiation of B-lymphocytes [98]. As previously discussed, mutation in TACI is a risk-enhancing factor for CVID [68, 69]. Although there is no direct evidence in human, murine models had demonstrated that deficiencies in TNF superfamily receptors or elevations of their respective ligands were strongly associated with the development of lymphoproliferative disorders with $TACI^{-/-}$ knockout mice developed aggressive lymphadenopathy, splenomegaly and B lymphocytosis. By 7 months, 15% of the $TACI^{-/-}$ animals had developed a strong B220 expressing B-cell lymphoma. It is important to highlight that none of the heterozygous animals developed lymphoma [99]. In another study, Batten *et al* showed that elevation of serum BAFF level promoted that survival of malignant B-cells using a murine BAFF transgenic TNF knockout model. Up to 35% of all animals in the study developed B-cell lymphoma [100]. APRIL also has a similar role and an anti-APRIL antibody has been shown to block survival of chronic lymphoid leukaemia [101]. Although these murine data are extremely interesting and provide putative causal associations between CVID and lymphoma, most TACI mutations described in human were heterozygous single nucleotide variants affecting a single amino acid position and cannot be directly compared to a murine knockout model [102]. The C76R TACI murine model, which resembles more closely to the C104R human variant, was associated with the development of moderate splenomegaly, suboptimal vaccine responses but not lymphomas [103]. On the other hand, high level of BAFF has been found in serum of CVID patients [104]. Both murine and human studies showed that BAFF can rescue B-cells from apoptosis and promote the survival of autoreactive B-cells, providing a plausible explanation for lymphomagenesis [105].

Overall, both infections and intrinsic B-cell defects appear to contribute to the increased malignancy risk in CVID and may work synergistically. It is possible that the continuous exposure to inadequately treated infections accumulating with intrinsic risk factors drive B-cells toward malignant changes and this state could be seen as the most extreme spectrum of antibody deficiency (Figure 2).

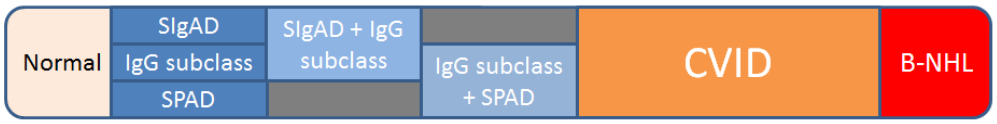

Figure 2. Spectrum of antibody deficiency.

Selective IgA deficiency (SIgAD), specific polysaccharide antibody deficiency (SPAD), Common Variable Immunodeficiency (CVID), B-cell non-Hodgkin's lymphoma (B-NHL).

1.7 Aetiology of CVID

In the previous sections, we discussed the characteristics of CVID and its relationship with selective IgA deficiency and B-cell non-Hodgkin lymphoma. The aetiology of CVID has been one of the most important questions for immunodeficiency research for the past 50 years. Genetics, infective and autoimmune aetiologies have all been considered and advances were made in all three areas. However, there are still many obstacles to overcome and the intrinsic heterogeneous nature of CVID poses a significant challenge.

1.7.1 Genetic mutations: (B-cell activation pathway)

The searches for monogenetic causes in CVID predominantly focused on patients with strong family histories of Mendelian inheritance. Due to the complexity of B-cell activation, a number of genetic mutations involving distinct molecular pathways have been identified in CVID, producing similar clinical presentation.

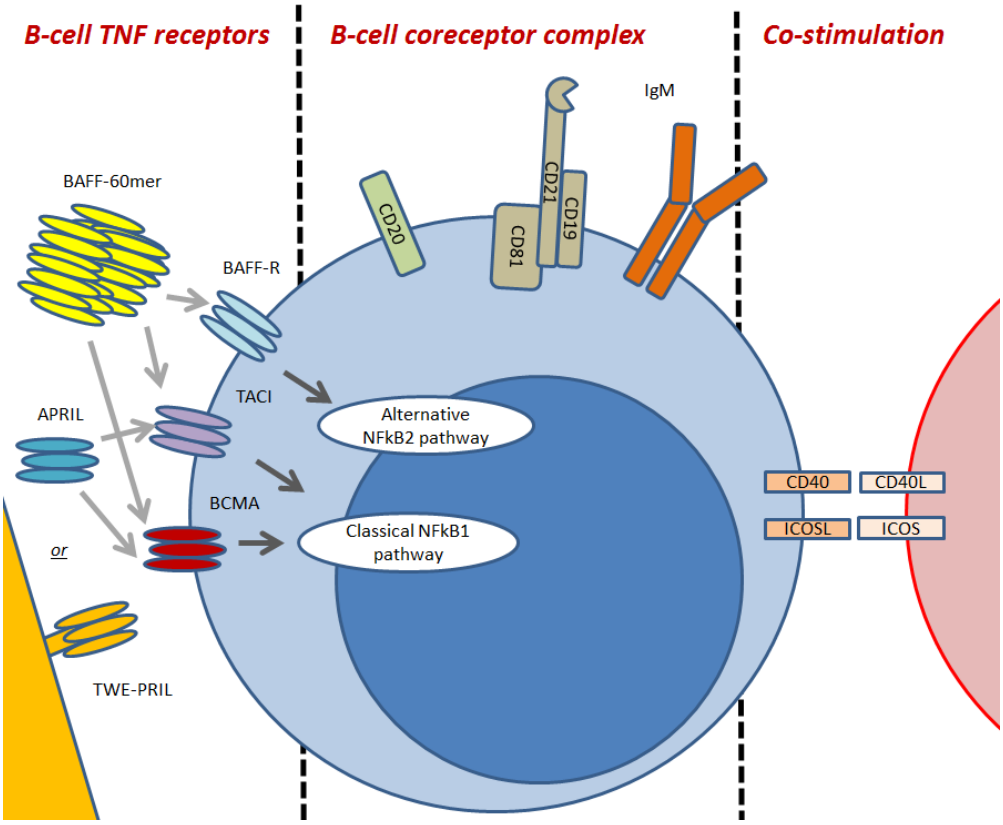

Figure 3. B-cell activation pathways and associating monogenetic mutations in CVID (ICOS, CD19, CD81, CD20, BAFF-R, TACI, TWE-PRIL & NFkB2).

1.7.1.1 Co-stimulatory signal

ICOS deficiency

Inducible T-cell costimulator (ICOS) was the first monogenetic mutation discovered in CVID [78, 106, 107]. *ICOS* is located on chromosome 2q33 and is an extend member of the T-cell co-stimulatory molecular family (CD28/CTLA4) expressed on activated T-cells, for augmenting the CD40:CD40L induced T-dependent humoral immune response as well as many other basic T-cell functions [108, 109]. Studies on $ICOS^{-/-}$ knockout mice suggested that ICOS play a key role in enhancing T-cell cytokine production, with marked reduction of IL-4 and IL-10 observed upon T-cell activation when compared to T-cells of the wide type animal. Both $ICOS^{-/-}$ and $ICOSL^{-/-}$ mice were shown to have poorly defined germinal centres and reduction in class-switched memory B-cells, highlighting its

importance in generating long term humoral memory and high affinity antibodies [110-112]. ICOS-deficient mice also showed greater susceptibility to the development of autoimmunity such as autoimmune diabetes and encephalomyelitis, making it an attractive candidate gene for CVID. However, other studies have shown that ICOS expression is essential for the development of collagen induced arthritis and experimental autoimmune myasthenia gravis in mice [113-116].

In 2003, Grimbacher *et al* reported four CVID patients from two families originated from the western end of the Danube River with adult onset hypogammaglobulinaemia. The families demonstrated autosomal recessive trait and were found to have homozygous large deletion of the *ICOS* gene, essentially removing both exon2 and exon3. *In vitro* stimulation of CD4 T-cells of these patients with anti-CD3 and anti-CD28 antibodies failed to induce ICOS expression. Consistent with the immunophenotype of CVID, these patients demonstrated severe reduction in total B-cells and class-switched memory B-cells [78]. To date, eleven ICOS deficient patients, all showing autosomal recessive trait, have been reported in the literature globally; predominately originated from the same geographical region. No reported sporadic cases of CVID were ever reported to carry the mutation [106, 107].

Although T-cells of ICOS-deficient patients were initially thought to be unaffected, a subtle form of cellular immune deficiency may exist, such as suboptimal control against herpes reactivation [117]. Consistent with murine model, histological examinations of lymph nodes showed reduction in T-cells and poor germinal centre formation. *In vitro* T-cell activation and cultures also showed impairment in IL-10 and IL-17 production [117]. In addition, profound reduction in follicular T-cells ($CD57^+CXCR5^+CD4^+$) can be seen in blood, lymph nodes and the spleen, providing a plausible mechanistic explanation for the poorly formed germinal centres and memory B-cells output observed in patients [118]. Despite the functional similarity between ICOS:ICOSL interaction and CD40:CD40L interaction, searches amongst uncharacterised hyper-IgM cohort (hypogammaglobulinaemia and absent germinal centre reaction) failed to identify any mutations in *ICOS* or *ICOSL* [119, 120].

In summary, both human and murine experimental data confirmed that T-cell co-stimulation via ICOS:ICOSL is crucial in the formation of germinal centres and demonstrated detrimental consequences in its absence. Despite ICOS deficiency offers an excellent explanation for the clinical and laboratory abnormalities observed in CVID, its rarity and geographical confinement make it unlikely to be a dominant aetiology of CVID. As it current stands, ICOS deficiency is a rare entity.

1.7.1.2 B-cell co-receptor complex and CD20

The B-cell co-receptor complex, consists of CD19, CD21, CD81 and CD225, plays a critical role in lowering B-cell activation threshold [121]. CD21 (Complement receptor type 2) binds C3d and other complement fragments generated during the activation of the complement cascade to promote B-cell responses, forming a crucial connection between the innate and adaptive immune system [122, 123]. Unsurprisingly, searches amongst the components of the B-cell co-receptor complex yielded a number of genetic mutations responsible for CVID.

CD19 deficiency

CD19 deficiency was identified as the second monogenetic cause of CVID [124]. Similar to ICOS deficiency, it was discovered in family pedigrees with an autosomal recessive trait. In 2006, van Zelm *et al* reported four children from 2 unrelated families with homozygous mutations in CD19. One family was clearly consanguineous while the second family originated from a small community, deeming it high risk for consanguinity. The homozygous germline mutations detected were different in the two families but both resulted in frameshift and a premature stop codon. Immunophenotypically, CD19 were absent on B-cells with normal expression of CD20 and reduced CD21 and CD5. Class-switched memory B cells were severely reduced and impairment in Ca^{2+} influx by IgM cross-linking was seen [124]. A further patient was reported one year later carrying a compound heterozygous *CD19*

mutation (A: frameshift from exon 6, B: large multi-gene deletion involving *ATP2A1*, *CD19* and *NFATC2IP*) [125].

Consistent with human CD19 deficiency, $CD19^{-/-}$ knockout mice demonstrated significantly impaired in mucosal IgA production and diminished responses to oral vaccination challenges [126]. $CD19^{-/-}$ mice were also reported to have reduced marginal zone B-cells for rapid polysaccharide antigen response [127] and severely impairment in T-dependent response via CD40 activation [128]. Altogether, these findings are in keeping with the clinical phenotype observed in human, strongly supporting the causal relationship between a deleterious change in CD19 and the development of antibody deficiency.

CD81 and CD21 deficiency

The expression of CD19 is dependent on CD81. In murine knockout model, CD81 plays a supplementary role in both T-dependent response and B-cell activation [129-131]. In 2010, van Zelm *et al* reported a case of *CD81* mutation in a 6 year old girl from a consanguineous Moroccan family with hypogammaglobulinaemia and glomerulonephritis [132]. Absent CD19 and CD81 expression on B-cells were noted during the diagnostic workup. Genetics analysis excluded a mutation in CD19 but a homozygous substitution G>A in exon 6 of *CD81* was found in the patient. IgA production was however relatively well-preserved in the patient and IgA deposition was noted on renal biopsy. However, the combination of nephrotic range proteinuria and the substantial use of immunosuppressant therapies, including corticosteroids, cyclophosphamide, mycophenate mofetil and azathioprine, in the patient obscured the proper interpretation of her immunology. Hence, the role of this single nucleotide variant in CD81 remains to be determined.

Similarly, a compound heterozygous CD21 deficiency was reported in a 28 year old man with childhood onset of recurrent respiratory tract infections. He was noted to have reduced IgG, impaired

functional antibodies and complete absent of CD21 on B-cell immunophenotyping and west blotting. Significant binding failure to both C3d containing immune complexes and PnPs14 pneumococcal polysaccharide antigen were demonstrated using patient's immortalised B-cell line, confirming the functional deficit [133].

Although both *CD81* and *CD21* mutations have advanced our understanding on the function of the B-cell co-receptor, their overall role in CVID will remain controversial in the absence of replicate cases/cohorts.

CD20 deficiency

CD20 is an enigmatic molecule constitutively expressed on the surface of all B-cells and it is one of the most widely used surface markers for identifying B-cells. Despite being an active therapeutic target (Rituximab, monoclonal chimeric anti-CD20 antibody) for a number of autoimmune diseases and haematological malignancies its true function remains debatable [134]. Similar to other B-cell co-receptor deficiencies, a case of human CD20 deficiency was reported in a 4 year old consanguineous Turkish girl in 2010 [135]. The patient had isolated reduction in IgG with normal levels of serum IgA and IgM. A homozygous 11-bp insertion in the splice site of exon 5 led to partial deletion of the splice site. The patient had normal number of B-cells (CD19) but impaired somatic hypermutation and vaccine response to polysaccharide antigens. Despite the arrays of *in vitro* abnormalities, the patient's clinical presentation was relatively mild. $CD20^{-/-}$ mice seemingly had normal B-cell functions, hence do not support a direct causal relationship in human antibody deficiency [136].

1.7.1.3B-cell TNF and TNF-receptor

Tumour necrosis factors (TNF) such as BAFF, APRIL and TWE-PRIL are crucial survival factors for B-cells. The B-cell TNF-receptor family consist of TACI, BCMA and BAFF-R receptor and signalling via these receptors represents another important B-cell activation pathway following direct ligation of CD40 by CD40L. BAFF and APRIL are expressed on surfaces of innate immune cells and are rapidly released by proteolytic cleavage. By contrast, TWE-PRIL (a fusion protein containing both TWEAK and APRIL) is only expressed on membrane surface. Soluble BAFFs undergo oligomerisation to form a super molecule, BAFF-60mer, to greatly enhance the signal transduction by engaging multiple receptors simultaneously [137, 138]. BAFF can bind BAFF-R, TACI and BCMA while APRIL is the natural ligand for only TACI and BCMA [139]. BAFF signalling through BAFF-R and APRIL is fundamental during the late transitional B-cell stage and it allows B-cells to complete its maturation process into naïve B-cells. Failure of this *signalling* pathway leads to the accumulation of transitional B-cells and retraction of the splenic marginal zone [72, 100].

BAFF-R is widely expressed by all subsets of human B-cells except plasma cells [140, 141]. Instead, survival of bone marrow long lived plasma cell is sustained by constant signalling through BCMA and the withdrawal of this signal will result in rapid disappearance of the plasma cell population. However, it seems that only BAFF but not APRIL is required for survival of long lived plasma cells as APRIL$^{-/-}$ knock out mice have relatively normal plasma cell survival [142]. To support this, BCMA$^{-/-}$ knockout also had severely impaired long-lived plasma cell survival, confirming this crucial interaction between BAFF and BCMA for long lived plasma cell survival [143]. TACI, on the other hand, is predominantly expressed on activated B-cells, B1 cells and marginal zone B cells [144]. TACI is capable of driving B-cells into plasmablasts and plasma cells via a T-independent manner [145, 146]. There is ample evidence to suggest that TACI and BAFF-R signalling could up-regulate activation induced cytosine deaminase (AID) to drive class-switching of IgA and IgG in the absence of T-cell help [147, 148]. TACI could also work synergistically with T-cell CD40-dependent response to further enhance B-cell differentiation [149]. Similar to BAFF-R, signalling through TACI promotes

the survival of activated B-cells and plasmablasts [144]. TACI also plays a unique regulatory role to prevent over-activation of B-cells. TACI$^{-/-}$ knockout mice developed fatal autoimmunity and lymphoproliferation [99]. In keeping with that, a number of studies confirmed that TACI is crucial in limiting proliferation and inducing apoptosis [99, 150]. Ligation to BAFF-R, BCMA and TACI trigger downstream signalling involving TRAF2, TRAF3 and TRAF6 in the eventual activation of the non-canonical NFkB pathways [137] and a number of genetic defects along this pathway have been found in CVID.

Transmembrane activator and CAML interactor (TACI) deficiency

TACI mutation is one of the most interesting discoveries in the field of CVID genetics. Unlike other genetic deficiencies, which are mostly found in consanguineous paediatric cases, *TACI* mutations were identified in sporadic cases of adult onset CVID across of multiple cohorts. Salzer *et al* discovered the lack of TACI, at the protein and transcript levels, on EBV transformed B-cell lines of CVID patients. Using targeted Sanger sequencing, the authors identified single nucleotide variants (two in the CRD2: S144X, C104R; one in transmembrane domain: A181E; one in intracellular domain: R202H) in 19 out of 162 individuals. Both C104R and A181E were missense mutations, altering the amino acid make-up of the protein. The majority of those individuals carried a heterozygous mutation but 4 were noted to be homozygous. Sequence analysis from 100 healthy donors and a search on SNPer database at the time suggested that those mutations were confined to CVID. Functional studies on homozygous patients also revealed that APRIL, but not BAFF, binding and B-cell proliferation were severely affected along with impairment of immunoglobulin class-switching and T-independent activation [68]. Similar findings were reported by Castigli *et al* by screening a smaller number of patients. Family screening of index cases further identified 7 sIgAD and 6 CVID patients carrying the heterozygous mutations. However, TACI expression on B-cells was largely normal for heterozygous state [69]. Furthermore, binding capacity to APRIL for heterozygous

individuals was later shown to be normal in heterozygous patients [151]. However, conflicting evidence exists with some suggesting that *in vitro* up-regulation of TACI by TLR activation may be impaired even in asymptomatic individuals [102]. Clinically, TACI patients were associated with higher incidence of lymphoproliferation, splenomegaly and autoimmunity [68, 151, 152], with histological examination of tonsillar biopsy showing follicular hyperplasia and enlarged mantle zone [68].

The genotype to phenotype relationship in TACI mutations has been under constant debate. Although a homozygous state does seem to be associated with more severe disease, many family members with a heterozygous mutation were unaffected. Murine studies using the C76R knock-in mutant mice, which was generated to mimic the human C104R mutation supported that APRIL binding is affected in both heterozygous and homozygous stats in a progressive manner [103]. Yet, even within a TACI-pedigree, CVID had been noted in family members without a mutation clinically. Later studies involving larger number of individuals demonstrated that TACI mutations can also be found amongst healthy donors in similar frequencies, although C104R and A181E appeared more prevalent in CVID. These studies also refuted the possible association between sIgAD and TACI mutations. Collectively, these studies estimated 5-7% of CVID patients and 0.5% of the healthy population carry at least one mutated allele of TACI. These figures translate into an estimated odd ratio (OR) of between 3.6 to 4.2 [70, 71, 151, 152]. According to open-access bioinformatics databases (Ensemble), the human C104R region is highly conserved amongst primates such as macaques, gorilla and chimpanzee. SIFT and Polyhen databases both listed C104R mutation as deleterious and probably/possibly damaging for most of its transcripts. The power of next-generation sequencing and genome projects around the world now offers a more accurate assessment of the prevalence of TACI mutation in human. A search in the phase 1 1000 genome projects on “Ensembl” revealed that 1.1-1.7% of American and European carry the C104R mutation but this mutation is also detectable in approximately 0.4% of Africans according the NHLBI exome sequencing project. These figures, hence, suggested the overall importance of *TACI* mutations might have been initially overestimated and may merely be a natural polymorphism amongst the population.

In conclusion, *TACI* represents a risk allele for CVID and *provides* a plausible biological explanation for humoral immunodeficiency in human. Moreover, it is relatable to the sporadic cases of CVID. However, *TACI* mutation could only account for the increase risk in 10% of CVID patients. As the high odd ratio and genetic association cannot be reproduced by genome wide association study, controversies will continue to remain in this area [153]. The overall impact of TACI in CVID is, thus, modest.

BAFF-R deficiency

Similar to *TACI* mutation, variants in BAFF-R was found to be more prevalent in CVID patients. Murine models had long indicated that BAFF-R could be a candidate gene for CVID. Losi *et al* discovered that at least two single nucleotide polymorphism (SNP) were more common in CVID patients. Patients with *BAFF-R* polymorphism may have low to normal expression of BAFF-R on their B-cells. However this study was under-powered and cannot conclude the role BAFF-R in the development of CVID [154]. A further search on patients with less than 5% peripheral B-cells identified one consanguineous patient with a homozygous in-frame deletion and BAFF-R was completely absent on western blotting. Consistent with murine models, the patient had very high serum level of BAFF, retraction of the splenic marginal zone and high proportional of circulating transitional B-cells ($CD19^{+}CD38^{++}IgM^{++}$). Interestingly, the patient had normal class-switched memory B cells and detectable IgA-plasma cell on biopsy. Paradoxically, a relatively well 80 year-old was later found to carry the same homozygous mutation [72]. Another patient with Good's syndrome presenting at the age of 63 was suggested to carry a compound heterozygous *BAFF-R* mutation [155].

TWEAK deficiency

TWEAK belongs to the same TNF superfamily of BAFF and APRIL and is structurally similar to APRIL [156]. Using high throughput gene-based sequencing chip, Wang *et al* identified a family of

CVID patients with autosomal dominant amino acid substitution in exon 6 of *TWEAK*. The index patient was a boy who presented with meningitis at the age of 3. The clinical phenotype included hypogammaglobulinaemia, low B-cell count, ITP, refractory warts and increase risk of lymphoma. In addition, reverse CD4:8 ratio and increase double negative T-cells was noted. The *TWEAK* mutation resulted in inhibition of plasma cell survival and proliferation. Functional assay also showed that the mutated *TWEAK* was unable to induce apoptosis to adenocarcinoma cell line [157].

NFκB2 deficiency

In recent years, next-generation sequencing has proven to be a massive success in identifying candidate genes for germline mutations. This approach had led to the discovery of 6 cases of autosomal dominant *NFκB2* mutation at the C-terminal of the protein in 3 families worldwide. NFκB2 represents the terminal component of the B-cell TNF signalling pathway and is directly involved in gene transcriptions and regulations [158]. Mutation in *NFκB2* has a distinct clinical presentation in comparison to the majority of CVID patients. Childhood onset hypogammglobulinaemia, adrenal insufficiency and debilitating neurological symptoms were central to the condition. Chronic reactivation of herpes infections was also reported [159, 160]. Murine knock out model showed the lack of NFκB2 can lead to impairment in peripheral B-cell development, hypogammaglobulinaemia and disrupted lymphoid architecture [161]. Although initially identified in patients labelled with CVID, its distinct clinical presentation makes it a unique clinical entity. However, it is worth noting that the full clinical spectrum might take a number of years to develop and the clinical presentation may still overlap with CVID during the early phase.

1.7.1.4High-throughput approach

To extend the genetic findings to sporadic cases, large genome wide association studies (GWAS) were carried out in CVID patients. Complementary to previous linkage analyses and fine mapping strategies, the HLA region was repeatedly highlighted in the Manhattan plots of GWASs. One study looking at both SNV and copy number variation additionally identified closer association at the *ADAM* and *ORC4L* loci. However these findings could not be reproduced in replicate cohorts, lessening their credibility [153]. Two separate GWASs highlighted *CLEC16A* in addition to the *HLA* loci as another risk allele for CVID and possibly sIgAD [63, 64]. It is however not clear how *CLEC16A* could lead to the failure of the humoral immune system although certain SNV/SNPs are linked with higher risk of organ-specific autoimmunity [162, 163]. Interestingly, none of loci containing those previously described monogenetic mutations, such as *CD20*, *TACI* etc, were highlighted in any of the GWASs, confirming the fact that those monogenetic mutations are restricted to rare family and cannot explain for the majority of CVID.

The application of whole genome sequencing has also revealed a number of new genes in families demonstrating clear Mendelian inheritance such as *CTLA4*, *LRBA* and *PLC-gamma 2* deficiencies [77, 164, 165]. However, results of sporadic cases of CVID remain disappointing. Furthermore, results of the WGS500 consortium suggest that TACI polymorphism is equally prevalent in other inflammatory and rare diseases, distancing a causal relationship between TACI and CVID. Intriguingly, whole genome data revealed that some patients were carrying multiple deleterious variants across their genome, suggesting a potential cumulative effect of multiple mutations [166]. Nonetheless, the data continue to support the polygenic and heterogeneous nature of sporadic cases of CVID without a single or dominant defining cause.

1.7.1.5Summary of CVID genetics

In the past decade, molecular studies have revealed monogenetic deficiencies in various B-cell activation pathways, including T-cell co-stimulation, B-cell co-receptor signalling and B-cell TNF receptor responsible for the clinical syndrome of CVID. It has also enhanced our biological insight of the functions of these molecules and the consequences of their absence. Yet, all these deficiencies are exceedingly rare with the majority affecting paediatric patients from consanguineous families. With the exception of *TACI*, monogenetic causes of CVID account for only about 100 cases in the literature (Table 2). Despite initial promising data, recent data continue to challenge to role of TACI in CVID. As it current stands it could only be considered as a susceptible allele and additional influences, either genetic or environmental, must play crucial roles in triggering the onset of CVID.

Mutations	No. of cases	Inheritance	Disease onset	References
ICOS	11	AR	Adulthood	[78, 106]
CD19	5	AR/CH	Childhood	[124]
CD81	1	AR	Childhood	[132]
CD21	1	CH	Childhood	[133]
CD20	1	AR	Childhood	[135]
TACI	~5%	Uncertain	Adulthood	[68, 167]
BAFF-R	1	AR	Childhood	[72]
TWEAK	2	AD	Childhood	[157]
NFκB2	6	AD	Childhood	[159, 160]
CTLA4	26	AD	Adulthood	[77, 168]
LRBA	22	AR	Childhood	[164]
PLCγ2	29	AD	Childhood	[165, 169]
CLEC16A	--	GWAS	--	[63, 64]
ADAM	--	GWAS	--	[153]
ORC4L	--	GWAS	--	[153]
HLA	--	GWAS	--	[64, 153]

Table 2. Summary of genetic mutations in CVID.

1.7.2 Intrinsic B-cell defects of CVID

Although molecular investigations have not identified the cause of CVID for the majority of patients, a number of *in vitro* abnormalities have been described, providing a glimpse of the pathophysiology of the disease. Being the most central feature of CVID, much of the effort has been invested in studying the humoral immune system and the functions of B-cells in hope of revealing a putative aetiology.

1.7.2.1B-cell Immunophenotypic data

In CVID, total peripheral blood B-cell count varies from normal in most patients to near absent in rare cases [170]. Early immunophenotypic data showed that markers such as CD86 [171, 172] and CD38 [173] were poorly expressed on activated B-cells of CVID patients whilst others have shown that B-cells express increased level of apoptotic factors such as FAS. More importantly, the expression of CD27 may be markedly reduced on surfaces of B-cells following activation with S.Cowan A, IL-2 and CD40L [174]. CD27 is a member of the TNF superfamily that is upregulated by plasmablasts, plasma cells and memory B-cells including class-switched memory B-cells ($CD20^+IgD^-IgM^-CD27^+$, smB) and marginal zone like B-cells ($CD20^+IgD^+IgM^+CD27^+$, MZB) [175], hence the lack of its expression in CVID is supportive of a defect in the terminal differentiation of B-cells. This suboptimal expression of CD27 has been repeatedly reciprocated in multiple CVID cohorts and these studies identified the lack or reduction in class-switched memory B-cells as the commonest finding on B-cell immunophenotyping. Moreover, a close association between the reduction of smB and increased $CD21^{lo}$ B-cell population and poor T-cell activation was demonstrated [176, 177].

Similar to peripheral B-cell count, disturbance in the B-memory compartment may be variable amongst patients. Attempts to stratify patients according to their B-cell immunophenotypes led to the

development of the Paris, Freiburg and Euro classifications [19, 177] and these classification systems have been adopted by a number of European centres in the past decade. Alachkar *et al* suggested that assessment of memory B-cells may be more useful than stratifying patients according to their ability to synthesise immunoglobulin in predicting the clinical outcome of paediatric CVID [178]. It is also generally agreed that patients with severe reduction in smB (<0.4% of peripheral blood lymphocytes) and expansion of $CD21^{lo}$ B-cells (>10% of total B-cells) are more likely to steer toward a more a complex clinical phenotype including splenomegaly, lymphadenopathy and granulomatosis. Consistent with that many of the monogenetic defects described in the previous section were characterised by the severe collapse of the class-switched memory B-cell population. The clinical relevance has led to the reduction in smB being included in the 2014-revised ESID diagnostic criteria. Moreover, the lack of MZB was linked to higher incidence of infections [179].

However, stratifying patients according to their B-immunophenotypes is not without its disadvantages. Firstly, normal ranges for B-cell subsets vary across age groups. Adults are more likely to accumulate higher levels of memory B-cells where as children have higher number of transitional and naïve B-cells [180]. Secondly, the origin of $IgM^+IgD^+CD27^+$ B-cells continue to draw vigorous debate. Although, phenotypically similar to marginal zone like B-cells and numerical reduction has been observed following splenectomy in human [181], recent studies suggest that $IgM^+IgD^+CD27^+$ B-cells are likely to represent a mixture of circulating marginal zone memory B-cells and post-germinal centre B-cells. In contrast to $IgD^-IgM^-CD27^+$ memory B-cells, these post-germinal centre $IgM^+IgD^+CD27^+$ memory B-cells are preprogramed to re-entering the secondary follicles on repeat antigen challenge for further rounds of affinity maturation. This process allows our humoral immune system to keep up with the evolutionary pressure from pathogens [182]. Thirdly, B-cell immunophenotypes observed in CVID are by no means unique to the condition. Reduction in IgD^+CD27^+ B-cells was also reported in autoimmune diseases such as SLE and Sjogren's [183, 184]. Similarly, low smB and expansion of $CD21^{lo}$ can be seen other conditions such as X-linked lymphoproliferative disorder (XLP), SLE and rheumatoid arthritis [185-188]. Regardless of its clinical

utility, the retraction of the memory compartment represents a crucial B-maturation defective in the pathophysiology of CVID.

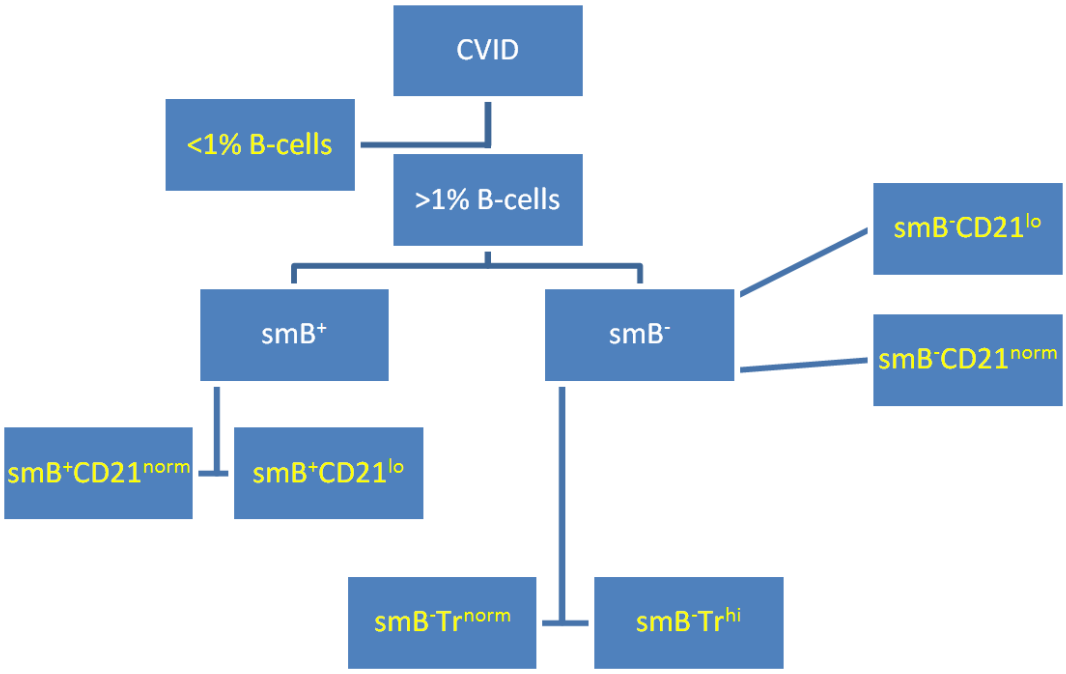

Figure 4. EUROCLASS classification for CVID.

Patients are stratified according to peripheral blood frequency of <1% (B^-) or ≥1% of total lymphocytes. Patients with B-cell frequency of ≥ 1% are further stratified according to switched memory B-cells (smB: $CD19^+CD27^+IgM^-$), $CD21^{lo}$ B-cells ($CD21^{lo}$: $CD19^+CD38^{lo}CD21^{lo}$) and transitional B-cells (Tr: $CD19^+CD38^{++}IgM^{++}$). (smB^- = <2%, smB^+ = >2%, $CD21^{lo}$ = >10%, $CD21^{norm}$ = <10%, Tr^{norm} = <9% and Tr^{hi} = >9% of total B-cells).

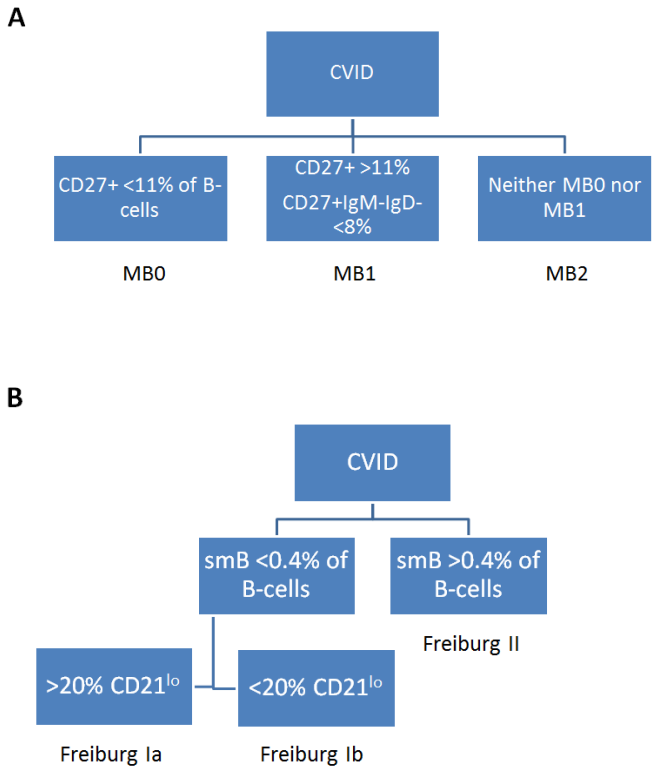

Figure 5. Paris and Freiburg classification.

(A) Paris classification; subdividing CVID patients according to frequency of $CD27^+$ and $CD27^+IgM^-IgD^-$ of total peripheral blood B-cells. (B) Freiburg classification; subdividing patients according to frequency of smB ($CD27^+IgM^-IgD^-$) of total peripheral blood lymphocytes and then frequency of $CD21^{lo}$ population of total B-cells.

1.7.2.2In vitro B-cell activation and proliferation

As previously discussed, the T-dependent response is considered to be the most central and potent of all humoral immune responses [189]. Interestingly, normal proliferation may be seen when B-cells of CVID patients are activated by anti-IgM and CD40L with the support of IL-4, although a huge amount of variability was seen as expected with many functional assays [190]. To further support this

residual functional ability, Borte *et al* showed that B-cells of CVID patients can upregulate CD38 and CD27 as well as produce normal amount of IgG using a combination cocktail of anti-CD40, IL-4 and IL-21 [191]. However, profound deficiency to generate immunoglobulins was observed in some patients when IL-10 was used as a substitute to IL-4, suggesting a highly specific defect [190, 192]. These *in vitro* results also showed a hierarchy in the deficiency of immunoglobulin isotypes with IgA being most severely affected while the ability to produce IgM was large retained. Interestingly, one study demonstrated that immunoglobulin production could be recused by co-culturing with activated allogenic T-cells [193].

Alternatively, B-cells may be activated via toll-like receptors (TLR), such as using unmethylated CpG oligodeoxynucleotide, in the absence of CD40:CD40L ligation *in vitro*. Impairment in proliferation, class-switching, CD86 up-regulation, IL-6 and IL-10 productions were observed when B-cells of CVID patients were stimulated with anti-IgM or via their TLR7/9. Similar to experiments using anti-CD40, results were highly variable with some patients demonstrating complete failure of B-cell activation while others had normal functions [194-197].

Measuring $Ca2^{+}$ intracellular influx from the endoplasmic reticulum (ER) have been used to assess B-cell intracellular signalling and it closely correlates with the up-regulation of Ki67, a proliferation marker. Upon IgM cross-linking, PLCγ mediates ER $Ca2^{+}$ channel to open and eventually lead to the activation of downstream transcription factors such as NFAT and NFκB [198]. Suboptimal $Ca2^{+}$ influx was reported in B-cells of CVID patients with higher frequency of $CD21^{lo}$ B-cells and reduced class-switched memory B-cells. The reduction in $Ca2^{+}$ influx was noted to occur along with the increased surface up-regulation of CD22, suggesting the overexpression of CD22 on CVID B-cells might have inhibited their full activation [199]. Cross-linking BCR was reported to induce suboptimal increased in intracellular pERK leading to poor endocytosis of BCR in the memory B-cells and $CD21^{lo}$ B-cells in CVID [200]. In addition, defective CD20 dissociation with the BCR complex may also impair of $Ca2^{+}$ influx in CVID [201].

Overall, these functional studies are often laborious and were usually done on limited number of patients. Direct comparison between studies is difficult as culture conditions tend to vary significantly. In addition, the concurrent use of immunoglobulin replacement therapy in patients poses a significant confounder given its potent inhibitory on B-cells [202]. Byrant *et al*, promoted the use of functional studies to sub-classify CVID but were halted by their impracticality [203]. However, it could be said that a large number of CVID patients from these historical studies demonstrated residual capacity and were able to generate comparable amount of immunoglobulin in the presence of CD40/CD40L ligation.

1.7.2.3Isotype class-switching and somatic hypermutation

Immunoglobulin isotype class-switching recombination (CSR) and somatic hypermutation (SHM) are two key processes that occur in germinal centres within secondary lymphoid tissues in generating high affinity and longer lasting antibodies. Defect in CSR is a hallmark of hyper-IgM syndrome but can also be seen in CVID [204], mostly reflected by the lack of IgA and IgG memory B-cells on peripheral blood immunophenotyping. In addition, *in vitro* studies frequently demonstrated a reduction in IgG and IgA production with retained IgM function. In keeping with this, IgE production was also shown to be defective [205]. CD73 is a critical trigger for CSR and was shown to be down-regulated on naïve and IgM memory B-cells of CVID patients [206]. Histologically, class-switched plasma cells, particularly IgA^+, were reduced or absence in number of lymph node biopsies [88]. Hence, orthogonal evidence supports a struggle to commit CSR in CVID.

Regarding antibody affinity maturation by somatic hypermutation (SHM), mutation rate at the variable region of immunoglobulin was initially estimated to be five times lower in CVID patients by studying the JH4-JH5 intron and V3–23-Cγ transcripts of IgM^-IgD^- B-cells [206-208]. Similar findings were reported when assessing the kappa light chain (IgκREHMA), for which 77% of patients had 6 to 7 time less mutation hotspots in their kappa regions. Impaired SHM in both heavy and light chains

have been linked to higher infection rate and was promoted to be a better predictor for severe infections [209, 210].Larger proportion of unmutated class-switched cells can be found in CVID B-cells, suggesting the defect in SHM may be independent from CSR. In the same study the overuse of certain mutational hotspots was noted; an observation also made in mice with defective UNG-dependent mismatched repair DNA machinery, hence, providing a plausible link to the increase risk of lymphoproliferative disorder in CVID [211]. Although impairment for SHM can be demonstrated consistently across all studies, more recent studies estimated that the magnitude of the deficiency to be less drastic [212]. Across all studies, it is estimated that 25-50% of all CVID patients had 2.5 to 5 fold reduction in SHM rate.

1.7.2.4Plasma cell: the true antibody producing cells

The study of peripheral B-cells has provided us with great insights regarding the functional state of the humoral immunity in CVID. Although *in vitro* B-cell activation represents an excellent model for primary and secondary humoral responses, baseline antibodies during the quiescent phase are not maintained by activating B-cells. In human, baseline antibody levels are instead maintained by bone marrow resident long-lived plasma cells ($CD19^{-}CD20^{-}CD27^{+}CD38^{++}CD138^{+}XBP1^{+}Blimp\text{-}1^{+}$) [213-215]. Long-lived plasma cells are notoriously difficult to study *in vitro* as they exist in very low number in peripheral blood. Bone marrow is the only reliable source for plasma cells but maintaining their survival *in vitro* had been a major obstacle. Although many studies were able to up-regulate CD38 on B-cell surface, these cells were likely to represent activated B-cells or short-lived antibody producing cells but not long-lived plasma cells. In 2009, Borte *et al* demonstrated marginal success in generating and isolating $CD138^{+}$ (Syndecan-1) plasma cells from frozen PBMCs of CVID and sIgAD patients, but our understanding of plasma cell functions in CVID is still very limited [191]. The limited insight of plasma cell functions were predominantly derived from histological data with small bowel biopsies often demonstrating reduced or absent plasma cells correlating with the degree of IgA

and IgM deficit in the serum [216]. Consistent with the serum and *in vitro* data, IgA plasma cells were almost always absent while IgG and IgM plasma cells were less affected [88]. Similar findings can be found in other parts of the gastrointestinal tract such as the stomach and the colon. This creates a clear distinction between CVID enteropathy and other intestinal inflammatory diseases such as sprue and inflammatory bowel disease (IBD) where B-cells and plasma cells are usually in abundance. Interestingly, the lack of plasma cells is frequently found along with abnormal lymphoid aggregation and inflammatory changes similar to graft-versus-host disease [217-219]. It was suggested these lymphoid aggregates and nodular lymphoid hyperplasia are likely to represent CD8 infiltration [74]. In lymph node biopsies, CD138 expressing cells can only be found in a third of the patients whilst Blimp-1 expression was detectable in most patients, suggesting a block at the final differentiation step for B-cells [220]. Similar to intestinal biopsies, significant reduction or absence of plasma cells can be seen in the bone marrow with adjacent T cell infiltration. The connection between these two findings is highly intriguing and is not described in other conditions [221].

Overall, the absence of plasma cells may be observed in 60-80% of patients' biopsy samples. This finding is consistent with poor B-cell activation and germinal centre activities leading to suboptimal terminal differentiation and hypogammaglobulinaemia. Finally, the consistent presence of T-cell aggregates warrants further investigations.

1.7.2.5Summary of B-cell defects

Similar to the clinical presentation, the study of B-cells demonstrated huge variability in all categories of B-cell function. The difficulty is in part due to heterogeneous nature of the condition but also a result technical variability. No single mechanisms current dominate our understanding of B-cell dysfunction in CVID but, the reduction of peripheral blood class-switched memory B-cells, defective proliferation, somatic hypermutation and finally the absence of tissue plasma cells would collectively

support attenuation in naïve B-cell activation. Furthermore, defects tend to be partial and residual functions were often demonstrated, raising the possibility of inadequate support from T-cells.

1.7.3 T-cell abnormalities in CVID

Although B-cells have been the central focus of CVID research, growing experimental data suggest that the T-cell compartment is also disrupted. T-cells are master players of our adapted immunity and play crucial roles in augmenting the humoral immune response. As previously discussed, the T-dependent antibody response is considered to be the most central mechanism of all humoral immune responses and constitutes to the production of high affinity antibodies and memory formation [222]. The discoveries of T-cell related molecular defects such as hyper IgM syndrome and ICOS deficiency highlighted the negative consequences to the humoral immunity in the absent of T-cell support [78, 120].

1.7.3.1 T-cell exhaustion

Global T-lymphopenia was the first T-cell abnormality noted amongst CVID patients [22, 223, 224]. Lymphopenia in CVID is predominantly restricted to the CD4 population, and could dramatically reverse the normal CD4:8 ratio when combined with expansion of the CD8 population; a feature not usually found in other antibody deficiencies [225]. In addition to the quantitative alterations, abnormalities in cytokine production, up-regulation of activation markers and cell proliferation have been reported. Experimental data for cytokine output in CVID have been well summarised by Varzaneh *et al* [226], for which sluggish production of IL-2 along with deficiencies in other Th2 cytokines such as IL-4, IL-5 and IL-10 were reported by a number of studies [226-228]. By contrast, high levels of IL-6, IFNγ and TNFα were observed [226]. This cytokine signature is similar

to an exhausted T-cell cytokine profile reported in chronic viral infections where the gradual inability to secrete IL-2 was observed following prolonged antigenic stimulation [229, 230].

Consistent with this observation, immunophenotypic data showed that T-cells of CVID patients exhibited high levels of activation markers including CD29, CD38, CD95, CD45RO and HLA-DR whilst CD27, CD62L and CD45RA were reduced. This activated memory phenotype was reported to correlate with the reduction of switched memory B-cells and less so with the expansion of $CD21^{lo}$ B-cells. Although the accumulation and expansion of T-cell memory is natural with advancing age, this process is greatly enhanced in CVID [21, 231-233]. In keeping with this, disproportional increased in terminally differentiated, senescent phenotype ($CCR7^{-}CD45RA^{+}$) with increased expression of CD57, and PD-1 were also found across multiple studies, supporting an exhausted cellular immune response in CVID [20, 225, 233, 234].

Cyclic AMP dependent protein kinase A type 1 (PKAI), a T-cell proliferation inhibitor, may accumulate in senescent T-cells [235, 236]. Early studies showed that T-cell proliferation responses to tetanus toxoid and TCR antibodies were suboptimal in CVID patients [237]. Aukrust *et al* later demonstrated that normal proliferation may be restored using a PKAI selective antagonist, hence suggesting that poor T-cell proliferation in CVID was a secondary feature to senescent [238]. More recently, the synergistic use of IL-2 therapy and checkpoint (PD-1) blockade demonstrated great potential in reversing CD8 T-cell exhaustion in a murine LCMV model [239]. Although anti-PD-1 antibodies have not been tried in CVID, IL-2 treatment in the past had demonstrated marginal success [240, 241]. Along with suboptimal proliferation responses, impaired apoptotic function may also contribute to the accumulation of activated T-cells in CVID [242-244].

Overall, orthogonal *in vitro* studies indicated that T-cells of CVID patients are driven toward exhaustion far greater than the expected physiological rate.

1.7.3.2 Exaggerated CD8 T-cell responses

In immunocompetent individuals, T-cell exhaustion is usually driven by a chronic infection or cancer. By stimulating CD4 T-cells with various bacterial antigens, Perreau *et al* showed that normal CD4 responses to various bacterial antigens were impaired but may be restored by blocking the PD-1–PD-L1/2 axis, suggesting that T-cell exhaustion was a result of heavier T-cells burden in the *absence* of a functional humoral system [234]. However, a key paradox for this hypothesis is the *relative* normality of the T-cell compartment in other antibody deficiencies [225]. Also, T-cell receptor assessments by spectratyping showed that T-cell repertoires were normal in patients with X-linked agammaglobuliaemia [245]. By contrast, CVID patients may carry very large, stable CD8 clonotypes skewing their entire repertoires [245, 246]. Preferential use of Vβ 4, 12 and 17 gene segments were reported in CD8 T-cells, particularly in patients with a reverse CD4:8 ratio [242, 247]. Together with the high degree of HLA sharing amongst CVID patients [56, 59], a putative antigenic driver had been proposed as the underlying cause for these CD8 T-cell clonotypes.

To further investigate for the putative antigenic driver behind the Th1-skewed and exhausted CD8 T-cells, Marashi *et al* examined the role of cytomegalovirus in CVID. Using pentamers, higher frequencies of $Ki76^{+}$ CMV-NLV peptide specific CD8 T-cells were detected in CVID, but not in XLA, whilst EBV responses were equivocal across all groups. The data suggested that 1-1.5% of CD8 T-cells in CVID may be proliferating against NLV-peptide [248, 249].

Autoimmune complications are other possibilities for the exaggerated CD8 responses. T-cell aggregates were often found in bowel and lymphoid tissues of CVID patients with granulomata, mimicking graft-versus-host disease [217-219, 221]. These lymphoid aggregates and nodular lymphoid hyperplasia were reported to predominately contain CD8 T-cells [74]. Intriguingly, CD8 infiltration was frequently noted along with the absence of plasma cells as previously discussed, raising the possibility of autoreactivity against plasma cells or their supportive environment [221]. Tissue infiltrated T-cells in CVID are not exclusively of CD8 origin. Histological examination of lung

tissue of CVID patients with interstitial lung diseases showed that tertiary lymphoid aggregates are dominated by CD4 and B-cells, similar to that of synovial joints in rheumatoid arthritis. Interestingly, the lack of plasma cells was not a routine feature in the lungs [250, 251]. Unfortunately, detail immunophenotyping on tissue resident T-cells of CVID patients are lacking.

As a whole, experimental data indicated that T-cells in CVID are driven towards exhaustion via an exaggerated CD8 immune response. Although both CMV and autoimmunity were considered as the underlying drivers, more evidence is still required. To further complicate this, recent TCR repertoire assessment using more powerful molecular and bioinformatics approaches favour an intrinsic T-cell defect as oppose to a chronic antigenic drive, disrupting the repertoire [252]. Hence the putative drivers behind the exaggerated T-cell immune response in CVID remain unknown and this area warrants further investigations.

1.7.3.3Diminishing thymic output complimenting CD8 exhaustion in CVID?

Chronic immune dysregulation provides an alternative explanation for T-cell exhaustion in CVID. Many studies have observed the imbalance between effector and regulatory T-cells in autoimmunity [253]. Fevang *et al* reported lower frequencies of $CD4^+CD25^+FOXP3^+$ T-cells, an immunophenotype widely adopted for regulatory T-cells (Treg), in the peripheral blood of CVID patients. In the same study, the frequency of Treg was inversely proportional to a serum neopterin, confirming their active anti-inflammatory role. RNA transcript levels for FOXP3 in CD4 T-cells were also lower in patients, particularly in those with splenomegaly [254]. Up to 50% reduction in peripheral blood regulatory T-cells ($CD4^+CD25^+FOXP3^+$ or $CD4^+CD25^+CD127^-$) had been demonstrated in multiple international cohorts with the greatest deficiencies identified in patients with autoimmune cytopenias or Freiburg group 1a [255-258]. In addition to the numerical deficiency in Tregs, lower expressions of CTLA-4 and GITR were demonstrated; both carry key regulatory functions for Tregs [259, 260]. Carter *et al*, further suggested that the reduction of Tregs in CVID was associated with activation of CD8 T-cells

but no associations between CD4 T-cells and Tregs were noted [259]. Similarly, reduced Treg frequency was also found in bronchoalveolar lavage fluid collected from CVID patients with interstitial lung disease and was inversely proportional to the level of TNFα [258]. Tregs isolated from CVID patients with autoimmune diseases were also shown to have inferior suppressive function when co-cultured with autologous $CD4^{+}CD25^{-}$ T cells [255]. Hence, the reduction of Tregs would provide a logical explanation for the overexpansion and exhaustion of CD8 T-cell as well as the development of autoimmunity CVID patients.

Examination with other T-cell subsets suggests that the reduction of Tregs may be part of a much broader picture. Using CD1d tetramer and Va24/Vb11 antibody staining, Fulcher *et al* demonstrated a deficiency in the invariant NKT-cell population (iNKT) in CVID. The deficiency was greatest in Freiberg group 1a CVID patients but not observed in XLA [261]. The numerical reduction of iNKT was recapitulated by other studies and may also be associated reduction of other innate cells, such as plasmacytoid dendritic cells and NK cells [262, 263]. In another study, nearly 50% of patients demonstrated no circulating iNKTs. Culturing T-cells with CD1d tetramer and α-galcer, a natural ligand for iNKT, also failed to adequately expand iNKT population [264]. The combined reduction in both Tregs and iNKTs suggest a potential problem in thymic output, as both are considered to be primary product of the thymus [265-267]. To further support this, more general immunophenotypic data revealed lower frequency of both naïve ($CD45RA^{+}CCR7^{+}$) CD4 and CD8 T-cells in CVID [231]. Although one would argue that lower frequency of naïve T-cell might be secondary to expanded of the memory and the activated compartments, reduction in naïve T-cells is not observed in other autoimmune diseases such as rheumatoid arthritis and systemic lupus erythematosus [268, 269]. Bateman *et al*, studied the T-cells of 58 CVID patients and enumerated various T-cell sub-populations using counting beads confirmed the numerical deficits within the naïve pool while XLA, IgA deficiency and IgG subclass deficiency were normal [225].

A number of studies also examined the level of T-cell receptor excision circle (TREC) in CVID patients. TREC is a gene segment by-product of VDJ rearrangement and is not replicated during cell division. It has been used as direct measurement of thymic output and recent thymic emigrants [270].

As much as 10x fold reduction in TREC was reported in both CD4 and CD8 T-cells of CVID patients. The magnitude of TREC reduction also correlated well with the level of activation marker on CD8 T-cells. Although the level of TREC naturally decreases with age due to physiological thymic involution, age-matched control data suggested that this process is greatly exaggerated in CVID [271, 272]. In addition to TREC, studies using immunophenotypic method ($CD45RA^{+}CD31^{+}$ as markers of recent thymic emigrants) also confirmed the reduction in thymic output in CVID [225, 273].

Therefore, there is compelling evidence to suggest a reduction in thymic output in CVID. As proposed by Liston *et al*, reduction in thymic output in other partial T-cell immunodeficiency may promote autoimmunity due to imbalance between effector and regulatory T-cells [274]. It is, thus, not surprising that the majority of the findings described above gravitate towards Freiberg group 1a patients whom naturally carry higher rate of autoimmune complications. In addition, the disappearance of iNKT would further hinder B-cell activation and memory formation [275]. However, it is not clear if this observed thymic involution is primary or secondary to recurrent infection and stress. In mice, infection with salmonella resulted in significant thymic atrophy due to the loss in thymocytes but recovery was seen post infection [276, 277]. Similar observations have been made in rabies, HIV, mycobacterium, turalemia and listeria infections but they are uncommon in CVID [278, 279].

1.7.3.4Summary of T cell defects

Although most patients do not clinically manifest as overt T-cell immunodeficiency, orthogonal evidence support an uncharacterised and exhausted T-cell immune response coupled with deficiency in thymic output in CVID. This can lead to the imbalance between regulatory T-cells and effector T-cells, driving T-cells toward greater exhaustion and perhaps increased risk of autoimmunity. However, it is still unclear how these T-cell abnormalities relate to hypogammaglobulinaemia and why most patients are spared from overt fungal and viral infections. The close proximity of T-cell aggregates

with the absence of plasma cells possibly suggests an inhibitory role in the functions and survival of long-lived plasma cells, an area warrant further investigations.

1.8 Hypothesis building

In this chapter, we discussed how CVID falls into the antibody deficiency spectrum from asymptomatic IgA deficiency to B-cell non-Hodgkin lymphoma. Linkage analyses and fine mapping strategies demonstrated the sharing of at risk alleles between these disorders, although the trigger of clinical disease appears to require additional factors.

Genetic studies of consanguineous families highlighted that defects in multiple B-cell activation pathways can converge into a single clinical entity whilst high throughput genomics data confirmed the polygenic nature of the disorder with no single gene mutations dominating our understanding of CVID. Much as, the exponential advance in molecular technique has led to the growing repertoire of monogenetic mutations and at risk alleles, a convincing aetiology for the majority of sporadic cases has yet to emerge. Hence for the majority of patients, their genetic information could only be translated into susceptibility.

Functional B-cell studies have consistently demonstrated the failure from the pre-germinal centre to the post-germinal centre stages whilst residual functions were observed. The absence of a specific intrinsic B-cell defect warrants the investigation of other external influences. In contrast to other antibody deficiency syndrome, most CVID patients exhibit sub-clinical T-cell abnormalities. As discussed, the exaggerated effector functions could impede on B-cell functions. To further support this, histological data often showed the paucity of plasma cells with T-cell aggregates. At the same time, the reduction of thymic output might limit the availability of cognate T-cells to support B-cells.

No genetic mutations or functional data are currently available to reflect on the relationship between B-cells and T-cells in CVID. This study characterises the relationship between the cellular and humoral compartments in CVID and tests if T-cells could play a key role in triggering the onset of humoral failure and unmasking clinical significant antibody deficiency in genetic susceptible patients (Figure 6).

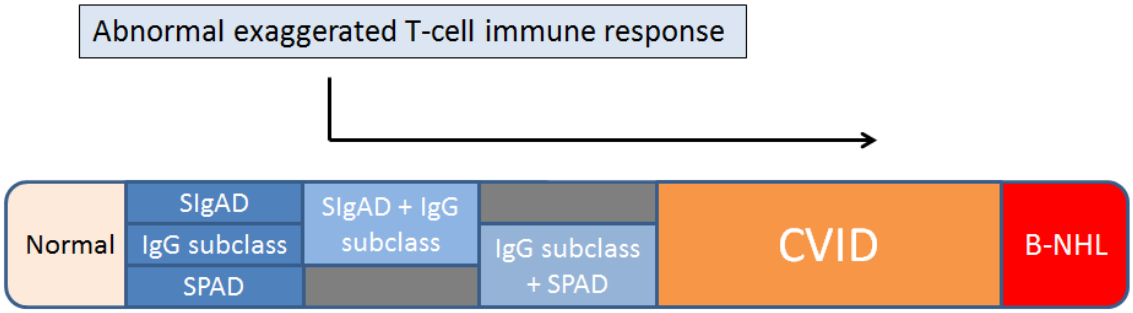

Figure 6. Putative mechanism of aberrant T-cell immune response inhibiting B-cell functions driving the development of CVID in genetic susceptible individuals.

1.8.1 Aims of the project

1) To further characterise the exaggerated T-cell immune response in CVID by comparing the TCR sequences of dominant clonotypes, testing the specificity to the disease.

2) To investigate the relationship between B-cells and T-cells in CVID and test if T-cells play an inhibitory role upon the humoral immune system.

1.8.2 Summary

Using a combination approach of next generation sequencing and multi-parametric flow cytometry, unique hyperexpanded CVID TCR clonotypes were identified in this study but *no* sharing was found between patients. Instead, the reduction in naïve T-cells was highlighted as the most prominent T-cell finding in CVID. Parallel study showed that many CVID patients failed to generate adequate number of long-lived plasma cells, rendering an intrinsic B-cell differentiation defect regardless of the presence of T-cells. The combined failure in naïve B-cells and T-cells led us to a second hypothesis of an acquired defect in lymphogenesis. Using DNA methylation as a marker for pre-VDJ clonality, this study suggests that arrest in thymic output and B-cell failure in CVID were the results of clonal haematopoiesis, linking CVID more closely to other general acquired haematological disorders as opposed to the tradition dogma of a mixture of germline monogenetic mutations.

Chapter 2

2. Material and Methods:

2.1 Ethics

This study was conducted according to protocols approved by the South Birmingham Research Ethics Committee, National Research Ethics Service, UK (REC ref: 11/WM/0041) and was sponsored by the University of Birmingham (Reference: RG_10-260). Written consent was obtained by all participants in accordance with the Declaration of Helsinki.

2.2 Patients and healthy donors

56 patients with CVID were recruited by convenience sampling from the West Midlands Immunodeficiency centre, UK. 4 patients with specific polysaccharide antibody deficiency (SPAD) who were receiving immunoglobulin replacement therapy were recruited as disease controls. All patients were diagnosed according to the ESID-PAGID criteria. According to accepted criteria, CVID patients were classified into Group1 (infection only +/- bronchiectasis) and Group2 (polyclonal lymphoproliferation, chronic enteropathy, interstitial lung disease, autoimmunity or combinations of these) [248, 252, 264]. Healthy donors were recruited within the University of Birmingham as controls.

2.3 T-cell receptor repertoire assessment

2.3.1 Genomic DNA extraction

Genomic DNA of healthy donors and CVID patients were obtained by extraction from 2.5 x 10^6 PBMCs using ISOLATE II Genomic DNA Kit (Bioline) or DNeasy Blood & Tissue Kit (Qiagen) accordingly to their standard manufacturer's protocols.

2.3.2 Next-generation sequencing of TCRγ repertoire

Next generation sequencing for TCRγ was conducted using LymphoTrack™ TCRG assays (Invivoscribe). Amplification and purification of the TCRγ complementarity determining region 3 (CDR3) were performed according to the manufacturer's instruction. DNA samples were resuspended to 200ng/µl with molecular grade water. 5µl DNA was added to 45µl of the corresponding master mix, containing a set of Vγ forward primers and Jγ reverse primers that were already linked to a sequencing primer and a unique identifier barcode at the 5' end. 0.25µl of AmpliTaq Gold® DNA polymerase was added to the mixture before polymerase chain reaction (PCR): Step 1: 95 °C for 7 minutes; Step 2: 95 °C for 45 seconds; Step 3: 60 °C for 45 seconds; Step 4: 72 °C for 90 seconds; Step 5: Repeat steps 2, 3, 4; for a total of 26 cycles; Step 6: 72 °C for 10 minutes; Step 7: 15 °C 'forever. The PCR products were then purified using the Agencourt® AM Pure® XP PCR Purification system (Beckman Coulter, Inc.) according to the manufacturer's instructions. Quantification of amplicons, with an approximately molecular size of 300bp, was performed using the High sensitivity DNA ScreenTape assays (Agilent Technologies). Library preparation was then carried out by diluting the amplicons with 10 mMTris-HCl pH 8.0 + 0.05% Tween 20 to equal molar and then pooled together to form a 1nM pooled library.

Sequencing was performed on MiSeq desktop sequencer (illumina) using the MiSeq reagent kit (v2). The prepared 1nM pooled DNA library was denatured into single-stranded DNA by 0.2M of NaOH (1:1) for 5 minutes. The library was diluted to a final concentration of 8pM using the HT1 buffer (MiSeq regent kit v2) and then loaded into the reagent cartridge. The flow cell was cleaned with microfiber before it was finally inserted into the sequencer. Using the Illumina experiment manager software, MiSeq was set to perform sequence read under the following settings: 'TrueSeqLT', 'paired end reading' and '151 cycles' for each end. FastQ files were analysed using the LymphoTrack™ DeepSeq™ Analysis tool version 1.1.

2.3.3 Next-generation sequencing of TCRβ repertoire

TCRβ repertoires were assessed by the ClonoSIGHT™ platform as previously described as part of an international collaboration with Sequenta/Adaptive Biotechnologies, USA [19]. All raw anti-sense TCRβ sequences obtained were re-verified by the IMGT web-based bioinformatics tool (www.imgt.org), HighV-Quest, under the following settings: species = human; locus = TCRB; single individual, nucleotide per line in alignments = 60; aligned reference sequences = 5.

2.3.4 Calculating T-cell repertoire diversity

Repertoire diversity was calculated by either Shannon entropy (natural log: ln) ($H = -\Sigma\, p(x) \ln p(x)$; p(x)=frequency of individual clonotype) or Simpson's diversity index ($D = 1-\Sigma\, ni(ni-1)/N(N-1)$; N=total read count; ni=read count for individual clonotype) as previously described [280, 281]. Higher scores are generated for polyclonal samples while lower scores indicate clonality.

2.3.5 TCR next-generation sequencing data cross-referencing

To assess the assay reproducibility and accuracy as well as identifying shared CDR3 sequences between individuals, TCRγ or β sequence data were converted to CSV files and analysed on Microsoft excel. CDR3 sequences were cross-referenced between samples using the in-built "vlookup" function (fx=vlookup ("*"&[X]&"*", List[Y], [Z], False), where X = the excel cell containing the primary search sequence, Y = area of search, Z = column number in the area of search of the desirable output data). Additional search within the Adaptive Biotechnologies healthy donor database was carried out directly by our international collaborators at Seattle.

2.3.6 Multiple sequence alignment and phylogenetic association

To assess the amino acid sequence similarity of CDR3 regions, a list of selected CDR3 amino acid sequences were converted into FASTA format and then upload onto the European Bioinformatic Institute online multiple sequence alignment tool (Clustal omega, www.ebi.ac.uk). The data was further analysed on Seaview software (Version 4.5.4) for phylogenetic analysis (Parsimony).

2.4 Flow cytometry

2.4.1 T-cell immunophenotyping by multi-parametric flow cytometry

Whole blood staining protocol was used for peripheral blood T-cell immunophenotyping. 450µl of EDTA blood was labelled with 20µl of the corresponding IOTest® beta mark TCR V-beta antibodies-FITC/PE depending on the finding on TCRβ next-generation sequencing. Anti-CD3-PE.Cy5, anti-CD4-BV711, anti-CD8a-APC, anti-CD45RA-BV510, anti-CD27-BV605, anti-CD28-PE.Cy7, anti-

CCR7-PE.Cy5.5 and anti-CD25-APC.Cy7 antibodies were used in the same experiment (Biolegend). Antibodies were used in 1 in 100 dilutions and incubated at room temperature for 20 minutes in the dark. Cells were washed with isotonic phosphate buffer saline with 2% fetal calf serum (FCS) and incubated with 2ml of 0.16M of NH4CL at room temperature in the dark for 10 minutes for red cell. A final wash with PBS and 2% FCS was carried out and 0.5ml of 1% paraformaldehyde was added. CountBrightTM Absolute Counting Beads (Life Technologies) were added according to manufacturer's protocol for accurate cell counting. Compensation of the 10-color experiment was done using Anti-Mouse Ig, κ/Negative Control Compensation Particles Set (BD biosciences) and automatically calculated by BD FACSDiVa software version 6.0. Acquisition was done by BD LSR Fortessa flow-cytometer (BD bioscience) and analysed by Flowjo version 7.6.5 software. Naïve T-cells ($CCR7^{+}CD45RA^{+}CD28^{+}CD27^{+}$), central memory ($CCR7^{+}CD45RA^{-}CD28^{+}CD27^{+}$), effector memory ($CCR7^{-}CD45RA^{-}$) and terminally differentiated effector memory T-cells (TEMRA: $CCR7^{-}CD45RA^{+}$) are defined accordingly.

2.4.2 Plasma cell immunophenotyping by flow cytometry

Cultured B-cells that were harvested from the upper transwell chambers under the plasma cell generation protocol were washed with PBS with 2% FCS twice. The cells were labelled with anti-CD20-FITC (Biolegend), CD27-PE (Biolegend), CD138-APC (MI15, Biolegend) and CD38-APC.Cy7 (Biolegend) on ice for 30 minutes. A human myeloma cell line, U266, was used as positive control for CD38 and CD138 expression. An isotype control (MOPC-21, Biolegend) was use to optimise the gating for CD138. A final wash was performed before CountBrightTM Absolute Counting Bead (Life Technologies) were added for accurate cell count. Cell counts were calculated according to the manufacturer's instruction. 7-AAD (BD Pharmingen™) dead cell stain was added prior to acquisition to exclude dead cells in the analysis. All experiments were performed by BD Bioscience FACS Canto flow-cytometer and analysed by Flowjo version 7.6.5 software. An example of plasma cell gating strategy is shown in Figure 7.

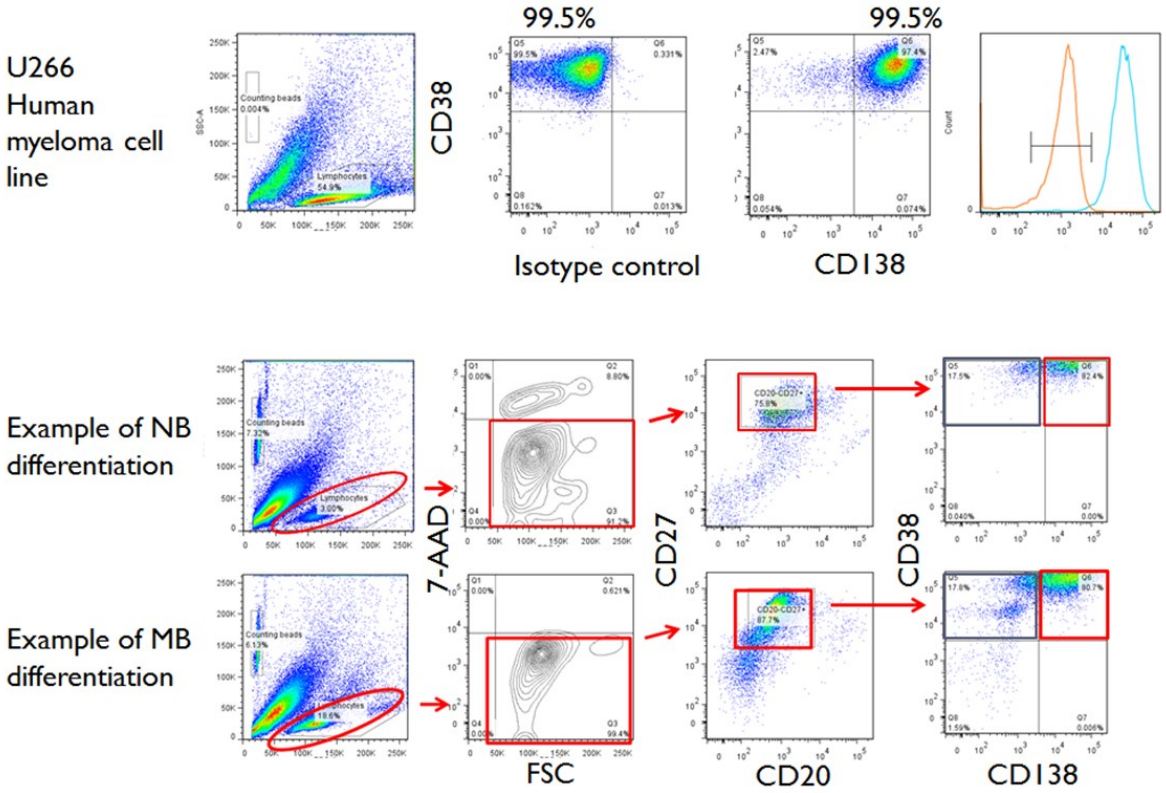

Figure 7. Gating strategy for long-lived plasma cells.

B-cells were separated into naïve B-cells ($CD27^-$) and memory B-cells ($CD27^+$) by magnetic beads and differentiated into long-lived plasma cell with the support of a murine bone marrow fibroblast cell line (M2-10B4). (Top panel) A U266 myeloma cell line was used to accurately determine positivity for CD138 expression. Clear differentiation between isotype control and MI15 anti-CD138 antibodies (99.5%) were demonstrated by histogram on the far right. (Middle panel) Example of naïve B-cell differentiation at Day 13 is shown. 7-AAD^+ dead cells were excluded. In the far right panel, short lived plasma cells were defined as $CD20^-CD27^+CD38^+CD138^-$ (blue box) whilst long-lived plasma cells were defined as $CD20^-CD27^+CD38^+CD138^+$ (red box). (Bottom panel) Example of memory B-cells differentiation is expressed in a similar fashion.

2.5 Plasma Cell culture

2.5.1 Naïve and memory B-cells separation

Peripheral blood mononuclear cells were prepared using standard density gradient centrifugation (Ficoll-Paque PLUS, GE Healthcare) and washed with PBS with 2% fetal calf serum (FCS). For the plasma cell generation experiment, naïve and memory B-cells were enriched by magnetic bead isolation (human Memory B cell Isolation Kit, Miltenyi Biotec) according to the manufacturer's instructions. All cells were washed with media or PBS twice before being used for downstream applications.

2.5.2 Cell-line maintenance

U266, human myeloma cell-line, were suspension cells maintained and grown in RPMI 1640 supplemented with 10% fetal calf serum (FCS) and 1% penicillin/streptomycin (P/S) (Sigma-Aldrich). 50% of medium was changed twice a week.

CD40L transfected L-cells (murine) were adherence cells grown in T75 culture flask (Corning) in Dulbecco's Modified Eagle's Medium (DMEM) (Sigma-Aldrich) supplemented with 10% FCS and 1% P/S. CD40L transfected L-cells were harvested by trypsin digestion and re-seeded (1:6 ratio) into a new flask every 3 days.

M2-10B4 murine bone marrow fibroblasts were also adherence cells grown in T75 culture flask (Corning) in Iscove's Modified Dulbecco's Media (IMEM) (Sigma-Aldrich) supplemented with 10% FCS and 1% P/S. M2-10B4 were harvested by trypsin digestion and reseeded (1:2 ratio) into a new flask every 3 days.

2.5.3 Plasma cell generation protocol

Plasma cells were generated using a protocol modified from Cocco *et al* [282].

Day 0-2: Naïve and memory B-cells were co-cultured separately with irradiated (100gy) CD40L transfected L-cells that had been adhered onto a 24-well plate 24 hours earlier. Cultures were grown in Iscove's Modified Dulbecco's Medium (IMDM) (Sigma-Aldrich) supplemented by 10µg/ml of affiniPure F(ab')2 fragment goat anti-human IgA + IgG + IgM (H + L) (Stratech), 50ng/ml of IL-21 (Affymetrix eBioscience), 20IU/ml of IL-2 (Proleukin ®), 10% FCS and 1% P/S for 72 hours at 37°C and 5% CO2.

Day 3-5: B-cells were then harvested away from CD40L stimulation and reseeded onto new wells in media (IMDM, 10% FCS, 1% P/S, 11µl/ml of HybridoMax (Gentaur), 5µl/ml of Lipid Mixture (Sigma-Aldrich) and 20µl/ml of MEM amino acids solution (Sigma-Aldrich) supplemented with 50ng/ml of IL-21 and 20IU of IL-2 and cultured for a further 72 hours.

Day 5: M2-10B4 murine fibroblast cell-line were irradiated (80gy) and pre-adhered to the bottom transwell chambers in IMDM supplemented with 10% FCS and 1% P/S at a concentration of 4.16 x 10^4cells/well.

Day 6: B-cells were harvested and reseeded onto the upper transwell chambers at 100,000 naïve or memory B-cells/well. The media was supplemented with 50ng/ml of IL-21, 10ng/ml of IL-6 (Biolegend) and 100IU of IFN-α (Roferon-A®).

Long term culture: The culture media were replaced every 3.5 days with IMDM with FCS, P/S, HybridoMax, Lipid Mixture and MEM amino acids solution supplemented with 50ng/ml of IL-21, 10ng/ml of IL-6 and 100IU of IFN-α onwards. IL-21 was withdrawn after Day 13. The upper chambers were transferred onto a new 24-well plate with freshly irradiated M210B4 on Day 24.

The upper transwell chambers were harvested at Day 13, Day 27 and Day 41 for flow cytometric analysis.

2.5.4 Sandwich ELISA for immunoglobulin output

Culture supernatant was collected from the bottom transwell chambers every 3.5 days when the media was being replaced. An in-house sandwich ELISA was designed to measure the IgM, IgA and IgG output of the cultures. Anti-human IgM antibodies (IgM AF6, Serascience), anti-human IgA antibodies (IgA MG4.156, Serascience) or anti-human IgG antibodies (IgG R10Z8E9, Serascience) were coated onto a NUNC plate (Thermo Scientific) overnight at 4°C in PBS (1μg/ml). The wells were washed with PBS with 0.05% tween 4 times and PBS twice and then blocked with PBS with 10% FCS for 1 hour at room temperature. The wells were washed as before and incubated with serial dilutions of a standard serum, with known IgM, IgA and IgG concentrations, or culture supernatant (1/100 dilution in PBS with 10% FCS) for 2 hours at room temperature. Following another wash, 1/4000 of HRP-conjugated mouse anti-human kappa (SouthernBiotech) plus 1/4000 of HRP-conjugated mouse anti-human lambda (SouthernBiotech) in PBS with 10% FCS were added to the wells and incubated for 1 hour at room temperature. A final washing step was done before 100μl of 1-step Ultra TMB substrate (Thermofisher) were added to the wells followed by 50μl of 10% hydrochloric acid to stop the reaction. Light absorbance was measured using GloMax 96-microplate luminometer. The amounts of immunoglobulins were determined according to the standard curve

2.5.5 Plasma cell gene expression assay

Total RNA was extracted from differentiated memory B-cells at Day 13 using the PureLink® RNA mini extraction kit (Life Technologies) according to the manufacturer's protocol. Total RNA was then converted to cDNA using the high-capacity RNA-to-cDNA™ kit (Applied Biosytstems®). Relative gene expressions were measured using TaqMan® gene expression assay (*BLIMP-*

1:Hs00153357_m1, *XBP1*: Hs00231936_m1, *IRF4*:Hs01056533_m1, *PAX5*: Hs00277134_m1 and *BCL6*: Hs00153368_m1). The expression averages of *beta-actin (ACTB)* (Hs01060665_g1) and *GAPDH* (Hs02758991_g1) were used as endogenous controls while Day 0 naïve B-cells of the same individuals were used as undifferentiated controls. All probes selected were designed to span the exons to minimise genomic DNA amplification. A final reaction mixture of 20µl was prepared; 1µl of Taqman® probes, 5µl of TaqMan® Gene Expression Master Mix (Applied Biosytstems®) and 30ng of cDNA in nuclease-free water. Nuclease-free water was used a non-template control for the experiment. Relative fluorescent intensity was measured using 7900HT Fast Real-Time PCR System (Applied Biosytstems®). The data was analysed on SDS manager version 2.4 software where CTs were determined when fluorescent intensity exceeded the threshold. Relative gene expressions were calculated by correcting to the endogenous and undifferentiated controls; $\Delta\Delta CT$ = (CT (target, untreated) - CT (ref, untreated)) - (CT (target, treated) - CT (ref, treated), Ratio = $2^{\Delta\Delta CT}$.

2.6 Pre-VDJ clonality assessment

2.6.1 Buccal sampling

Donors were asked to restrict from any oral intake for 1 hour prior to sampling. 20mls of distilled water were used to rinse off any residual food immediately before sampling. Donors were asked to take 10mls of sterile saline into their oral cavity and rub their tongues around the inside of their cheeks lightly for about 60 seconds to encourage dislodgement of the surface epithelial layer without causing any trauma. The fluid is then recollected into a sterile universal tube. Cells were spun down and washed with PBS twice before genomic DNA extraction.

2.6.2 Leukocyte subset isolation

PBMCs were prepared as previous described. Granulocytes were prepared by aspirating the layer immediately above the red blood cells following density gradient centrifugation of whole blood. Excess red cells were lysed by incubating in 0.16M ammonium chloride (NH4CL) for 10 minutes to purify the granulocytes collection. Granulocytes were washed with sterile PBS twice before genomic DNA extraction. PBMCs were then enriched in to naïve and memory B-cells using EasySepTM Human Memory B Cell (Stem cell technologies) or fluorescence-activated analysis sorting. Fluorescence-activated sorting was done by labelling PBMCs with anti-CD3 APC.Cy7 antibodies (clone SK7, Biolegend), anti-CD20 PerCP antibodies (clone SH7, Biolegend), anti-CD27 Pacific blue antibodies (clone MT-271, Biolegend), anti-CD45 PE antibodies (clone HI30, Biolegend) at a concentration of 1/100 dilution in PBS with 2% FCS and 2mM of EDTA for 20 minutes at 4°C. Cells were washed with the same buffer and prepared for FACsorting (MoFlo® Astrios™, Beckman Coulter Inc.). Lymphocytes that were $CD45^{+}CD3^{-}CD20^{+}CD27^{-}$ were collected as naïve B-cells and lymphocytes that were $CD45^{+}CD3^{-}CD20^{+}CD27^{+}$ were collected as memory B-cells.

2.6.3 Assessing X-inactivation by HUMARA assay:

Genomic DNA of healthy donors and CVID patients were extracted from buccal tissue, whole blood, PBMCs, granulocytes, enriched naïve B-cells and memory B-cells using PureLink® Genomic DNA Kits (Life Technologies) accordingly to their standard manufacturer's protocol.

Restriction enzyme digestion: Undigested DNA (Reaction A) and restriction enzyme digested DNA (Reaction B) was prepared from each individual. Reaction A contained 50ng of genomic DNA, 2µl of Buffer A (Promega), 0.2µl of acetylated BSA (Promega) and nuclease-free water to a final volume of 20µl. Reaction B contained 50ng of genomic DNA, 0.5µl of HpaII restriction enzyme (Promega), 2µl of Buffer A (Promega), 0.2µl of acetylated BSA (Promega) and molecular grade water

to a final volume of 20µl. The reactions were incubated in a thermocycler at 37°C for 2 hours to destroy the unmethylated AR allele.

PCR amplification of human androgen receptor (AR) gene: PCR were performed using the AccuPrime™ Taq DNA Polymerase High Fidelity kit (Invitrogen) as follows: 5µl of each digested or undigested DNA, 5µl of 10X AccuPrime™ PCR Buffer II, 0.2µl of AccuPrime™ Taq High Fidelity, 37.8µl of molecular grade water, 1µl of 10 µmol/l of FAM-labelled forward primer (AR-F: FAM 5′ TCC AGA ATC TGT TCC AGA GCG TGC 3′) and 1µl of 10 µmol/l of reversed primer (AR-R: 5′ GCT GTG AAG GTT GCT GTT CCT CAT 3′). PCR was set as follows: step 1: 94 °C for 30 seconds, step 2: 94 °C for 30 seconds, step 3: 56 °C for 30 seconds, step 4: 68 °C for 60 seconds, step 5: Repeat steps 2, 3, 4; for a total of 34 cycles, step 6: 4 °C forever.

Capillary reaction: Following PCR, reactions were diluted in 1:50 in molecular grade water. In a 96-well PCR plate, 1µl of the diluted reaction was added to a mixture containing 8.5µl of Hi-Di formamide and 0.5µl of GeneScan™ 600 LIZ® dye Size Standard v2.0 (Life Technologies). The plate was then sealed with an adhesive film. The PCR products were denatured by a further cycle of 95°C for 5 minute. The plate was then placed on ice until being analysed by an ABI 3730 DNA analyser (Applied Biosystems). The data were analysed on Gene Mapper version 4.0. X-chromosome skewing was estimated as previously described [283]. Germline corrected ratio was calculated by dividing X-skewing of lymphocyte subset by X-skewing of buccal tissue.

2.7 Analyses and Statistical tests

Statistical analyses were performed using GraphPad Prism version 5.0. and comparisons between non-parametric data sets were done using the 2-tailed Mann-Whitney U test. Multiple linear regression

and Kruskal-Wallis test were done using IBM SPSS statistic 21. 2-way ANOVA was used when multiple groups were analysed. P-values of <0.05 (*), <0.01 (**) and <0.001 (***) were considered to be statistical significant.

Chapter 3

3. T-cell receptor characterisation in Common Variable Immunodeficiency.

In Chapter 1, we discussed how T-cells might limit the full potential of the humoral immune response. Previous studies suggest the presence of a specific exaggerated T-cell immune response in CVID although the antigenic targets of these T-cells are not known. Proliferation of T-cells is a hallmark of the cellular immune response, generating progenies to exert *their* effector functions, as well as establishing memory [284]. Hence, the size of a T-cell clone may be used as a surrogate marker for the magnitude or chronicity of an immune response.

3.1 Next generation sequencing of T-cell receptors

3.1.1 Immune repertoire assessment by CDR3

During T-cell development, the process of VDJ rearrangement grants each T-cell its unique complementarity determining region 3 (CDR3) on each of the T-cell receptor chains (alpha and beta). Coupling the vast permutation of available V, D and J gene segments with nucleotide editing during the joining of each segments, the immune repertoire has enormous potential for diversity. Immune diversity is further enhanced by the combination of an α-chain and a β-chain to form the final TCR for antigen recognition [285]. In human, pairing of the αβ chains could theoretically lead to 10^{15} different TCR receptors, although the full potential of the TCR repertoire is likely to be limited by the process

of central tolerance and convergent recombination [286, 287]. Deep sequencing approach currently estimates the human αβ TCR repertoire to be around 10^7 [285].

Given the uniqueness of the CDR3 region on each T-cell, it has been used as a molecular signature to dictate and track clonal proliferation. T-cells carrying identical CDR3s are defined as a "clonotype" [288]. Furthermore, the CDR3 region represents the most important peptide binding site for a TCR while other regions such as CDR1 and CDR2 predominantly make contacts with the MHC molecule [289]. Hence, the CDR3 region could potentially narrow done the putative antigenic targets of a T-cell; developing areas which warrant further investigations [290, 291].

The evaluation of the immune repertoire was previously carried out by assessing the lengths of the CDR3 sequences using PCR-based method such as spectratyping or capillary reaction [292]. Using a set of V-forward and J-reverse primers, millions of CDR3 genes can be amplified and visualised on a gel or a spectrophotometer. While V families of a normal immune repertoire have a Gaussian distribution in CDR3 length, immune dysregulation or expansion of large T-cell clonotypes may disrupt this pattern showing abnormal clonal or oligoclonal peaks (Figure 8A). Such techniques offer a global view of the immune repertoire but are unable to provide any detailed information. Inherently, large peaks may compose of multiple clonotypes and falsely identified as a clonal population (Figure 8B).

In recent years, the use of next generation sequencing has gained popularity in assessing the immune repertoire. Instead of measuring the length of the CDR3 regions, unprecedented level information can be obtained by massive parallel sequencing of the amplicons, allowing researchers to access information regarding the frequencies and actual DNA sequences for millions of clonotypes simultaneously [293]. Supported by open-sourced bioinformatics, for example the IMGT webtool, further information such as the V/D/J gene segment usage, amino acid composition, frequency of nucleotide insertion and deletion as well as repertoire diversity could be derived [294]. (Example data is shown in Figure 9). Although, there is ongoing debate regarding the accuracy of these high throughput data, such as amplicon PCR bias and sequencing error, deep TCR sequencing represents a

major technical advance in immune repertoire research [295]. By synthetically generating a known TCRγ library, Carlson et al showed that it was possible to correct amplification biases computationally and allowing the data to more accurately represent the immune repertoire of the sample. However, this information is not yet available for the TCRβ repertoire [296]. Nevertheless, deep TCR sequencing has proven its worth and usefulness in the field of basic science, autoimmune and cancer researches [297-299].

Therefore, deep TCR sequencing provides us with the opportunity to re-characterise the immune repertoires of CVID patients in greater details and identify expanded dominant T-cell clonotypes which might play an inhibitory role on the humoral immune system. This chapter will examine the precision of deep TCR sequencing, search for disease specific hyperexpanded T-cell clonotypes and attempt to elucidate their role in the pathophysiology in CVID.

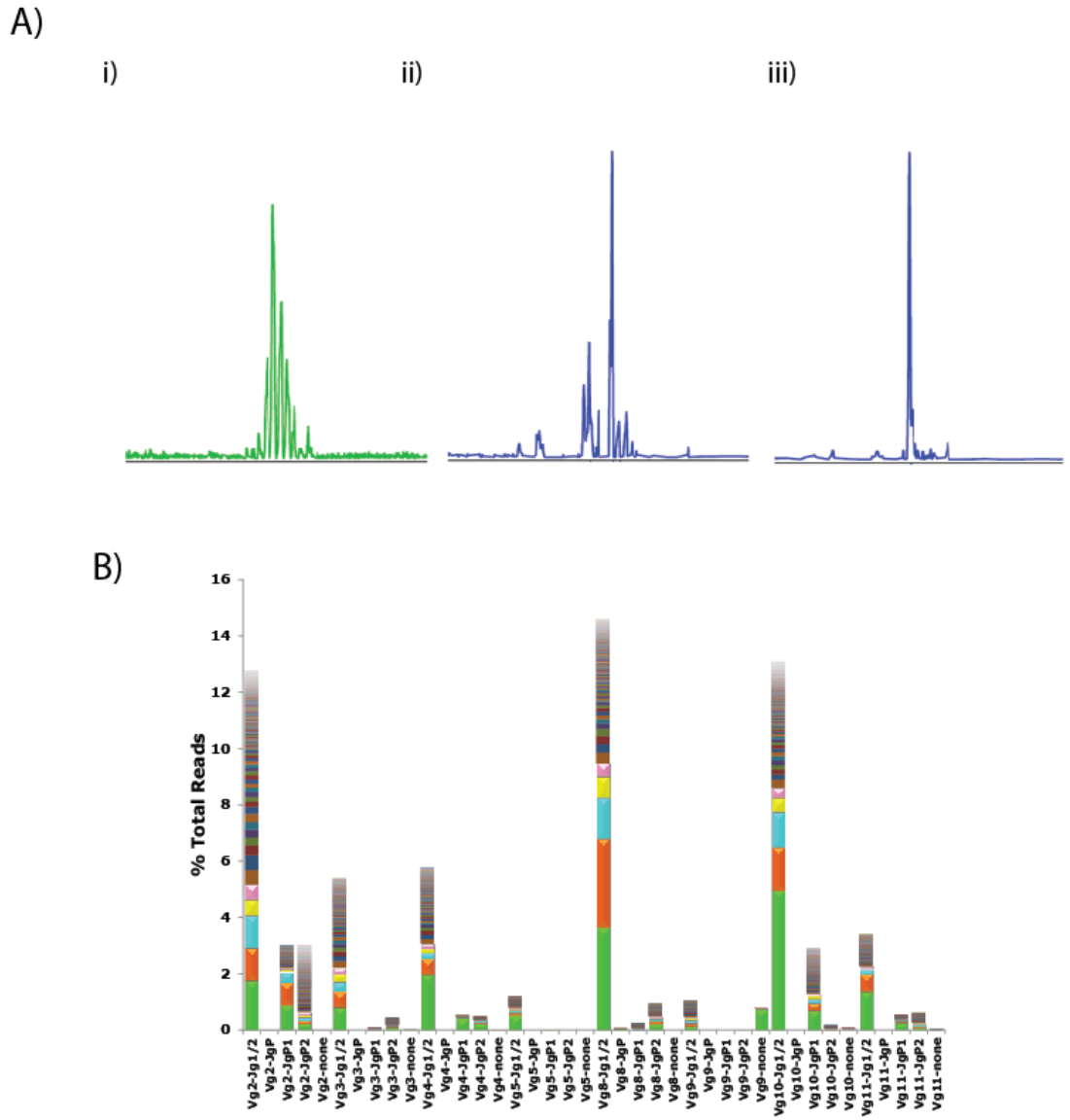

Figure 8. Examples PCR-based CDR3 assay.

(A) Fluorescent PCR-based technique by capillary reaction (GeneScan) provides qualitative assessment of immune repertoire. Example of a polyclonal sample with near perfect Gaussian distribution (i), an oligoclonal sample with distinct peaks disrupting the repertoire (ii) and a clonal sample (iii) are shown. (B) Deep sequencing of the TCRγ repertoire provides detailed qualitative and quantitative assessment of immune repertoire. V-family usage and clonotype frequency are additionally available. An example of an oligoclonal sample reveals that large peaks may compose of multiple small clonotypes.

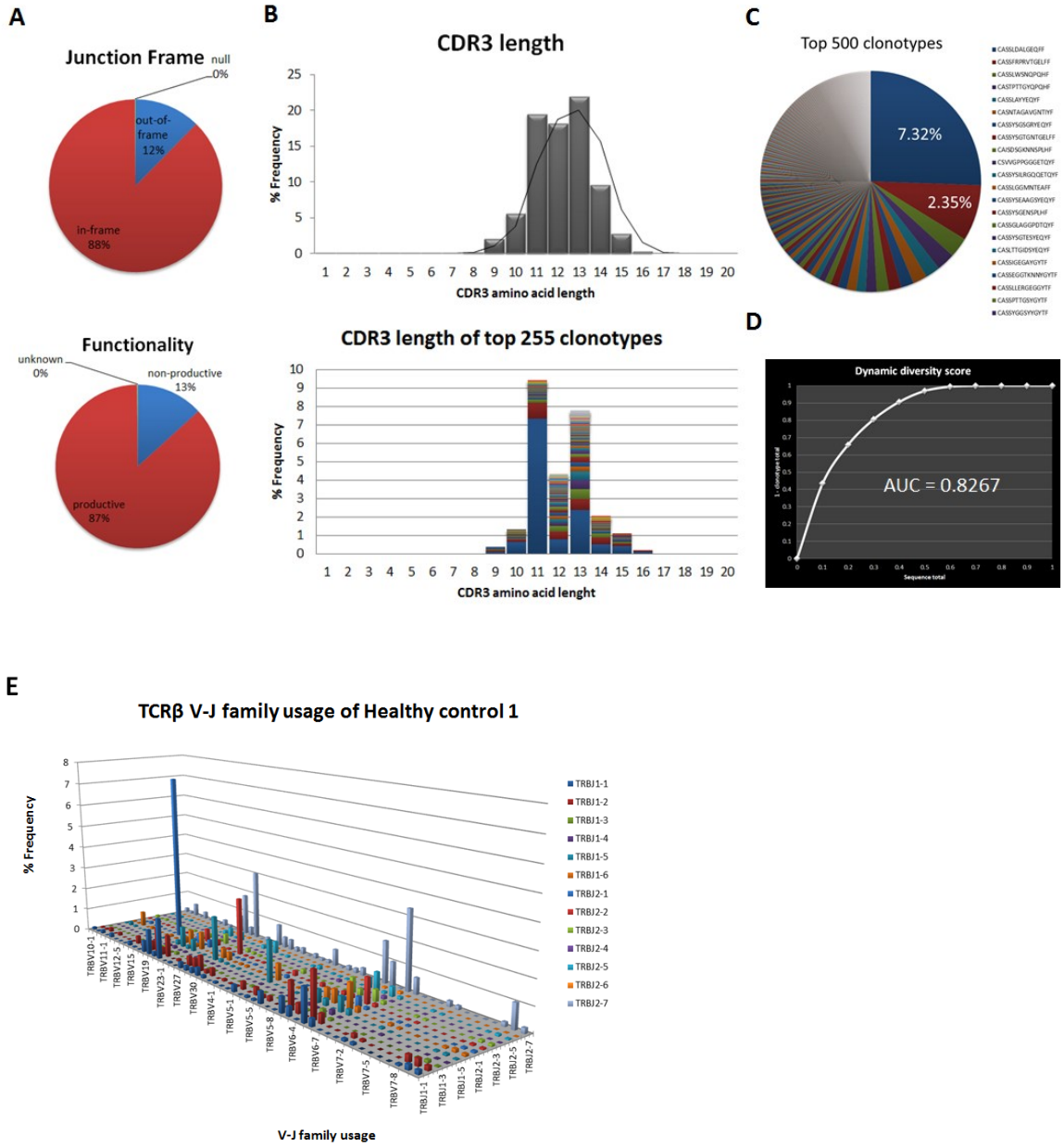

Figure 9. Example of deep TCRβ sequencing.

Deep TCRβ sequencing was carried out on genomic DNA extracted from peripheral blood of a healthy donor, generating a total of 5,944,046 DNA reads. Of all DNA reads, 245,833 DNA clonotypes and 194,048 amino acid clonotypes were identified (A) The relative frequencies of in-frame versus out-of-frame sequences (top) and productive versus non-productive sequences (bottom) are shown. (B) CDR3 length of all clonotypes demonstrated a Gaussian distribution (top) but larger clonotypes were less evenly distributed (bottom). (C) Of 194048 amino acid clonotypes identified, the top 500 clonotypes are expressed in a pie char. (D) Repertoire diversity was calculated by the area under the curve (1 – cumulative clonotype frequency against the 1 – cumulative sequence frequency). (E) The relative frequency of V and J gene usage is shown.

3.1.2 Precision and reproducibility of deep TCR sequencing

To test if deep TCR sequencing was a suitable tool to screen for expanded T-cell clonotypes in CVID, a validation experiment was conducted. Given the relative simplicity of the TCRγ repertoire in comparison to the TCRβ repertoire as it lacks nucleotide editing and has less V and J gene segments and no D segments, deep sequencing using the LymphoTrack^{TM} TRG assay was first carried out. Genomic DNA of a patient with a known T-cell acute lymphoblastic leukaemia (clonal) and a healthy donor (polyclonal) was tested in duplicates. Samples were sequenced to a depth of 1.5 to 3x10^6 reads. Both polyclonal and clonal samples demonstrated excellent precision. Using the Run 1 as the baseline, all clonotypes of >0.0625% were re-detectable on Run 2. However, re-detection of smaller clonotypes of less than 0.015% was less likely especially in the polyclonal sample (Figure 10, A and B). The frequencies of individual clonotypes were also reproducible with the best result achieved with larger clonotypes (Figure 10, C and D). Hence, the data suggests that a high level of precision can be achieved by deep sequencing of the TCRγ repertoire.

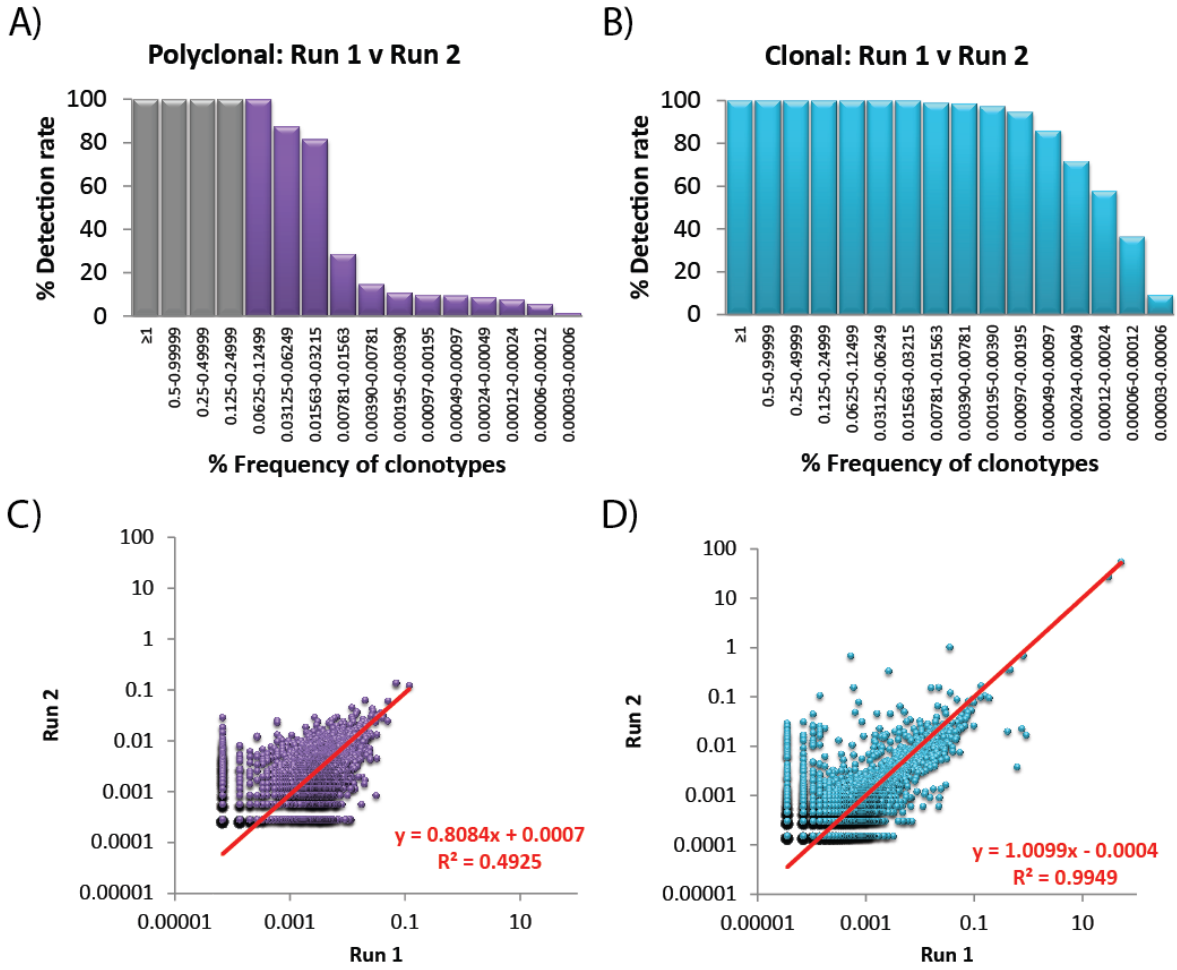

Figure 10. Precision of TCRγ repertoire sequencing.

TCRγ sequencing of a clonal and a polyclonal samples were conducted in duplicate using the LymphTrack™ assay and results from Run 1 and Run 2 compared. (A-B) The cumulative detection rates of clonotypes of various sizes are shown (Purple = polyclonal, Turquoise = clonal). (C-D) Clonotype size concordance for those that could be detected on repeat runs are shown with each individual data point represents a unique clonotype (left; polyclonal; n = 3426, right; clonal; n = 5620). The X and Y axes represent % frequency (size) of a clonotype.

Given the excellent results demonstrated by TCRγ sequencing, a similar experiment was conducted for the TCRβ repertoire. Data were generated by the ClonoSIGHT™ assay (Sequenta Inc) as described in the method section. Although reproducibility was slightly inferior to the TCRγ experiment, a similar pattern was seen with the result of TCRβ sequencing (Figure 11). This is however expected given the greater permutation of V/D/J gene segments with the additional complication of nucleotide editing in the TCRβ repertoire, deriving much greater natural diversity. For both TCRγ and TCRβ repertoires, accuracy could not be examined in the absence of a gold standard. Nevertheless, the data indicate that deep sequencing technology can deliver reasonably precise results with minimum sequencing errors for clonotypes greater than 0.01%.

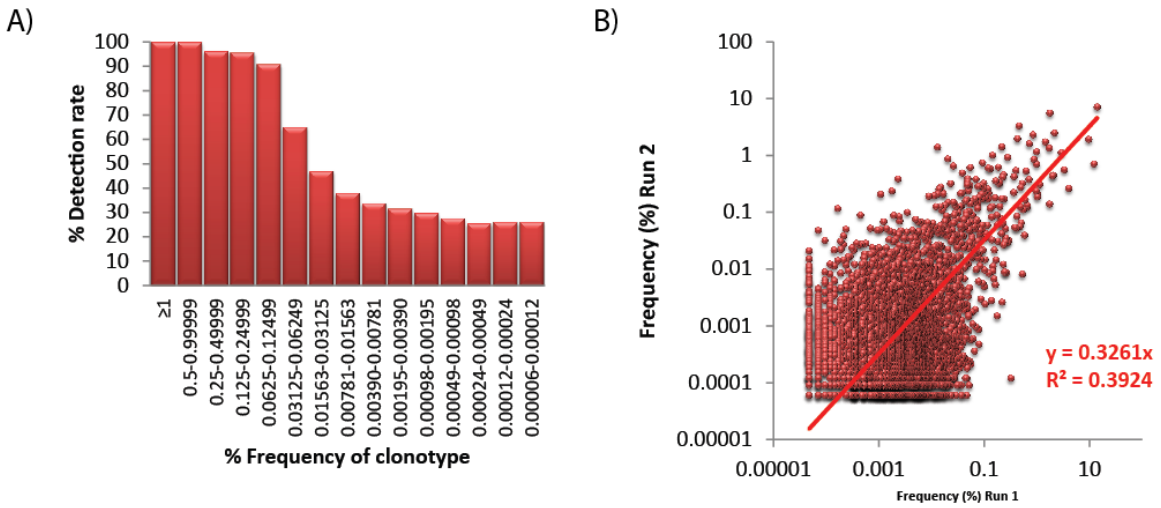

Figure 11. Precision of TCRβ sequencing.

ClonoSIGHT™ assay was performed on a polyclonal sample in duplicate. Data were cross-referenced to determine the re-detection rate. (A) The cumulative detection rates of clonotypes of various sizes are shown. (B) Clonotype size concordance are shown with each individual data point represents a unique clonotype (n = 4369).

3.1.3 Mathematical model for repertoire diversity

A number of diversity indices have been used to calculate immune repertoire diversity. These indices measure the degree of evenness of a given sample, according to the "information theory". For immune repertoire, a polyclonal sample is considered to be relatively even and by contrast, a clonal sample will exhibit a significant degree of bias. Of all, Shannon Entropy (SE) and Simpson's diversity index (SDI) were most frequently employed, mostly due to their relative simplicity and user friendliness. Comparison studies in ecology have shown good agreement between both indices although the Simpson's diversity index tends to weight heavier toward dominant species within the population, increasing its sensitivity for clonality [300]. To understand the utility of these mathematical models, we compared the TCRβ repertoire diversity score of 57 samples (15 healthy controls and 42 CVID) derived from both SE and SDI. Consistent with published reports, our data showed a direct relationship between SE and SDI when used in calculating DNA clonotype diversity (r^2 = 0.7252) with improved correlation if only amino acid clonotypes of >0.01% were considered (Figure 12, A and B). This improvement in correlation suggests that SDI will tend to represent diversity of larger clonotypes while small background clonotypes may be ignored.

Equation for Shannon Entropy and Simpson's diversity index are listed below:

Shannon entropy (natural log: ln)

$$H = -\Sigma\, p(x) \ln p(x)$$

(p(x) =frequency of individual clonotype)

Simpson's diversity index

$$D = 1-\Sigma\, n_i(n_i-1)/N(N-1)$$

(N=total read count; n_i=read count for individual clonotype)

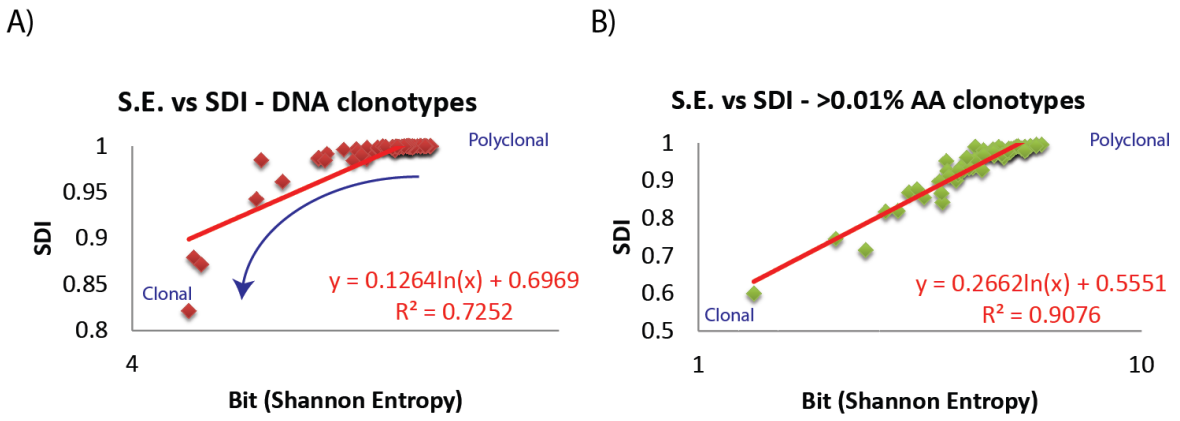

Figure 12. Immune repertoire diversity by Shannon Entropy (SE) and Simpson's diversity index (SDI).

SE and SDI score of 15 healthy and 42 CVID TCRβ repertoires were compared. (A) Log (SE) v linear (SDI) are shown. Polyclonal samples are located at the top right corner, while more clonal samples are located at the bottom left corner. The blue curved arrow indicates that clonality is greater emphasised by SDI than SE. (B) Only amino acid clonotypes of >0.01% were considered in the calculation. Solid red lines represent the best fit lines with their equations and r^2 values depicted adjacently.

3.2 Immune repertoire assessment of Common Variable Immundeficiency

3.2.1 TCRγ and TCRβ repertoire restriction secondary to the loss of small background clonotypes in CVID.

To characterise the immune repertoire of CVID patients, repertoire diversity was calculated using the mathematical models described in 3.1.3. Given that both αβ and γδ T-cells contribute to the immune repertoire, next-generation sequencing of the TCRγ and TCRβ repertoires were carried out.

Read depths of 1.5 to 3 x 10^6 reads for TCRγ sequencing and 2.5 to 3 x 10^6 reads for TCRβ sequencing were achieved. CVID patients were subdivided into Group1 (infection only +/- bronchiectasis) and Group2 (polyclonal lymphoproliferation, chronic enteropathy, interstitial lung disease, autoimmunity or combinations of these) [248, 264].

The data showed that TCRγ diversity was lower in CVID patients, but statistical significance was not observed (median SE: HC=10.8 vs CVID=10.1 vs Group1=10.4 vs Group2=9.9) and similar pattern was seen in the TCRβ repertoire (median SE: HC=11.0 vs CVID=10.8 vs Group1=11.1 vs Group2=10.5). Interestingly, repertoire diversity did not differ when only amino acid clonotypes of >0.1% (prominent immune response) were considered or when SDI, which weigh more heavily on dominant species, were calculated (Figure 13A). To correct the potential confounding effect of age-related repertoire restriction, TCRβ repertoire diversity by Shannon Entropy was examined against the age of the individuals. Reduction in repertoire diversity in CVID was noted to occur across all ages with a subgroup of patients skewing the overall picture (Figure 13B).

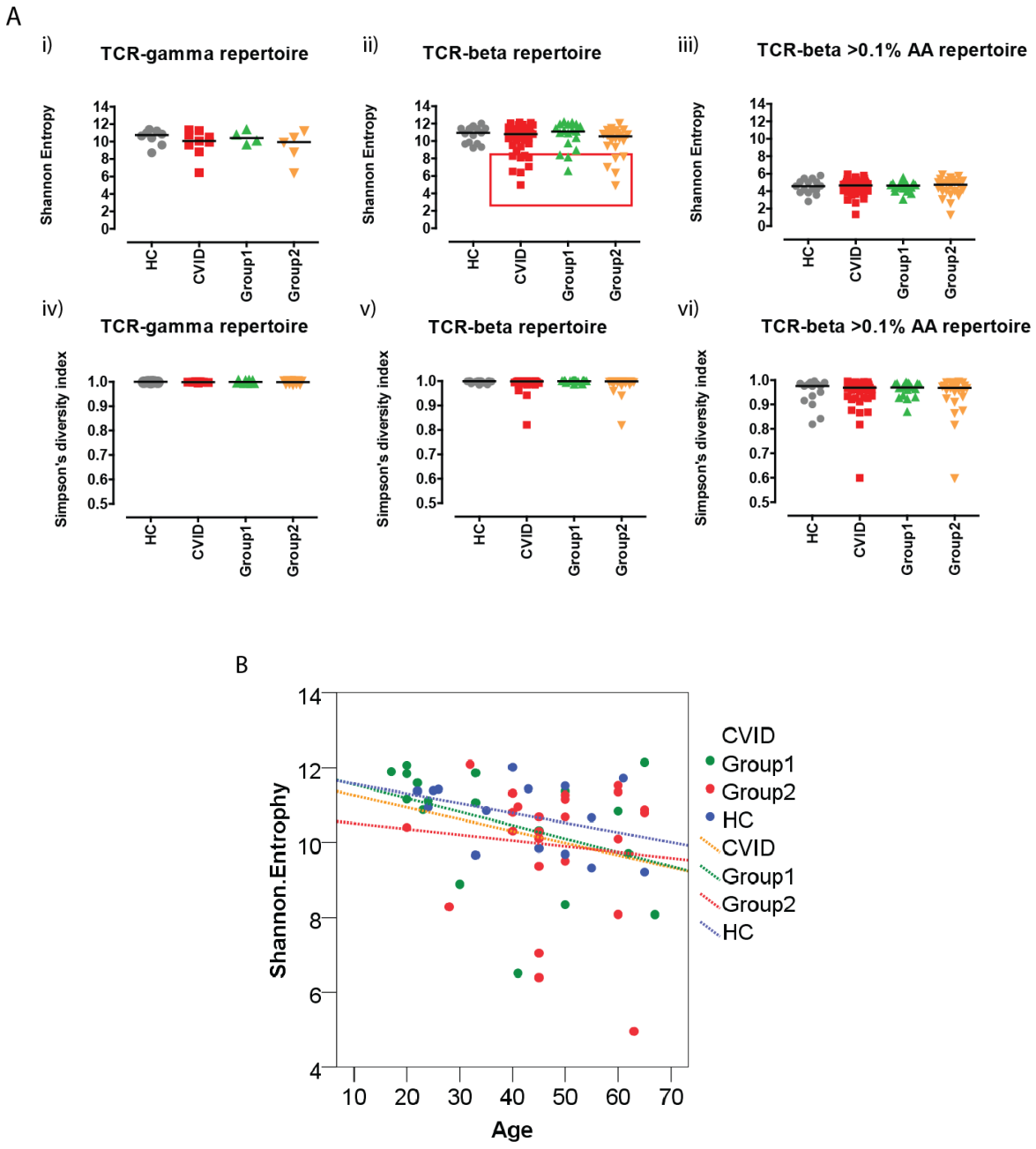

Figure 13. Assessment of repertoire diversity by deep TCRγ and TCRβ sequencing.

(A) TCRγ and TCRβ repertoire diversities of healthy donors (n=15, grey), CVID patients (n=42, red), Group1 patients (n=18, green) and Group2 patients (n=24, orange) were calculated using Shannon Entropy (i-iii) or Simpson's diversity index (iv-vi). All DNA clonotypes were considered in Ai, ii, iv & v but only in-frame and productive amino acid (AA) clonotypes of >0.1% were used in the calculation in (iii) & (vi). Medians are shown. (B) Shannon Entropy score against age (dotted lines represent the best fit lines for each group). Statistical differences are highlighted by *, ** or ***.

To further dissect the origin of this subtle reduction in repertoire diversity, the counts and frequencies of hyperexpanded, large, medium and small background clonotypes of each individuals were compared. The size definitions of clonotypes are listed in Table 3. The data revealed that the differences in repertoire diversity were predominantly secondary to the numerical reduction of small background clonotypes (<0.001%) in CVID patients (Figure 14A) while numerical counts and overall occupancies of medium to hyperexpanded clonotypes were unaffected (Figure 14B). The normality of the medium (0.001-0.01%), large (0.01-1%) and hyper-expanded (>1%) compartments suggest that the reduction of small background clonotypes as the source of the difference. Hence, the data indicate that the magnitude of established immune responses were relatively unaffected in CVID patients while the reduction of small background clonotypes was the major driver for reducing repertoire diversity. Contrary to the original hypothesis, the presence of an exaggerated T-cell immune response in CVID disrupting the function of the humoral immune system is not supported.

	% of immune repertoire	**T-cell ratio**
Hyperexpanded clonotypes	>1%	>1 in 100 T-cell
Large clonotypes	0.01 - 1%	1 in 100 -10000 T-cell
Medium clonotypes	0.0001 – 0.0099%	1 in 10000 - 100000 T-cell
Small clonotypes	<0.0001%	<1 in 100000 T-cell

Table 3. Size definition of Vβ clonotypes.

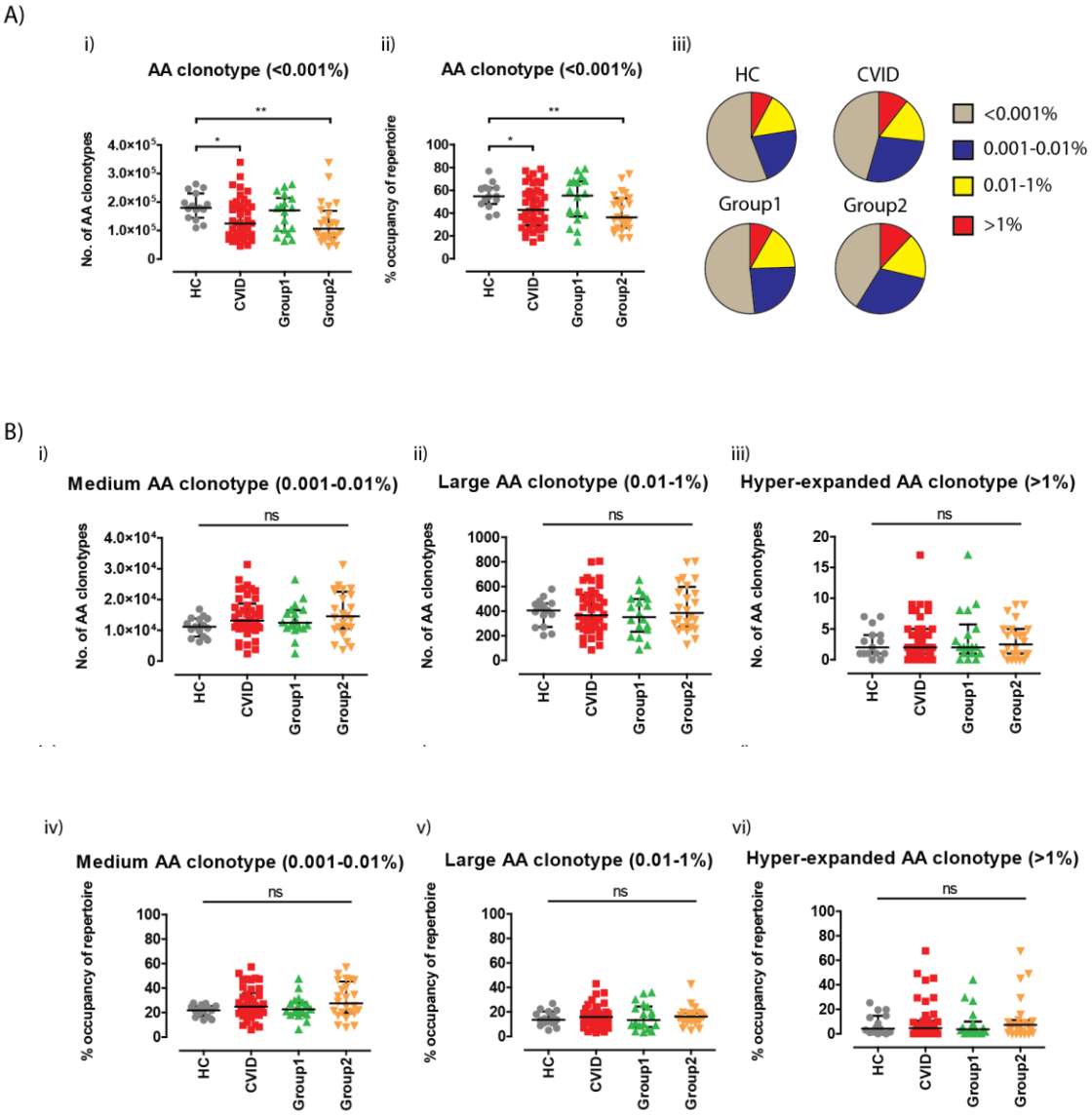

Figure 14. Numerical counts and the relative occupancies of small, medium, large and hyper-expanded clonotypes.

Amino acid clonotypes of each repertoire were further separated into various size groups according to Table 3. (A) Small background clonotypes (<0.001%) of healthy donors: n=15, grey; CVIDs: n=42, red; Group1 patients: n=18, green; and Group2 patients: n=24, orange are shown in (i) & (ii). The average size proportions of clonotypes of each group are shown by the pie charts (iii). (B) The numerical counts and % occupancy of the repertoire of medium (0.001-0.01%), large (0.01-1%) and hyper-expanded (>1%) AA clonotypes are shown. Medians and interquartile ranges are depicted. Statistical differences are highlighted by *, ** or ***.

3.2.2 Both background and established clonotypes in CVID exhibit characteristics of normal TCR synthesis.

Next, we compared the various parameters of the TCR sequences of small background (<0.001%) and established (>0.1%) clonotypes as qualitative markers for VDJ rearrangement. Genomic DNA often contains more than one copy of β-chain CDR3 genes as T-cells may go through multiple rounds of VDJ rearrangement before a successful TCR could be synthesised. The data showed that small clonotypes (<0.001%) in healthy controls were composed of approximately 85% in-frame, productive sequences while a smaller fraction (15%) was made up of out-of-frame and unproductive sequences. Similar proportions of in-frame, productive sequences were reflected in the other established clonotypes groups, indicating they were unbiasedly selected from the small clonotype pool. A similar pattern was observed in CVID patients (Figure 15A). In both healthy donors and CVID patients, the CDR3 lengths of small clonotypes demonstrated an expected Gaussian distribution, peaking at 13 amino acids in length. The CDR3 lengths of larger and established clonotypes were also equivocal between healthy donors and CVID patients (Figure 15B).

In contrast to previous studies, major differences in V-gene usage were not observed between healthy donors and CVID patients. Certain V-families were more likely to be selected into the established clonotype pool but this process was not significantly altered in CVID patients (Figure 16). Collectively, the data show that small clonotypes within a certain V-family are equally likely to be selected into the large clonotype pool, suggesting the programme required for a normal T-cell response is intact in CVID.

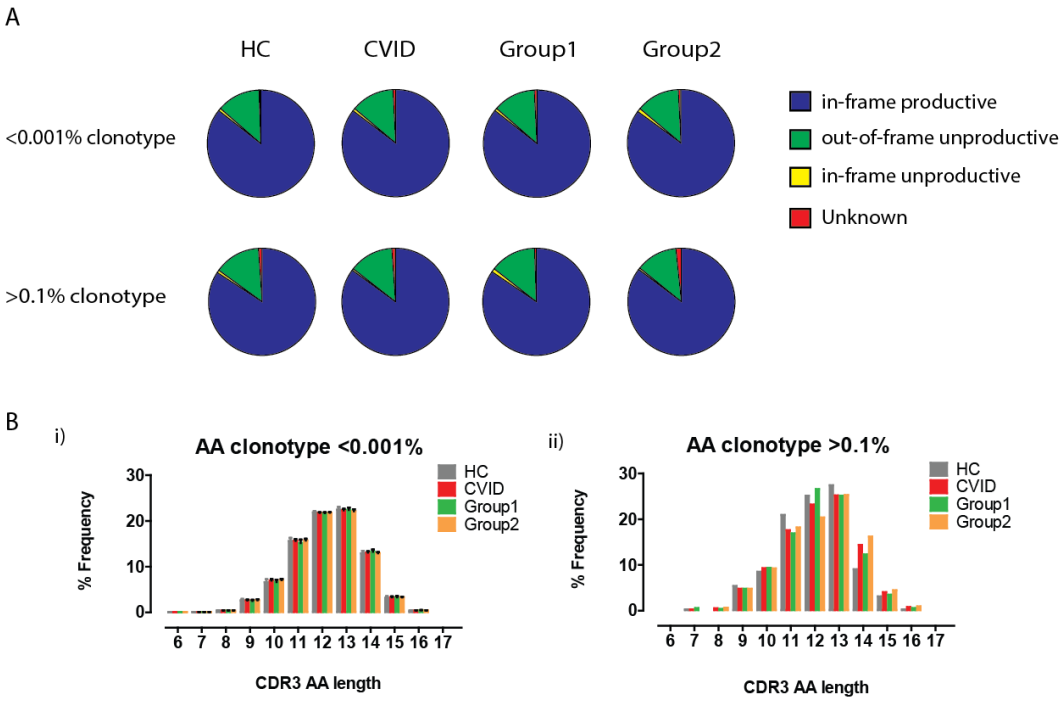

Figure 15. Analysis of in-frame productive sequences and CDR3 length in TCRβ repertoire.

Comparison between small background clonotypes (<0.001%) and more established clonotypes (>0.001%, >0.01%, and >0.1%) were made. Established clonotypes of all three cut-offs demonstrated identical results and data of >0.1% clonotypes are used here as an example. (A) The average proportion of in-frame productive (blue), in-frame unproductive (yellow), out-of-frame (green) and unknown (red) sequences of background (<0.001%) and established (>0.1%) clonotypes of healthy donors (n=15), CVIDs (n=42), Group1 patients (n=18) and Group2 patients (n=24) are shown. (B) The frequencies of CDR3 amino acid length are shown. No statistical differences were noted in (A) and (B).

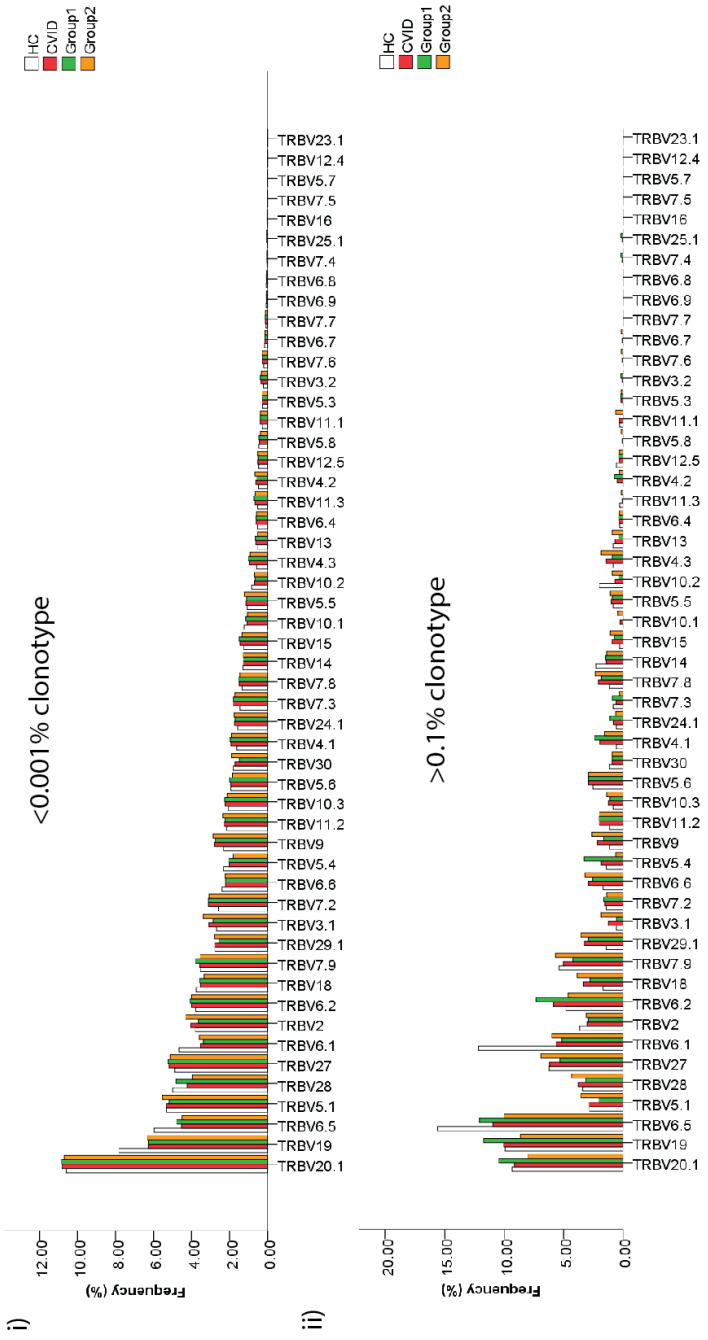

Figure 16. Analysis of in-frame V-gene usage in TCRβ repertoire.

The frequencies of V gene usage are shown. The left panel (i) represents clonotypes of <0.001% while an example of established clonotypes (>0.1%) is shown on the right panel (ii). No statistical differences were noted.

3.2.3 Clonotype sequence analysis suggests non-specific immune dysregulation driving clinical complications in CVID.

Although the magnitude and general properties of established T-cell clonotypes in CVID were normal, a search for disease specific clonotypes was conducted to further test the original hypothesis. Cross-referencing of >0.01% clonotypes of all individuals were performed to identify shared CDR3 sequences; a cut-off that was selected given the excellent reproducibility shown during the validation exercise (3.1.2). Across all 57 individuals, 437 shared clonotypes were identified. 209/437 clonotypes were shared between healthy donors and CVID patients; 33 (2.2/individual) were unique to healthy donors and 195 were unique to CVID patients. Of those 195 CVID unique clonotypes, 96 were shared between both Group1 and Group2 patients, 31 (1.72/individual) were unique to Group1 and 68 (2.83/individual) were unique to Group2 patients (Figure 17A). The frequencies of unique clonotypes within each group were proportional to the sizes of the groups, although Group2 patients exhibited a slightly higher expected number of unique clonotypes (Figure 17B). Amino acid analysis of CDR3 sequences using Weblogo version 2.8.2 demonstrated a huge variety of sequences within groups, although a glycine is more likely to locate in the centre of the CDR3 region for CVID patients (Figure 17C). All shared unique clonotypes are listed in Table 4.

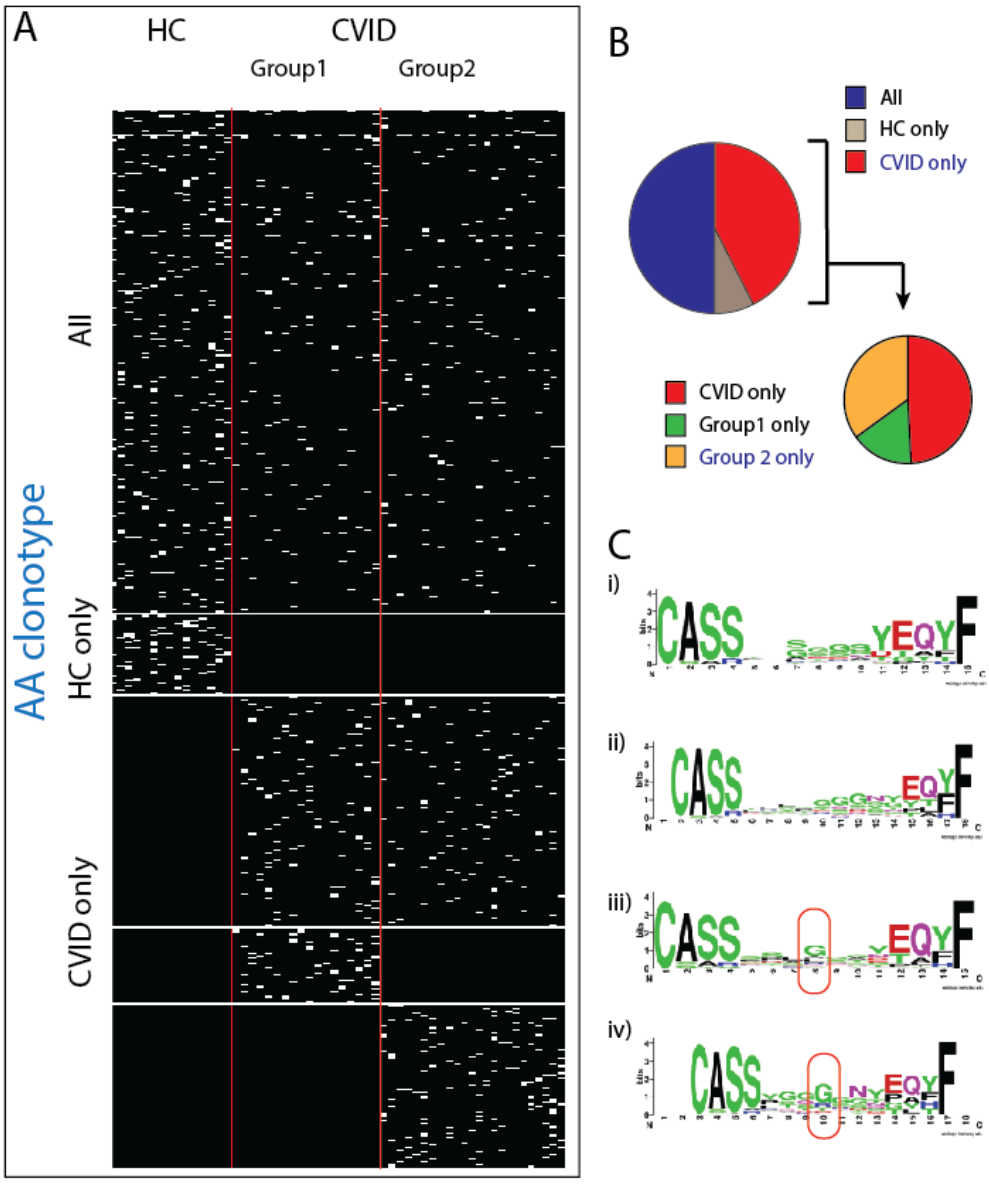

Figure 17. Shared TCRβ amino acid clonotypes between individuals.

(A) Amino acid clonotypes of >0.01% were cross-referenced between all 57 individuals (healthy donor; n=15, Group1 CVID; n=18, Group2 CVID; n=24). CDR3 sequences that could be found in more than 1 individual are shown (Row = clonotype, Column = subject). The three groups are separated by vertical red lines. Clonotypes that are uniquely identified in healthy donors, Group1 or Group2 patients are shown. (B) The proportion of clonotypes shared between all, healthy donors, CVID patients are illustrated in the large piechart. The small piechart shows the proportion of shared clonotypes within CVID patients. (C) The odds of each amino acids occurring in each position are represented by logo plots (i) = HC, (ii) = CVID, (iii) = Group1 & (iv) = Group2.

Shared clonotype	Amino acid sequence	Shared clonotype	Amino acid sequence	Shared clonotype	Amino acid sequence
CMV1	CASSAYTGTVYGYTF	Group1.8	CSARDPAGRDTEAFF	Group2.23	CASSYSKDTQYF
CMV2	CASSLSTGTSYGYTF	Group1.9	CASSLVADTQYF	Group2.24	CASSLWGSPLHF
CMV3	CASSEALLGRANYGYTF	Group1.10	CASSLEPSYEQYF	Group2.25	CASSYLGSNQPQHF
CMV4	CASSPLTGTGVYGYTF	Group1.11	CASSEVGEQYF	Group2.26	CASSYSLGNTEAFF
		Group1.12	CSARDNYEQYF	Group2.27	CASSMTSGSYNEQFF
HC1	CASSIFGELFF	Group1.13	CASSQDGGSYNEQFF	Group2.28	CASSPQGYGYTF
HC2	CASSGLAGGPDTQYF	Group1.14	CASSFGGSYEQYF	Group2.29	CASSLGRGTEAFF
HC3	CASSDSYEQYF	Group1.15	CASSLGLQETQYF	Group2.30	CASSYDRDYGYTF
HC4	CASSHGENTEAFF	Group1.16	CASSFPGQPYEQYF	Group2.31	CASSLGDGYEQYF
HC5	CASSYSSGSSYEQYF	Group1.17	CASSYSTDTQYF	Group2.32	CASSLVYEQYF
HC6	CASSAGYEQYF	Group1.18	CASSFGNEQFF	Group2.33	CASSLSGYTEAFF
HC7	CASSLGLAGAYEQYF	Group1.19	CASSPGSNQPQHF	Group2.34	CASSYGETQYF
HC8	CASSDGVSGNTIYF	Group1.20	CASSPGTAYEQYF	Group2.35	CASSSGTNYGYTF
HC9	CASSFEGNYGYTF	Group1.21	CASSSPLHF	Group2.36	CSARDSTGNGYTF
HC10	CASSEASGSSYEQYF	Group1.22	CASSLAGTGELFF	Group2.37	CASSPGGGSGNTIYF
HC11	CASSPGTSSYEQYF	Group1.23	CASRGSNQPQHF	Group2.38	CASSYSKGGSSPLHF
HC12	CASSYSGGSYEQYF	Group1.24	CASSVGTEAFF	Group2.39	CASSLGQGNYGYTF
HC13	CASSREGDQPQHF	Group1.25	CASSFTDTQYF	Group2.40	CASSYSNSPLHF
HC14	CASSELAGGPDTQYF	Group1.26	CASSYGDTGELFF	Group2.41	CASSPDRGNQPQHF
HC15	CASSIQSEAFF	Group1.27	CASSYSGGGAYEQYF	Group2.42	CSAPGQGSTEAFF
HC16	CASSTRSSYEQYF	Group1.29	CASSRPYNEQFF	Group2.43	CASSQAYEQYF
HC17	CASSYVRTGGGYGYTF	Group1.30	CASSEELAGANEQFF	Group2.44	CASSYRISYEQYF
HC18	CASSYPGQGNYEQYF	Group1.31	CASSLQGGTEAFF	Group2.45	CASSLGGNSYEQYF
HC19	CASSYDRNYGYTF			Group2.46	CASSPGQGPYEQYF
HC20	CASSRVPSYEQYF	Group2.1	CASSSSTGLGNSPLHF	Group2.47	CASSLTDREAFF
HC21	CASSPGGTDEQYF	Group2.2	CASSPQRNTEAFF	Group2.48	CASSWGQGAVEQYF
HC22	CASSDSGYSPLHF	Group2.3	CAGGFNQPQHF	Group2.49	CASSPGLNYGYTF
HC23	CSAREREYEQYF	Group2.4	CASSITGGDQPQHF	Group2.50	CASSPGGQGYEQYF
HC24	CASSPGQVSYEQYF	Group2.5	CSARFADTQYF	Group2.51	CASSQSGSNQPQHF
HC25	CASSERLAGAYEQYF	Group2.6	CASSLQETQYF	Group2.52	CASSYGRGNTEAFF
HC26	CASSFGYGYTF	Group2.7	CASSPDSLNTEAFF	Group2.53	CASSLQGNTEAFF
HC27	CASSYADTQYF	Group2.8	CSAPGQGTDTQYF	Group2.54	CASSFGGGNTEAFF
HC28	CSARVGDTEAFF	Group2.9	CASSYSSYEQYF	Group2.55	CASSYANSPLHF
HC29	CASRGTGSSYEQYF	Group2.10	CASSPTGWEQYF	Group2.56	CASSYGTGNSPLHF
HC30	CASSSGTSSYEQYF	Group2.11	CASSITSGDYNEQFF	Group2.57	CASSPGQETQYF
HC31	CASSPGNTEAFF	Group2.12	CASSSTTNYGYTF	Group2.58	CASSPGHSYEQYF
HC32	CASSYSEADTQYF	Group2.13	CASSYGNEQFF	Group2.59	CASSPDRDYGYTF
HC33	CASSLDSYEQYF	Group2.14	CASSYGTVSYEQYF	Group2.60	CASSSNYGYTF
		Group2.15	CSARFSDTQYF	Group2.61	CASSPSGNTIYF
Group1.1	CASSYTRQGYGYTF	Group2.16	CASNPTGSNQPQHF	Group2.62	CASSRDRGYEQYF
Group1.2	CSAGDRGFQETQYF	Group2.17	CASSLYRDNQPQHF	Group2.63	CASSRGTANYGYTF
Group1.3	CASSLAGYEQYF	Group2.18	CASSPGPGNTIYF	Group2.64	CASSYSGGSSYEQYF
Group1.4	CASSPPSGGETQYF	Group2.19	CASSYRYEQYF	Group2.65	CASSYGDSNSPLHF
Group1.5	CASSYSASSYEQYF	Group2.20	CASSRQNYGYTF	Group2.66	CASSSTGIYEQYF
Group1.6	CASSPGQTYEQYF	Group2.21	CASSYTGTGGYEQYF	Group2.67	CASSEEGPTYEQYF
Group1.7	CATSRDAGPGNTIYF	Group2.22	CASSYQGTEAFF	Group2.68	CASRATGTYEQYF

Table 4. List of shared amino acid clonotypes >0.01%.

HLA-A2 CMV specific clonotypes, shared clonotypes unique to healthy donors, unique to Group1 CVID and unique to Group2 CVID are highlighted in blue, grey, green and orange respectively.

To further examine the shared unique clonotypes, sequence similarly was conducted by multiple sequence alignment (Clustal omega, Seaview version 4.5.4) with their phylogenetic relationship determined (Parsimony). Four known HLA-A2 CMV specific clonotypes were used as positive controls in this in silico experiment to determine if motif-related sequences could be accurately group together. The analysis revealed a total of 8 distinct branches. Results showed that all 4 CMV sequences were closely located together at the end of "Branch1" (Figure 18A). While shared unique clonotypes of healthy donors (HC) tended to congregate towards the centre of the phylogenetic tree

and formed closer relationship with shared unique clonotypes of Group1 patients, shared unique clonotypes of Group2 patients demonstrated greater distant from the centre and an inverse relationship with HC and Group1 clonotypes (Figure 18B). In particular, "Branch 2" and "Branch 5" contained predominantly clonotypes from Group2 patients. Clonotypes of "Branch 2" and "Branch5" were derived from 14 and 12 Group2 patients respectively demonstrating a range of clinical complications without specific bias (Figure 19A). This non-specific association with clinical complication suggests a global immune dysregulation. In keeping with that, immunophenotypic data showed that $CD4^{+}CD25^{+}$ T-cells were significantly lower in Group 2 patients ($p = 0.0061$) (Figure 19B). Although true FoxP3 expression regulatory T-cells were not examined.

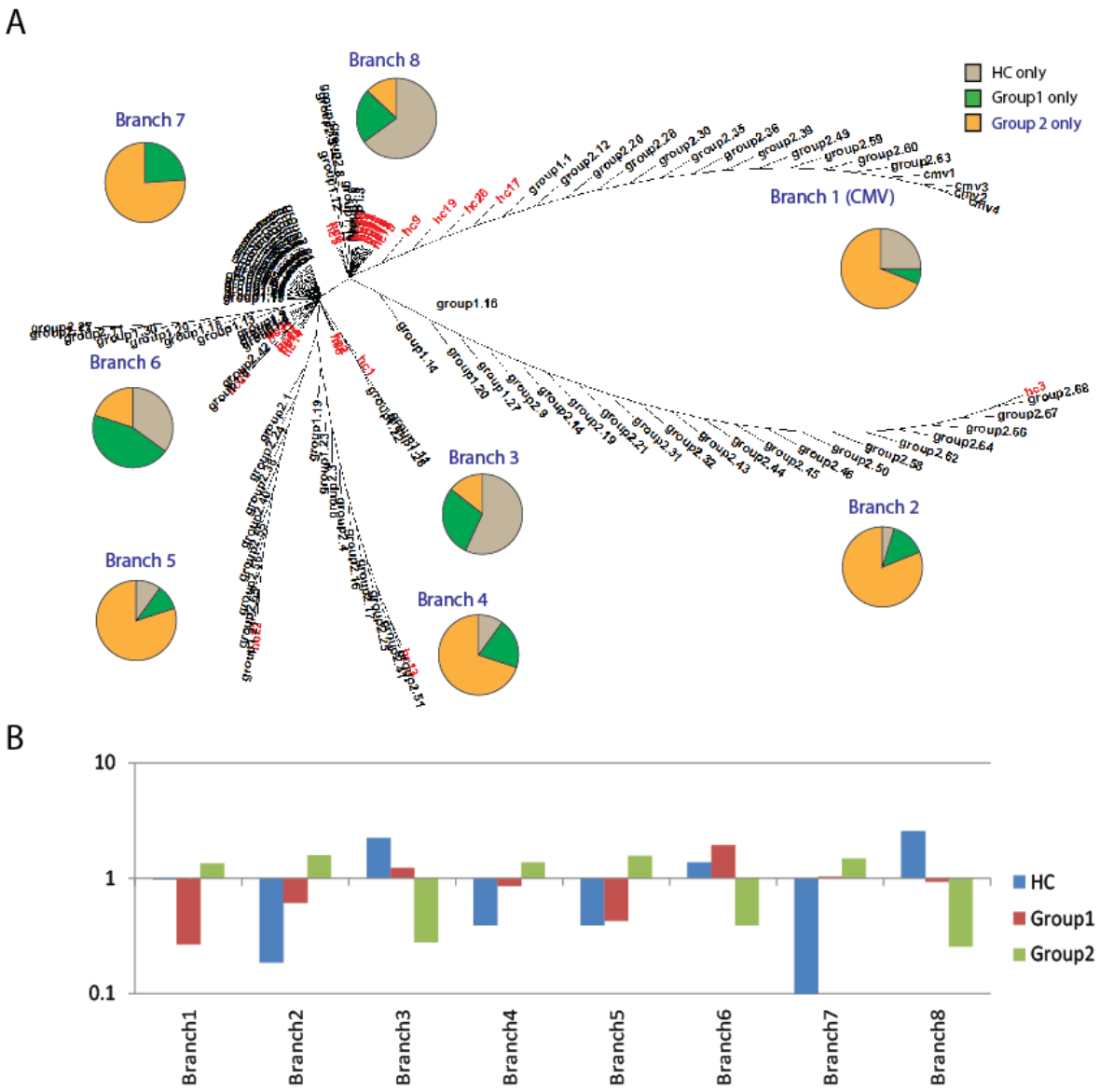

Figure 18. Phylogenetic relationship between shared unique clonotypes of each subgroup.

Phylogenetic distance of shared clonotypes were calculated using Parisomy according to sequence alignment by Clustal-Ω. Four well-published HLA-A2 CMV clonotypes were used as controls (far end of Branch 1). (A) The relationship between all shared unique clonotypes of each subgroup (healthy donor; n=33, Group1 CVID; n=31, Group2 CVID; n=68) are shown. Healthy control shared unique clonotypes are highlighted in red. For each branch, the proportion of HC (grey), Group1 (green) and Group2 (orange) clonotypes are shown in piecharts. (B) The proportional ratios of each branch corrected to their expected frequencies are shown.

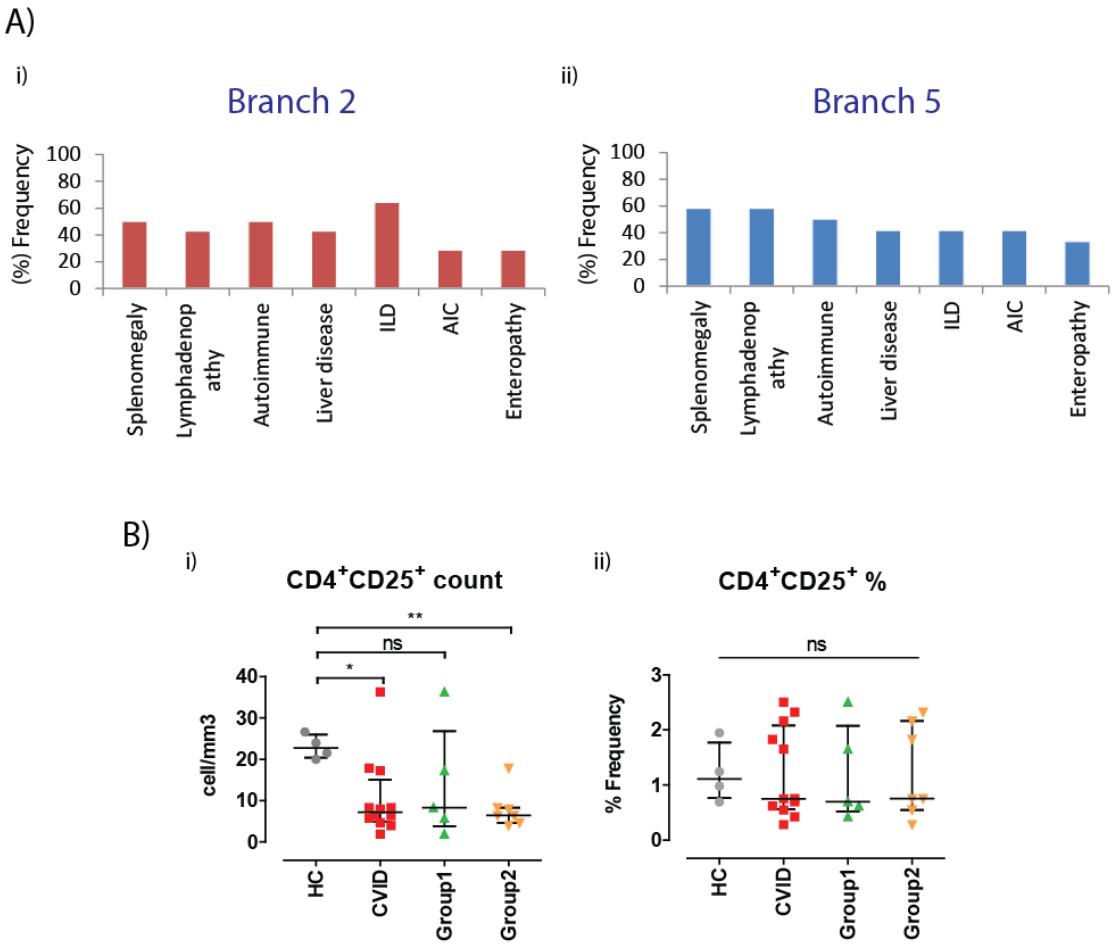

Figure 19. Clinical complications in relation to Branch 2 and Branch 5 clonotypes and $CD4^+CD25^+$ T-cells in CVID.

(A) 14 and 12 Group2 CVID patients were identified as owners of Branch 2 and Branch 5 clonotypes respectively. The frequencies of clinical complications occurring are shown (ILD = interstitial lung disease, AIC = autoimmune cytopenia). (B) Numerical counts and frequencies of $CD4^+CD25^+$ T-cells of healthy donors (n=4, grey), CVIDs (n=12, red), Group1 patients (n=5, green) and Group2 patients (n=7, orange) are shown. Medians and interquartile ranges are depicted. Statistical differences are highlighted by *, ** or ***.

3.2.4 Dominant CD8 clonotypes in CVID largely compose of CCR7$^-$CD45$^-$ effector memory T-cells.

To further test the uniqueness and functions of established clonotypes in CVID, multiparametric flow cytometry was carried out to complement the deep sequencing data. Due to the limited resolution of flow cytometry, only hyperexpanded clonotypes (>1%) were examined. Sixteen individuals (HC = 4, CVID = 12) with hyperexpanded clonotypes were identified. To assess the phenotypic expression of these hyperexpanded clonotypes, tailored TCR Vβ specific antibodies in combinations with other T-cell surface markers were used for flow cytometric analysis. Naïve T-cells were excluded from the analysis to better reflect the occupancy of a hyperexpanded clonotype within the memory compartment (Figure 20A). The details of hyperexpanded clonotypes are shown in Table 5.

V-families of hyperexpanded clonotypes in healthy donors and CVID patients predominantly contained CD4$^+$T-cells, while a smaller proportion was made up of CD8$^+$ T-cells (Figure 20B). In healthy donors, the majority of hyperexpanded CD8$^+$ clonotypes within the memory compartment were of TEMRA phenotype (median %: HC=68.5, CVID=17.5, Group1=13.8, Group2=21.2, P=ns) whilst hyperexpanded CD8$^+$ clonotypes from CVID patients were more likely to be effector memory T-cells without re-expression of CD45RA (median %: HC=22.6, CVID=59.7, Group1=77.5, Group2=57.1) (Figure 20, C and D). No differences in CD8$^+$ central memory or CD4$^+$ subpopulations were otherwise seen (Figure 21).

To further test if the CVID hyperexpanded clonotypes were unique to the disease, an extended search in the Adaptive immunoSEQ healthy donor public database was conducted. The result showed that all 4 healthy donor hyperexpanded clonotypes were detectable in other individuals in lower frequencies. By contrast, a large proportion (8/12) of the CVID hyperexpanded clonotypes did not matched any of the clonotypes listed in the healthy donor databases, suggesting their uniqueness to CVID or its associating complications (Table 5). Overall, the greater proportion of effector CD8$^+$

memory indicated an ongoing immune response and impaired clearance of a unique set of antigens in CVID patients. As a by-product, reduction in naïve T-cells were noted in these few CVID patients, consistent with the initial finding of lower number of small background clonotypes detected in 3.2.1. , warranting further investigations.

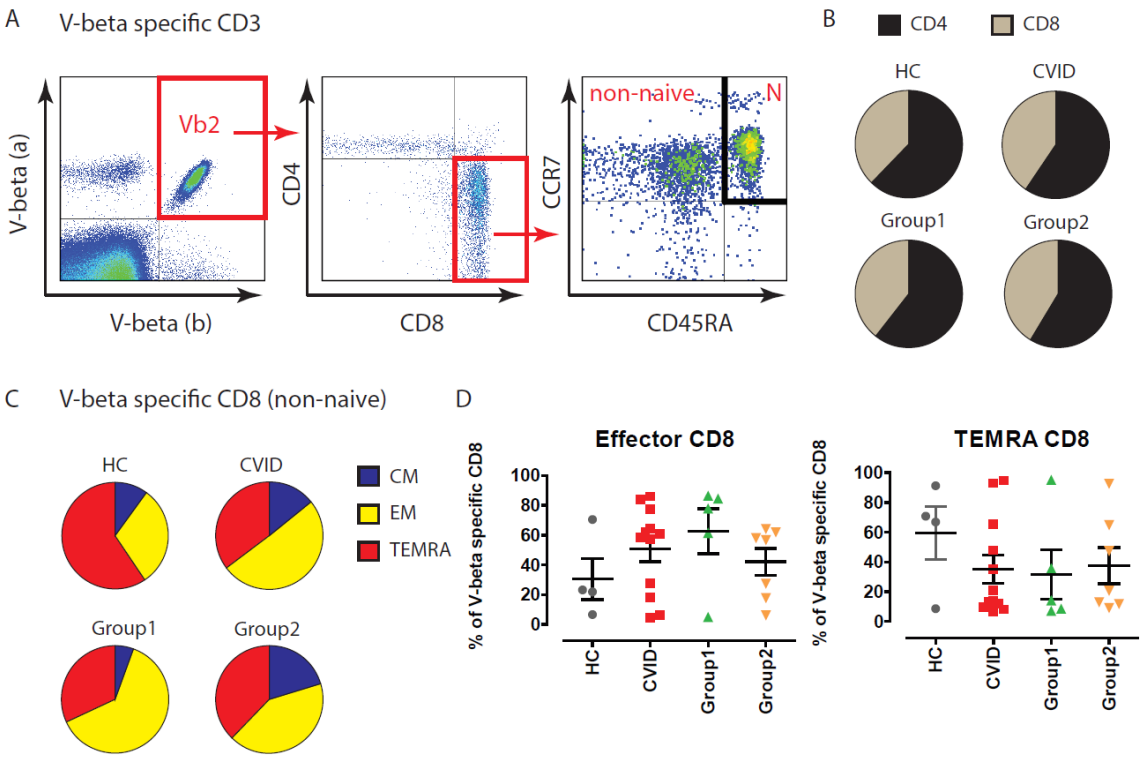

Figure 20. Immunophenotypic features of hyper-expanded clonotypes.

Corresponding IOTest V-beta specific antibodies were used to identify hyper-expanded clonotypes found by TCRβ sequencing. (A) Example of gating is shown. (B) The average frequencies of CD4 and CD8 T-cells of the V-beta family containing the hyper-expanded are shown (CD4=black, CD8=grey). (C) CD8 T-cells were further subdivided into non-naïve subsets: central memory, effector memory and TEMRA compartments (CM=blue, Effector memory=yellow, TEMRA=red). (D) Individual data points for CD8 effector memory and TEMRA are shown respectively. Medians and interquartile ranges are depicted.

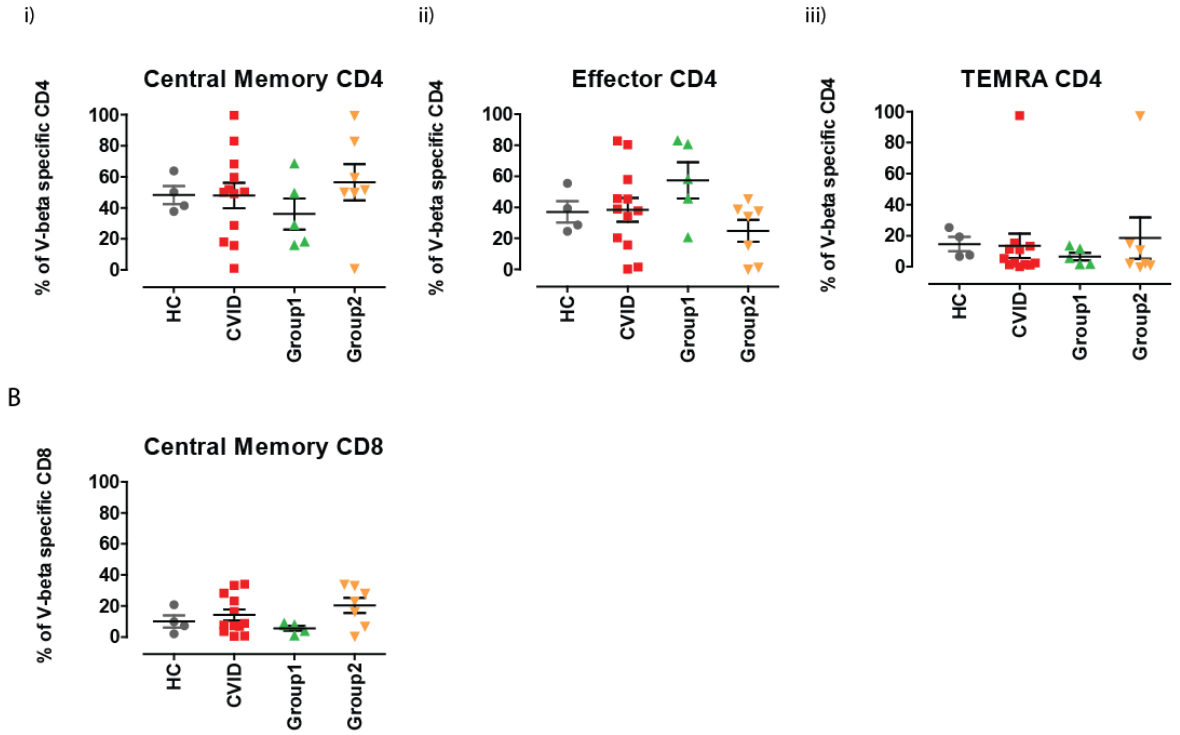

Figure 21. Immunophenotypic feature of hyperexpanded clonotypes (2).

Corresponding IOTest V-beta specific antibodies were used to identify hyper-expanded clonotypes found by TCRβ sequencing. CD4 and CD8 compartments were further subdivided into non-naïve subsets: central memory, effector memory and TEMRA compartments (A) Individual data points for CD4 central memory, effector memory and TEMRA are shown. (B) Individual data points for CD8 central memory are shown in (B). Medians and interquartile ranges are depicted. (two tailed Mann-Whitney U test).

	V-gene	CDR3 AA	J-gene	% of Repertoire	Dominant CD8 phenotype	Unique to CVID	Group
HC1	*TRBV14*	CASSLDALGEQFF	*TRBJ2-1*	9.3	TEMRA	--	HC
HC4	*TRBV27*	CASKVGQGYEQYF	*TRBJ2-7*	3.2	TEMRA	--	HC
HC5	*TRBV20-1*	CSARPPGQTYEQYF	*TRBJ2-7*	7.9	TEMRA	--	HC
HC10	*TRBV20-1*	CSAGGASGSLEQYF	*TRBJ2-7*	1.5	EM	--	HC
CVID3	*TRBV19*	CASSIDLDAYNEQFF	*TRBJ2-1*	8.5	EM	Y	1
CVID7	*TRBV5-6*	CASSPRGTGVTYEQYF	*TRBJ2-7*	8.5	EM	Y	1
CVID10	*TRBV12-3, 12-4*	CASSLANYGYTF	*TRBJ1-2*	5.1	TEMRA	--	1
CVID18	*TRBV19*	CASSSGNNQPQHF	*TRBJ1-5*	3.1	EM	--	1
CVID16	*TRBV19*	CASQGTGGIYEQYF	*TRBJ2-7*	3.7	EM	Y	1
CVID20	*TRBV10-3*	CAISARGAGANVLTF	*TRBJ2-6*	1.8	TEMRA	Y	2
CVID38	*TRBV19*	CASSIVPGQNYGYTF	*TRBJ1-2*	1.0	TEMRA	Y	2
CVID41	*TRBV6-2*	CASSYSSGSGEAFF	*TRBJ1-1*	2.7	EM	--	2
CVID37	*TRBV5-1*	CASSPPMGGSNYGYTF	*TRBJ1-2*	0.9	TEMRA	Y	2
CVID26	*TRBV14*	CASSQDFTGHYGYTF	*TRBJ1-2*	3.1	EM	Y	2
CVID22	*TRBV29-1*	CSVKPTYEGYEQYF	*TRBJ2-7*	3	EM	Y	2
CVID24	*TRBV29-1*	CSVGGGLSYEQYF	*TRBJ2-7*	3.0	EM	--	2

Table 5. Hyperexpanded clonotypes in health controls and CVID patients.

EM = Effector memory CD8 T-cells, TEMRA = terminally differentiated effector memory CD8 T-cells and HC = healthy donor.

3.3 Immunophenotyping and repertoire diversity in CVID

3.3.1 Collapse of naïve T-cell pool correlates with reduction in repertoire diversity.

In section 3.2, reduction in small background clonotypes was observed amongst CVID patients while immunophenotypic data continue to support a reduction in naïve T-cells as reported by other studies. To closer examine the relationship between immune repertoire diversity and changes in T-cell subpopulations, numerical counts and frequencies of various T-cell subpopulations were correlated with Shannon Entropy score. Using multi-parametric flow cytometry, naïve ($CCR7^+CD45RA^+CD28^+CD27^+$), central memory ($CCR7^+CD45RA^-CD28^+CD27^+$), effector memory ($CCR7^-CD45RA^-$) and terminally differentiated effector memory (TEMRA: $CCR7^-CD45RA^+$) were defined accordingly. Cell counts were accurately determined using counting beads. An example of gating strategy is shown in Figure 22A.

Of all results, the most striking abnormality was noted in the naïve T-cell compartment. Severe reductions in numerical count and frequency of naïve CD4+ T-cell counts were seen in CVID patients regardless of their clinical phenotypes. Both Group1 and Group2 patients exhibited nearly 10 fold reduction in peripheral blood naïve $CD4^+$ T-cell count. Moreover, strong positive correlations were also found between naïve $CD4^+$ T-cells and repertoire diversity (Figure 22, B and C). Similar magnitude of reductions in naïve $CD8^+$ T-cell counts were seen in both Group1 and Group2 patients with strong positive correlations demonstrated with repertoire diversity (Figure 22, D and E).

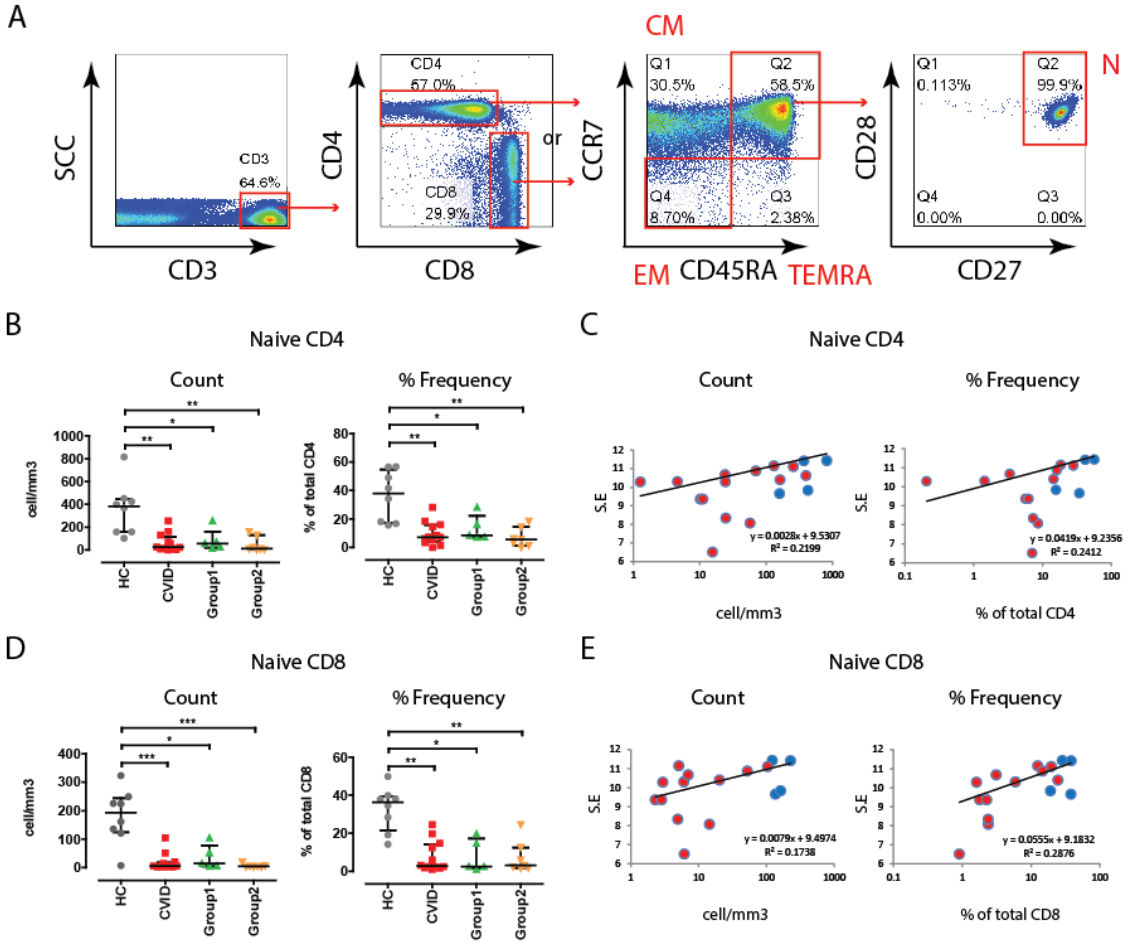

Figure 22. Correlations between repertoire diversity and peripheral naïve T-cells.

(A) Peripheral blood T-cell subpopulations were enumerated using counting beads. An example of the gating strategy is shown. (B) Naïve (N:CCR7^{+}CD45RA^{+}CD28^{+}CD27^{+}) CD4 T-cell counts and frequencies of healthy donors (n=8, grey), CVIDs (n=12, red), Group1 patients (n=5, green) and Group2 patients (n=7, orange) are shown. (C) Naïve CD4 T-cell counts and frequencies are plotted against TCRβ repertoire diversity (Shannon Entropy: S.E.). Black lines represent the best fit line with the equation and r2 value depicted adjacently (HC=blue dots, CVID=red dots). (D) Naïve CD8 T-cell counts and frequencies of healthy donors, CVIDs, Group1 patients and Group2 patients are shown. (E) Naïve CD8 T-cell counts and frequencies are plotted against TCRβ repertoire diversity. Medians and interquartile ranges are depicted. Statistical differences are highlighted by *, ** or *** (two tailed Mann-Whitney U test).

To determine if the reduction of naïve T-cells was related to thymic output, the thickness, anteriorposterior, craniocaudal and transverse lengths of thymus on high resolution CT scans were examined. Notably smaller and hypodense thymi was observed amongst CVID patients when compared to age-matched published reference range (Figure 23, A and B) [301], with all dimensions positively correlating with the numbers of small background clonotypes (<0.001%) by TCRβ sequencing (Figure 23C). Hence, our data suggest a reduction in thymic output leading to the peripheral reduction in naïve T-cells, limiting repertoire diversity in CVID.

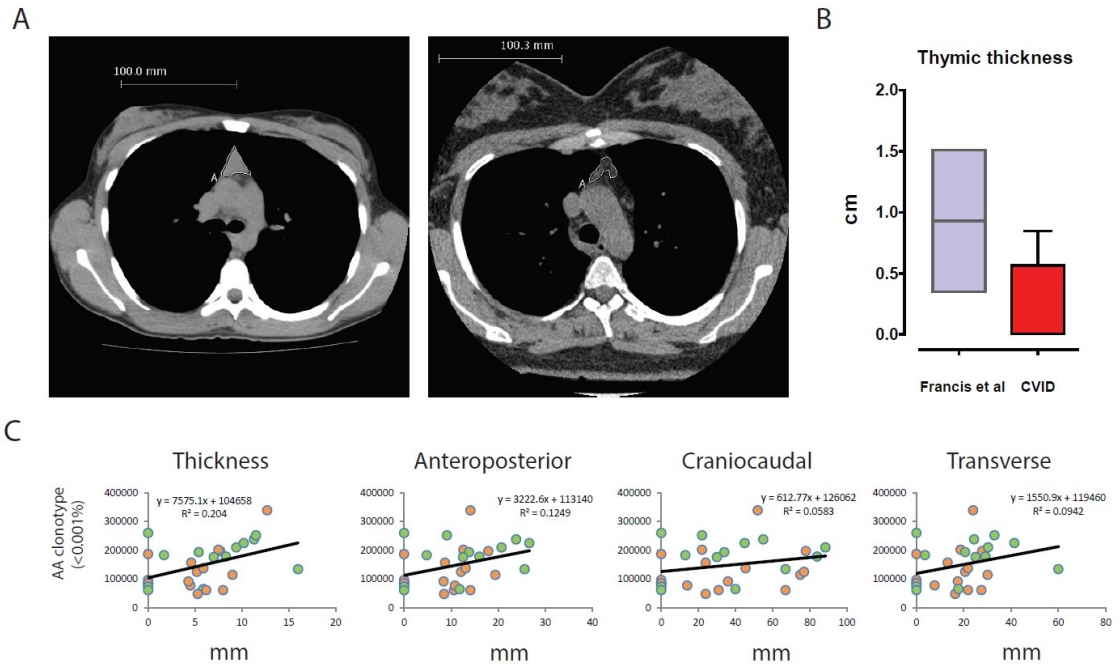

Figure 23. Reduced thymic dimension in CVID.

Thymic size was assessed using high resolution CT scan and compared to age-matched published reference ranges and the numbers of AA clonotypes (<0.001%). (A) Examples of a full thymus (left: 20yr old CVID patient) and a small hypodense thymus (right: 29yr old CVID patient) are shown. (B) The thymic thickness in cm of CVID patients (red, n=30) and the expected range of individuals between 40-50 yr (grey, mean and standard deviation) obtained from Francis *et al* are shown. (C) Thymic dimensions (thickness, anteroposterior, craniocaudal and transverse length in cm) are plotted against AA clonotypes (<0.001%). Black lines represent the best fit line with the equation and r^2 value depicted adjacently (Group1=green, Group2=orange dots). Medians and interquartile ranges are depicted.

3.3.2 *Effector memory T-cells play a relatively minor role in shaping repertoire diversity in CVID patients.*

So far, limited evidence has been generated to support an exaggerated T-cell immune response within this cohort of CVID patients. In keep with that, similar work (with 3.3.1) on other T-cell subpopulations such as effector memory ($CCR7^{-}CD45RA^{-}$), central memory ($CCR7^{+}CD45RA^{-}CD27^{+}CD28^{+}$) and terminally differentiated memory T-cells (TEMRA:$CCR7^{-}CD45RA^{+}$) did not reveal any convincing correlation between repertoire diversity. The data show that effector memory $CD4^{+}$ T-cells were normal in CVID and played no roles in shaping the repertoire diversity (Figure 24, A and B). Although a marginal difference in the frequencies of effector memory $CD8^{+}$ was observed which inversely correlated with repertoire diversity, numerical changes was not seen. The marginal difference was therefore likely to be secondary to the reduction of naïve T-cells and not the dominant driver for shaping the repertoire diversity (Figure 24, C and D). Similarly, neither central memory ($CCR7^{+}CD45RA^{-}CD28^{+}CD27^{+}$) nor terminally differentiated effector memory (TEMRA: $CCR7^{-}CD45RA^{+}$) demonstrated convincing correlations with repertoire diversity (Figure 25). Overall, there was no exaggerated T-cell immune response exerting major influences on the immune repertoire diversity.

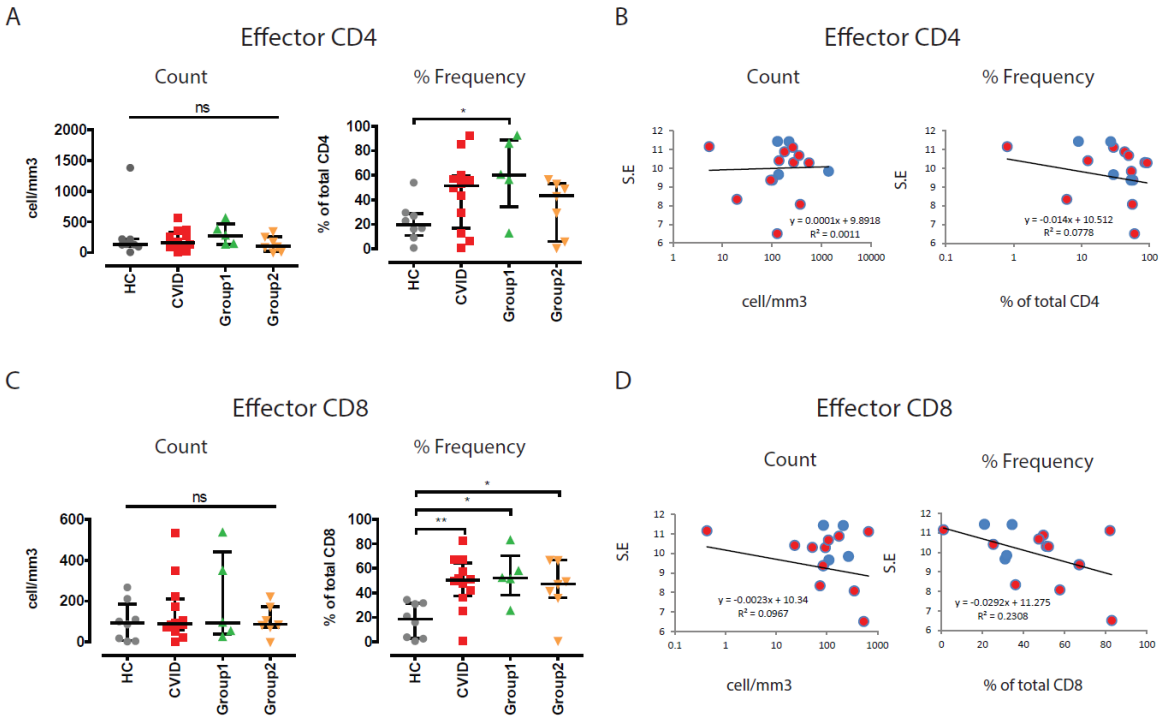

Figure 24. Correlations between repertoire diversity and peripheral effector memory T-cells.

(A) Effector memory (EM:CCR7$^-$CD45RA$^-$) CD4 T-cell counts and frequencies of healthy donors (n=8, grey), CVIDs (n=12, red), Group1 patients (n=5, green) and Group2 patients (n=7, orange) are shown. (B) Effector CD4 memory T-cell counts and frequencies are plotted against TCRβ repertoire diversity (Shannon Entropy: S.E.). Black lines represent the best fit line with the equation and r2 value depicted adjacently (HC=blue dots, CVID=red dots). (C) Effector memory CD8 T-cell counts and frequencies of healthy donors, CVIDs, Group1 patients and Group2 patients are shown. (D) Effector CD8 memory T-cell counts and frequencies are plotted against TCRβ repertoire diversity. Medians and interquartile ranges are depicted. Statistical differences are highlighted by *, ** or *** (two tailed Mann-Whitney U test).

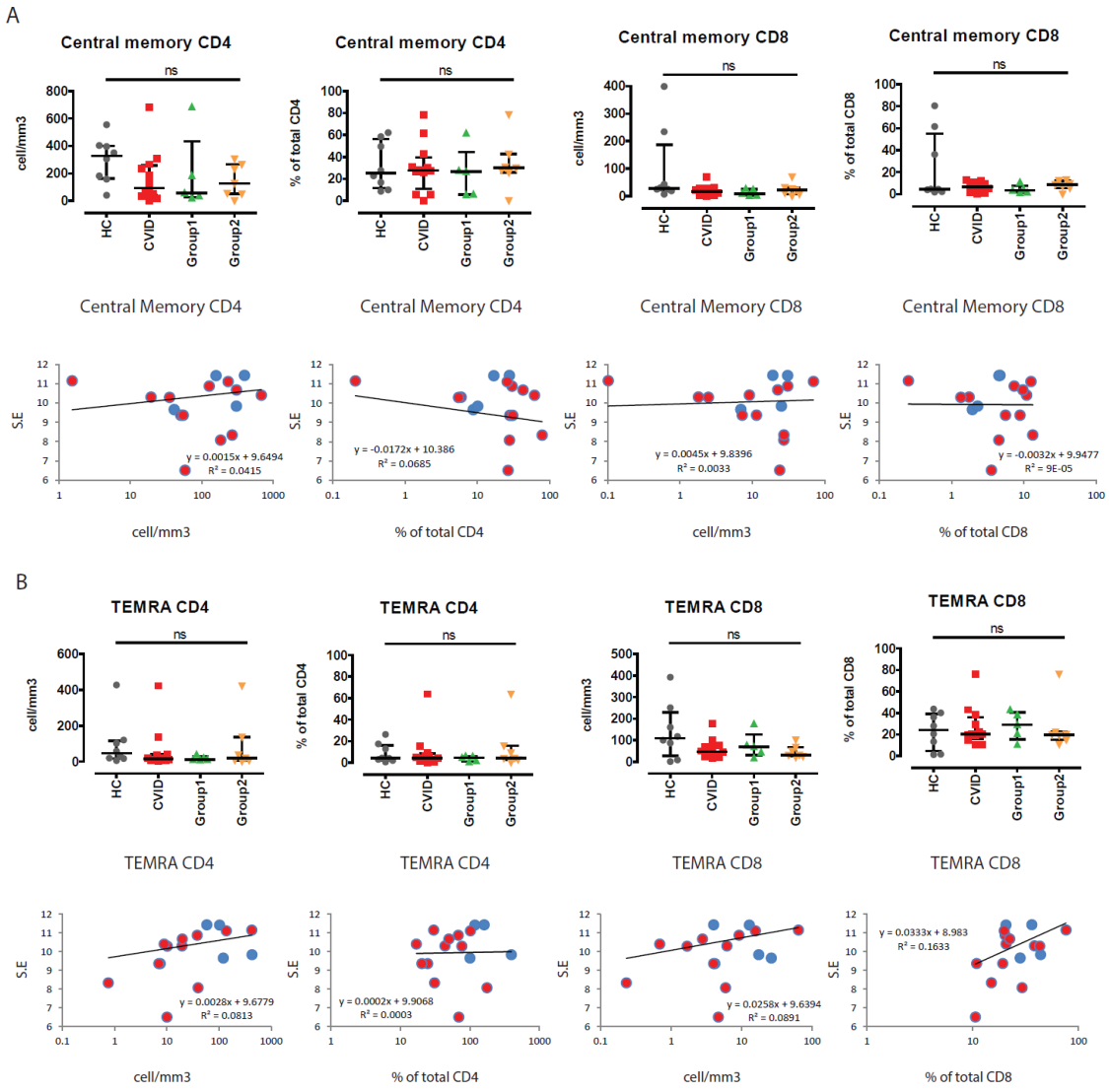

Figure 25. Peripheral blood immunophenotyping and correlations between repertoire diversity, central memory and TEMRA T-cells.

(A) Central memory (CM:CCR7^{+}CD45RA^{-}CD28^{+}CD27^{+}) CD4 and CD8 T-cell counts and frequencies of healthy donors (n=8, grey), CVIDs (n=12, red), Group1 patients (n=5, green) and Group2 patients (n=7, orange) are shown (top). CM T-cell counts and frequencies are plotted against TCRβ repertoire diversity (Shannon Entropy: S.E.). (B) Similarly, results of TEMRA (CCR7^{-} CD45RA^{+}) CD4 and CD8 T-cells are shown in (B). Black lines represent the best fit line with the equation and r^2 value depicted adjacently (HC=blue dots, CVID=red dots). Medians and interquartile ranges are depicted. Statistical differences are highlighted by *, ** or *** (two tailed Mann-Whitney U test).

3.4 Repertoire diversity and clinical outcome

3.4.1 The reduction in repertoire diversity correlates with severity of bronchiectasis and infection outcome in CVID.

In view of the reduction of repertoire diversity and naïve T-cells, I further hypothesise that the limited availability of cognate T-cells would affect T-dependent antibody responses against new antigens, hence, resulting in more frequent infections. To test this hypothesis, repertoire diversity was tested against severity of bronchiectasis and the annual requirement for antibiotics. The severity of bronchiectasis was graded into none, mild or moderate to severe according to CT findings. A reduction in repertoire diversity was observed in patients with moderate to severe bronchiectasis (Figure 26A). Similarly, patients with reduced repertoire diversity required more courses of antibiotics (Figure 26B). Finally, despite statistical significances were not observed, peripheral blood naive $CD4^+$ and $CD8^+$ counts also showed similar correlations with the severity of bronchiectasis (Figure 26C), demonstrating an association between the reduction in repertoire diversity, naïve T-cells and increase infection rate.

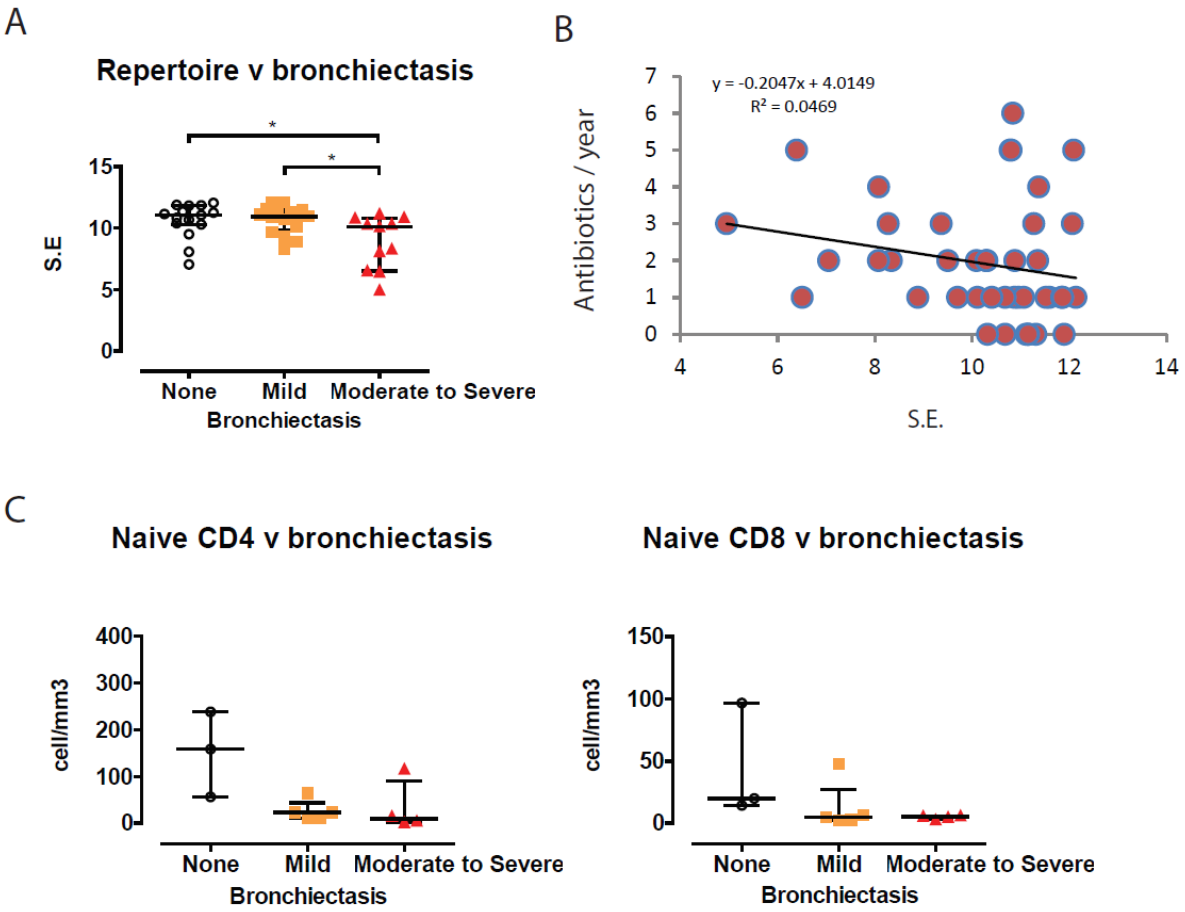

Figure 26. Repertoire diversity and infection burden.

(A) Bronchiectasis was sub-classified into none (open circle white), mild (orange square) or moderate to severe (red triangle) according to CT scan findings (n=42). Repertoire diversities by Shannon Entropy versus severity of bronchiectasis are shown. (B) The numbers of courses of antibiotics required by the patients were plotted against Shannon Entropy. Black lines represent the best fit line with the equation and r^2 value depicted adjacently. (C) Peripheral blood naïve CD4 and CD8 T-cell counts versus severity of bronchiectasis are shown. Medians and interquartile ranges are depicted. Statistical differences are highlighted by *, ** or *** (two tailed Mann-Whitney U test).

3.5 Discussion

This chapter advances on our understanding of T-cell oligoclonality in CVID and provides evidence that a restriction in T-cell repertoire diversity is a consequence of a reduction in the naïve T-cell pool rather than an exaggerated hyperexpanded clonotype picture. The resolution of high throughput TCR sequencing allowed us to demonstrate significant reduction solely in the small clonotype pool but no other compartments. Depletion of naïve T-cells irrespective of clinical complications was noted and could be as low as a tenth of healthy donors. Furthermore, reduction in naïve T-cells was associated with heavier infection burden and bronchiectasis. The collective reduction in naïve T-cells, repertoire diversity and thymic size was consistent with other published reports supporting the reduction of thymic output in CVID patients [252, 302]. Molecular studies have shown that the numbers of copies of T-cell receptor excision circles (TRECs) were significantly reduced and $CD31^+$ recent thymic immigrants were lower when compared with healthy donors [225, 271, 272]. Moreover, other thymic-derived populations including naïve, regulatory and invariant NK T-cells were all reported in lower frequencies in patients with CVID [20, 254, 264, 302]. Although it is recognized that the thymic output gradually declines with age, it is known to be active well into the 7^{th} decade [303]. These data would support a complete or near complete arrest in thymic output in CVID.

In agreement with the report by Giovannetti *et al*, the data show that naïve T-cells, repertoire diversity and infection outcome are all intricately linked together [242]. Infection burden was seen in the form of bacterial infections and bronchiectasis, indicating the lack of cognate T-cells for supporting T-dependent antibody responses, although this is unlikely to be the sole factor leading to humoral failure in CVID. Despite the severe reduction in naïve T-cells, the majority of patients did not present with overt T-cell immunodeficiency, perhaps prevented by their well-preserved memory T-cell compartments. One possible explanation would be that the collapse of the naïve pool occurred after firm establishment of the memory and effector repertoires in adulthood and secondary to recurrent infections induced thymic sequestration as previously discussed. It would be of interest to see if arrest

in thymic output coincides with the timing of humoral failure and if recovery could be seen in some patients with better infection control. Finally, these findings call for caution in the use of immunosuppressive therapies targeting T-cells in CVID patients or it risks further compromising the existing T-cell immunity in the absence of adequate thymic replenishment.

Large expanded $CD8^+$ clonotypes in CVID were mostly $CCR7^-CD45RA^-$, but $CCR7^-CD45RA^+$ in healthy donors. The differentiation origins of $CD45RA^-$ and $CD45RA^+$ memory are subjected to ongoing debate, and expression of CD45RA on $CD8^+$ memory may be dynamic [304]. Nonetheless, in human CMV and HIV infections, CD45RA re-expression on $CD8^+$ memory correlated well with better control of the viruses and the removal of antigenic stimulation [305-307]. Therefore, the larger proportion of $CCR7^-CD45RA^-$ $CD8^+$ T-cells in CVID may indicate the persistent presence of an antigenic driver. However, the data suggest that their overall influences on repertoire diversity are limited and the alteration in the frequency of $CD8^+$ effector memory was likely to be a bystander of the reduction in naïve T-cells.

In contrast to previous studies, preferential V-gene usage in CVID patients was not observed [245-247, 252]. Unfortunately, cross-scanning of repertoires and multiple sequence alignment bioinformatics could not clearly identify unique shared clonotypes or motif related CDR3 sequences that were associated with polyclonal lymphoproliferation, enteropathy, interstitial lung disease or autoimmunity [290, 308]. Further studies are needed to test the specificities of those CVID hyperexpanded clonotypes.

CDR3 sequence analysis revealed a number of unique shared sequences in Group2 CVID patients that were phylogenetic more distinct, supporting the notion that many of the inflammatory complications of CVID are driven by altered T-cell immune responses. The alter T-cell immune responses were not specific to a particular clinical presentation, reflecting a more universal mechanism for immune dysregulation, perhaps relating to the reduction of regulatory T-cells. Given that an alter immune response was not found in Group1 patients, our data do not currently support that T-cells play a direct inhibitory role against the humoral immune system or the survival of plasma cell as we

initially hypothesised. It is worth noting that these bioinformatics data should be interpreted in extreme care. Although similar approaches have been used by other studies [290, 308], our analysis was subjected to high background signal and bioinformatics errors in the absence of full HLA matching.

Another limitation of the experimental design is the inherent PCR bias of the genomic DNA approach for TCR sequencing [309]. Hence the size estimation of each clonotype may be biased. Regardless, our data show that hyperexpanded clonotypes were well-reflected by flow cytometric analysis using the Vβ-specific antibodies. Our experimental design could be improved by performing high throughput sequencing on enriched T-cell subpopulations which will allow us to more accurately compare the naïve and memory repertoires of $CD4^+$ and $CD8^+$ T-cells, although the resources requiring to generate such data set would exponentially increase.

3.6 Summary and conclusion

In summary, the data suggest that the T-cell compartment of CVID is severely disrupted as a result of thymic failure, whilst its full extent might be masked by a well-preserved memory T-cell compartment generated prior to the onset of disease, preventing patients from an overt T-cell immunodeficiency syndrome and controlling latent viral infections. Immune dysregulation appears to arise from a universal mechanism, predisposing patients to a number of inflammatory complications.

In fact, the lesser availability of cognate T-cells would limit the ability to generate a competent T-dependent antibody response against new antigens. Although thymic failure might be secondary to B-cell deficiency, these findings raise the possibility of a global arrest in lymphogenesis occurring late in life. In the bone marrow, the late onset arrest in lymphogenesis might lead to increased homeostatic proliferation of pre-existing B-cells to maintain the population, subjecting B-cells to replicative senescence and impaired functions.

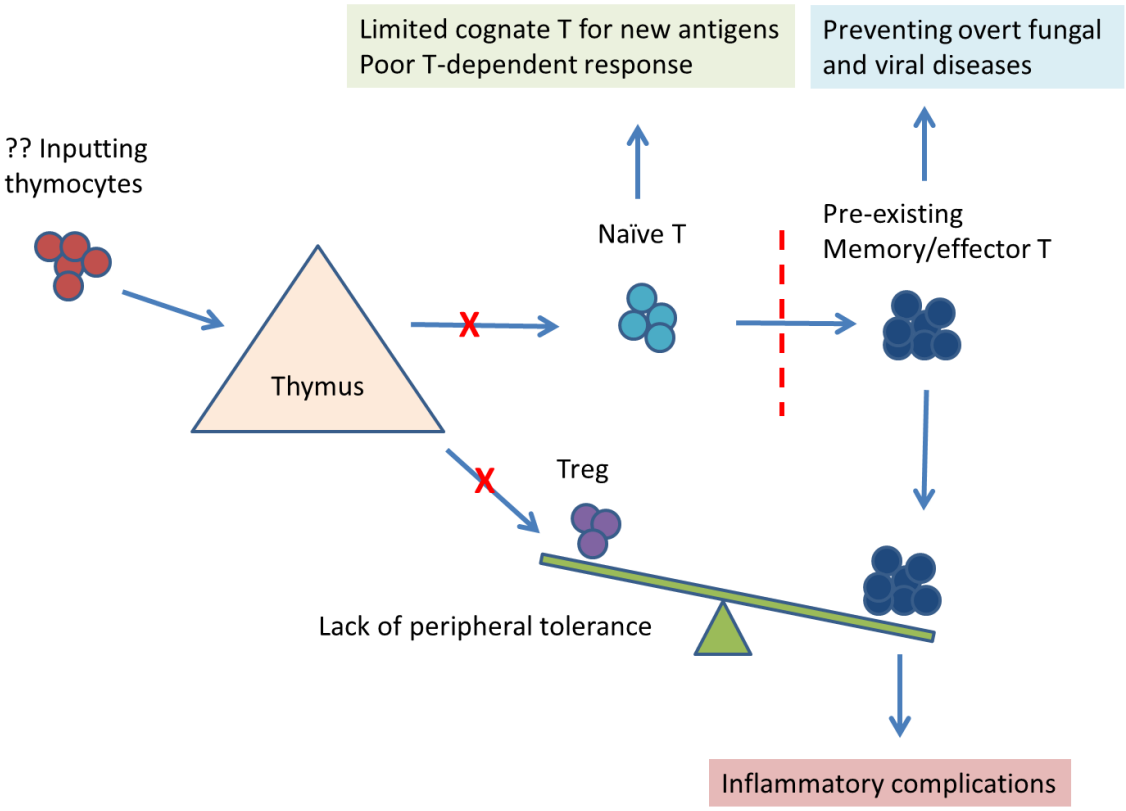

Figure 27. Model of T-cell defect of CVID.

Chapter 4

4. Assessment of plasma cell survival suggests mosaicism in the B-cell pool of CVID patients.

In the previous chapter, the study on T-cells highlighted an arrest in T-cell lymphogenesis later in life in CVID patients, suggesting a simultaneous collapse of B-cell and T-cell outputs as a plausible aetiology for the condition. In keeping with that, both KRECs (kappa deleting recombination excision circle) and TRECs were shown to be reduced proportionally in CVID patients [310]. However, the normality of total B-cell and naïve B-cell counts ($CD27^-$) act as a key paradox for this hypothesis and warrant further investigations.

4.1 Naïve versus memory B-cells in CVID

Similar to naïve T-cells, naïve B-cells are maintained by a combination of continuous bone marrow output and homeostatic proliferation [311]. While T-cells progressively rely on homeostatic proliferation as one ages and thymic involution accelerates [303], bone marrow output of B-cells remains relatively constant throughout life [312]. Studies have shown that naïve B-cells in both mice and human demonstrated minimal proliferative events before the germinal centre stage [311].

Interestingly, by isolating B-cells into various subsets Driessen *et al* showed that homeostatic proliferation of naive B-cells can be as high as 3 times in CVID patients when compared to healthy donors, a finding closer associated with patients with low level of transitional B-cells and memory B-

cells. This level of replicative senescence was suggested to have detrimental effects on sequential B-cell functions, such as poor proliferation, somatic hypermutation and antibody production [212].

For B-cells, replicative senescence is best described in the $CD21^{lo}$ subpopulation as this population was shown to be largely maintained by homeostatic proliferation [313]. Consistent with previous descriptions, expansion of this population is frequently observed in CVID patients [176]. Furthermore, $CD21^{lo}$ B-cells were shown to be ANA antibodies positive and have poor proliferative capacity [314]. Therefore, evidence is mounting up to support that the canonical mechanism to maintain total B-cell population in CVID is being shifted from primary bone marrow generation toward homeostatic proliferation. This compensatory effect may hence mask the true deficit of bone marrow output with the effect of replicative senescence only being manifested during B-cell activation and all downstream functions including memory formation and the maintenance of baseline antibody levels by bone-marrow resident long-lived plasma cells (LLPC) [213, 214].

As a proportion of memory B-cells would likely be generated prior to bone marrow arrest, they may be spared from the effect of replicative senescence and retain normal plasma cell generation and survival ability upon reactivation. We therefore hypothesise that naive B-cells and memory B-cells might varies in their functional deficits in CVID, particularly in those patients demonstrating a residual memory B-cell population.

4.2 Plasma cell culture

4.2.1 3-step in vitro culture system in generating and maintain long-lived plasma cells

The study of plasma cells, in particular for their survival, has been extremely difficult to conduct in the past due to technical limitations. Plasma cells are found in peripheral blood in extremely low frequency and bone marrow is their only reliable source. In addition, plasma cells die rapidly in culture environment as their survival requires specific niches difficult to replicate *in vitro* [315]. The *in vitro* replication of such micro-environment poses as a major technical challenge in studying human plasma cells. In recent years, a number of research groups successfully differentiated human peripheral B-cells into strong syndecan-1 (CD138) expressing LLPC using very similar three-step culture techniques [282, 316, 317]. In these culture environments, the T-dependent antibody response is activated to the best with data showing that LLPCs were able survive for up to 63 days or as long as the experiments continued with the support of various cytokines and murine bone marrow fibroblasts [282]. This offers an opportunity to examine the full spectrum of the humoral immune response by comparing the terminal differentiation and survival of activated naïve and memory-B-cells in CVID.

4.2.2 Long term culture of naïve-derived and memory derived $CD20^{-}CD27^{+}CD38^{+}CD138^{+}$ long-lived plasma cells.

Previously described protocols for long-lived plasma cell (LLPC) generation were conducted using total B-cells or isolated memory B-cells. However, the differentiation potentials for naïve and memory B-cells under such *in vitro* environment are not clear. To understand how healthy naïve and memory B-cells may response to the protocol adopted in this study, naïve and memory B-cells from healthy donors were tested. Plasma cells were generated from magnetic isolated naïve or memory B-cells using a 3-step culture system (see method for details) and then maintained for 6 weeks in an *in vitro* system replicating the bone marrow niche. The schema for long-lived plasma cell culture supported by murine bone marrow fibroblast cell line (M2-10B4) and the gating strategy to define plasma cells are shown in Figure 28.

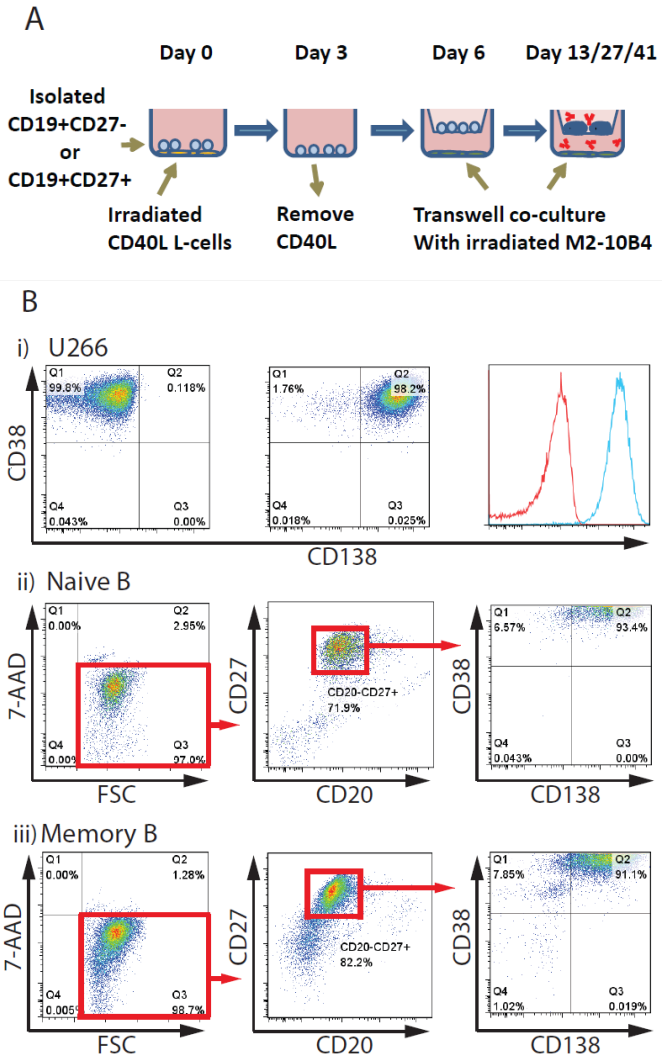

Figure 28. Schema of modified long-term plasma cell generation protocol culture and flow cytometry gating strategy.

(A) Naïve ($CD27^-$) and memory ($CD27^+$) B-cells were enriched by magnetic bead isolation and terminal differentiated into plasma cells using a 3-step culture system. B-cells were initially activated by CD40L-expressing L-cells supplemented by IL-2, IL-21 and anti-IgA/M/G F(ab)2 and then transfer to a transwell system supported by murine bone marrow fibroblast (M2-10B4) on Day 6. The wells were harvested on week 2/4/6 for flow cytometric analysis. Short-lived plasma cells (SLPC = $7\text{-}AAD^-CD20^-CD27^+CD38^+CD138^-$) and long-lived plasma cells (LLPC = $7\text{-}AAD^-CD20^-CD27^+CD38^+CD138^+$) were enumerated using counting beads. (B) A U266 myeloma cell line was used to optimise CD38 and CD138 gating. Events within the upper left quadrant of the far right plot were considered to be SLPC whilst events within the upper right quadrant were considered to be LLPC. Examples of both naïve and memory B-cells differentiations of a healthy donor at Day 13 are illustrated.

Equal number of naïve and memory B-cells (100,000/well) were plated out on Day 6. Whilst proliferating plasmablasts are generated at Day 6, all cells in the differentiation system ceased to proliferate after Day 10, thus defining the functional transition from plasmablast to plasma cell state. However, the rate of phenotypic maturation to the $CD138^{+ve}$ state varies such that cultures harvested on Day 13, Day 27 and Day 41 were composed of $CD138^{-ve}$ plasma cells ($7\text{-}AAD^{-}CD20^{-}CD27^{+}CD38^{+}CD138^{-}$) which have a shorter survival (short-lived PC = SLPC), and $CD138^{+ve}$ PCs ($7\text{-}AAD^{-}CD20^{-}CD27^{+}CD38^{+}CD138^{+}$) which represent long-lived plasma cells (LLPC).

Under such experimental condition, memory B-cells ($CD27^{+}$) were far more potent than naïve B-cells ($CD27^{-}$) in generating both SLPCs and LLPCs (Figure 29A). Both naïve-derived SLPCs and naïve-derived LLPCs rapidly declined in numbers and were almost undetectable by Day 27. By contrast, memory-derived LLPCs gradually increased in number between Day 13 and Day 27 and were able to maintain their population until Day 41, a likely effect from the progressive upregulation of CD138 in the culture (Figure 29, B and C). Similarly, supernatants from memory B-cell cultures contained significantly more IgG and IgM than those from naïve B-cell cultures. Sustained IgG production was noted until the end of the experiment from memory-derived PCs, indicating that these cells are responsible for long term antibody production (Figure 29D).

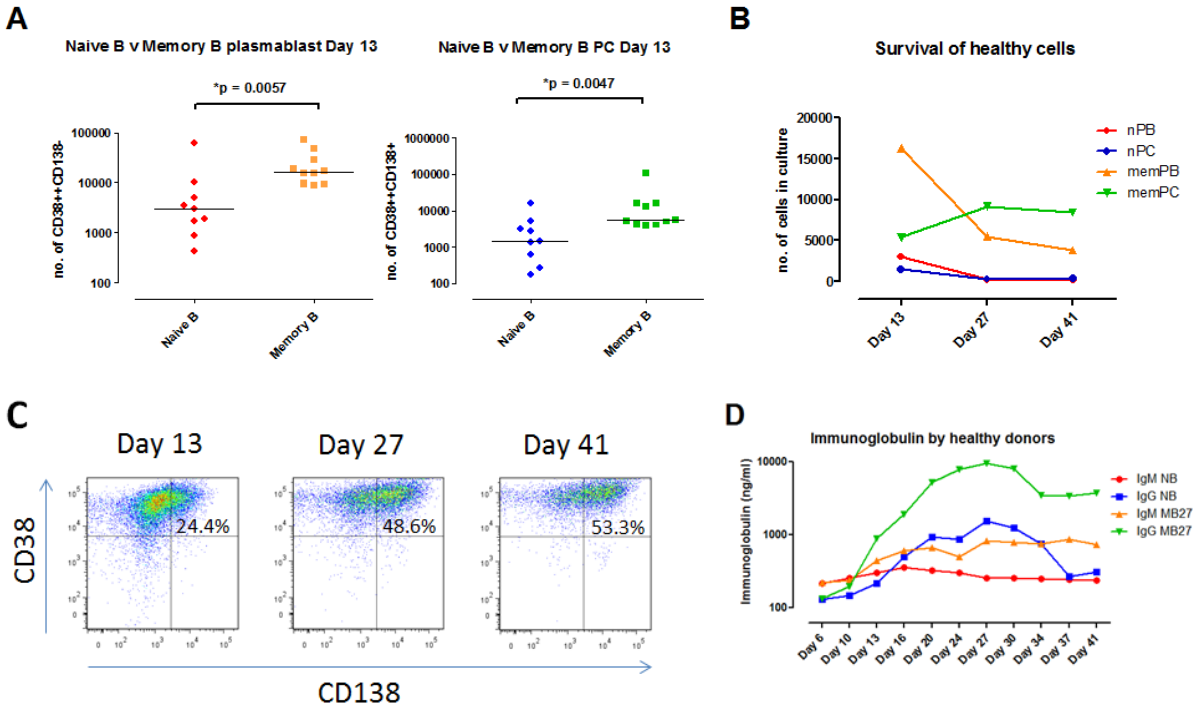

Figure 29. Naïve and memory B-cell terminal differentiation in healthy controls.

Culture-wells were harvested on week 2/4/6 and analysed by flow cytometry. (A) The calculated SLPC and LLPC counts on Day 13 are shown (median naïve-derived SLPC:memory-derived SLPC = 3019:16263 cells/well, median naïve-derived LLPC:memory-derived LLPC = 1469:5414 cells/well). The dynamics median cell counts for each subset (red = naïve-derived SLPC, blue = naïve-derived LLPC, orange = memory-derived SLPC and green = memory-derived LLPC) over a 6-week period are shown in (B). An example of the progressive expression of CD138 within the memory culture is shown in (C). (D) The IgM and IgG concentrations (ng/ml) within the supernatants were measured by sandwich ELISA and their medians are shown (red = IgM in naïve cultures, blue = IgG in naïve cultures, orange = IgM in memory cultures and green = IgG in memory cultures). Statistical differences are highlighted by *, ** or *** (two tailed Mann-Whitney U test).

4.3 Long-lived plasma cell generation in CVID.

4.3.1 CVID patients demonstrate greatest deficit in generating of $CD38^{+}CD138^{+}$ plasma cells from naïve B-cells.

With the assay established in-house and patterns of normal naïve and memory B-cell differentiation defined, the functions and differentiation potential of CVID B-cells were examined. Naïve and memory B-cells from 14 CVID patients, 4 disease control patients and 10 healthy donors were isolated and examined. The data show that generation of naïve-derived LLPCs and memory-derived LLPCs at Day 13 were suboptimal in CVIDs ($p = 0.015$ and $p = 0.017$ respectively). Greatest deficit was noted in the generation of naïve-derived LLPCs (7-fold less), whilst memory-derived LLPCs were only moderately affected (1.5-fold less) (Figure 30). Similarly, memory-derived SLPCs were only subtly affected. Plasma cell counts in CVID patients also showed no signs of recovery at Day 27 and Day 41. Sub-classifying patients into Group 1 (infection only) and Group 2 (autoimmune complications, enterpathy, interstitial lung disease and polyclonal lymphoproliferation) as the previous chapter showed similar results. To further control the confounding effect of variable memory B-cell subpopulations, $CD138^{+}$ LLPCs counts from memory cultures were correlated with class-switched memory B-cells ($IgD^{-}IgM^{-}CD20^{+}CD27^{+}$) in patients' peripheral blood. Similarly, LLPCs counts from naïve cultures were correlated with $CD21^{lo}$ B-cells ($CD20^{+}CD21^{lo}CD38^{-}$) in peripheral blood. The analysis did not demonstrate any correlation between these rarer B-cell subsets and *in vitro* LLPC outputs (Figure 31). In addition, the numerical PC deficits in patients were not exerted by immunoglobulin replacement therapy as the disease control group demonstrated normal long-lived plasma cell generation. Consistent with the T-cell data, although both the naïve and memory compartment were affected, the failure of naïve B-cells transforming into plasma cells was much greater in CVID whilst memory function was better preserved.

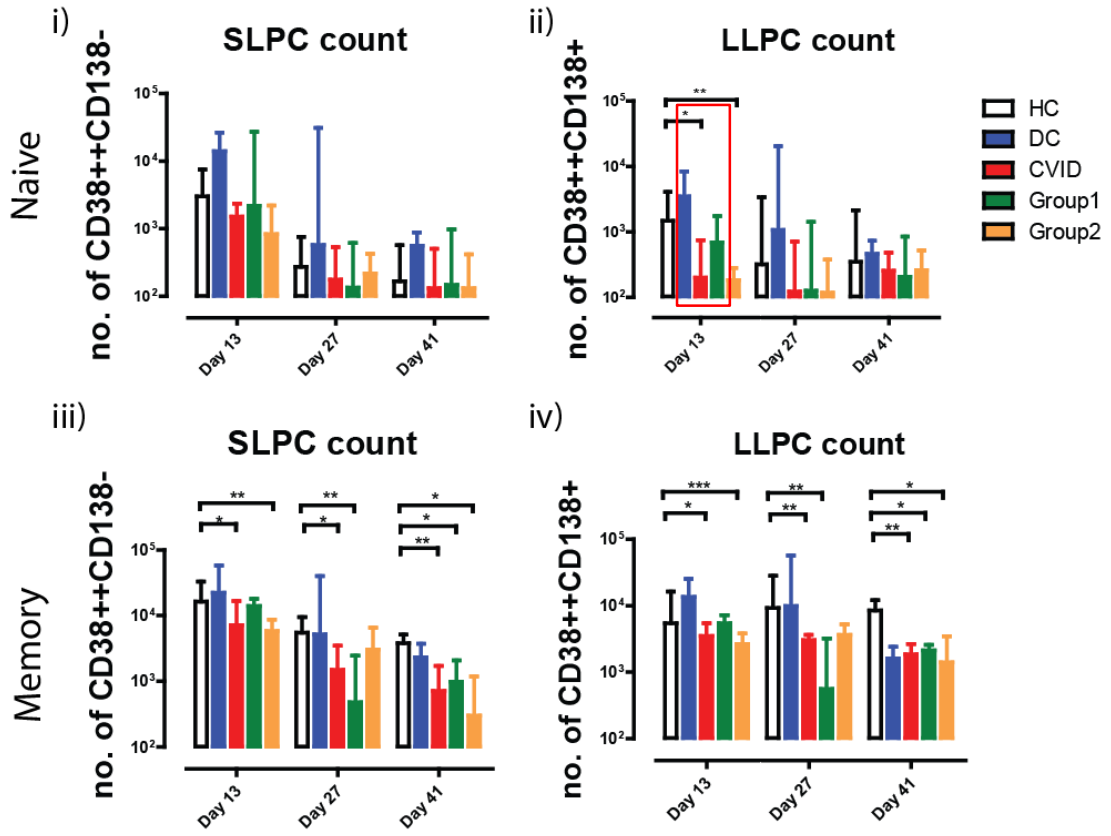

Figure 30. Comparison of SLPCs and LLPCs generation and survival from naïve and memory B-cells of CVID patients and controls.

SLPC and LLPC counts generated from naïve and memory cultures at Day 13, Day 27 and Day 41 of healthy donors (n=10-6), disease controls (n=4-2), CVID (n=14-8), Group1 patients (n=7-5) and Group2 patients (n=7-3) are depicted. Some cultures died out before Day 41 and the minimum (n) is reflected by the latter number. Medians and interquartile ranges are represented by the height and error bar respectively. The red box indicates the greatest deficit in naïve LLPC output at Day 13. Statistical differences are highlighted by *, ** or *** (two tailed Mann-Whitney U test).

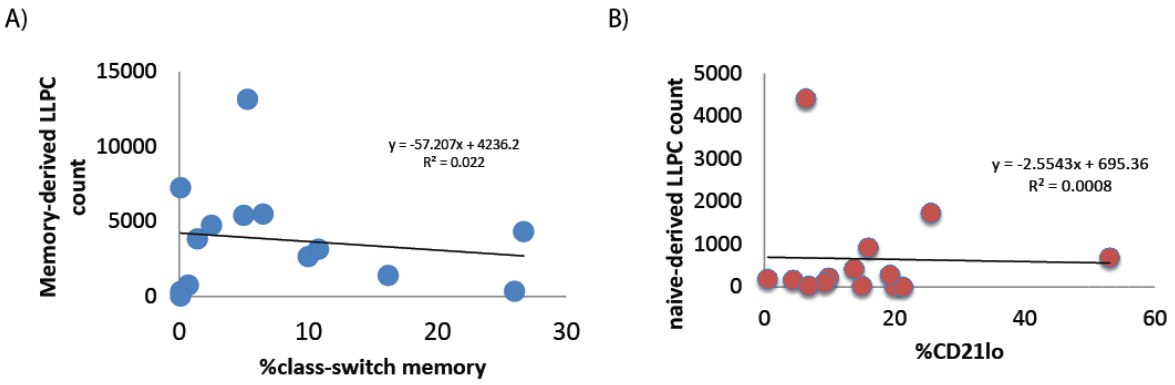

Figure 31. Correlations between plasma cell functions and peripheral blood B-cell subpopulations.

(A) Percentage frequencies of smB ($CD19^+IgM^-CD27^+$) of total B-cells of CVID patients versus the number of LLPCs ($CD20^-CD27^+CD38^+CD138^+$) in the memory-derived culture at Day 13 is shown (n = 14). (B) Percentage frequencies of $CD21^{lo}$ ($CD19^+CD38^-CD21^{lo}$) of total B-cells of CVID patients versus the number of LLPCs ($CD20^-CD27^+CD38^+CD138^+$) in the naïve-derived culture at Day 13 is shown (n = 14). No correlations were demonstrated. Black lines represent the best fit line and correlations (r^2) are illustrated.

To investigate whether the reduction in LLPCs was related to a block in phenotypic maturation, the frequencies of persisting SLPCs ($CD38^+CD138^-$) and LLPCs ($CD38^+CD138^+$) at Day 13, Day 27 and Day 41were compared (Figure 32). Within the naïve cultures, maturation from $CD138^-$ to $CD138^+$ plasma cells was clearly impaired in CVID patients with less than 50% of surviving cell at the end of the 6-week period upregulating CD138. Although a slight delay in maturation towards LLPC phenotype was observed in the memory CVID cultures at Day 27, upregulation of CD138 normalised at Day 41. Together, both numerical count and maturation profile suggest that the deficit in CVID was greater from the naïve pool. Nonetheless, the ability to express the cardinal phenotype of LLPC was partially retained in most patients, suggesting a healthy subpopulation of B-cells might exist in CVID contributing to the suboptimal baseline antibody production observed clinically.

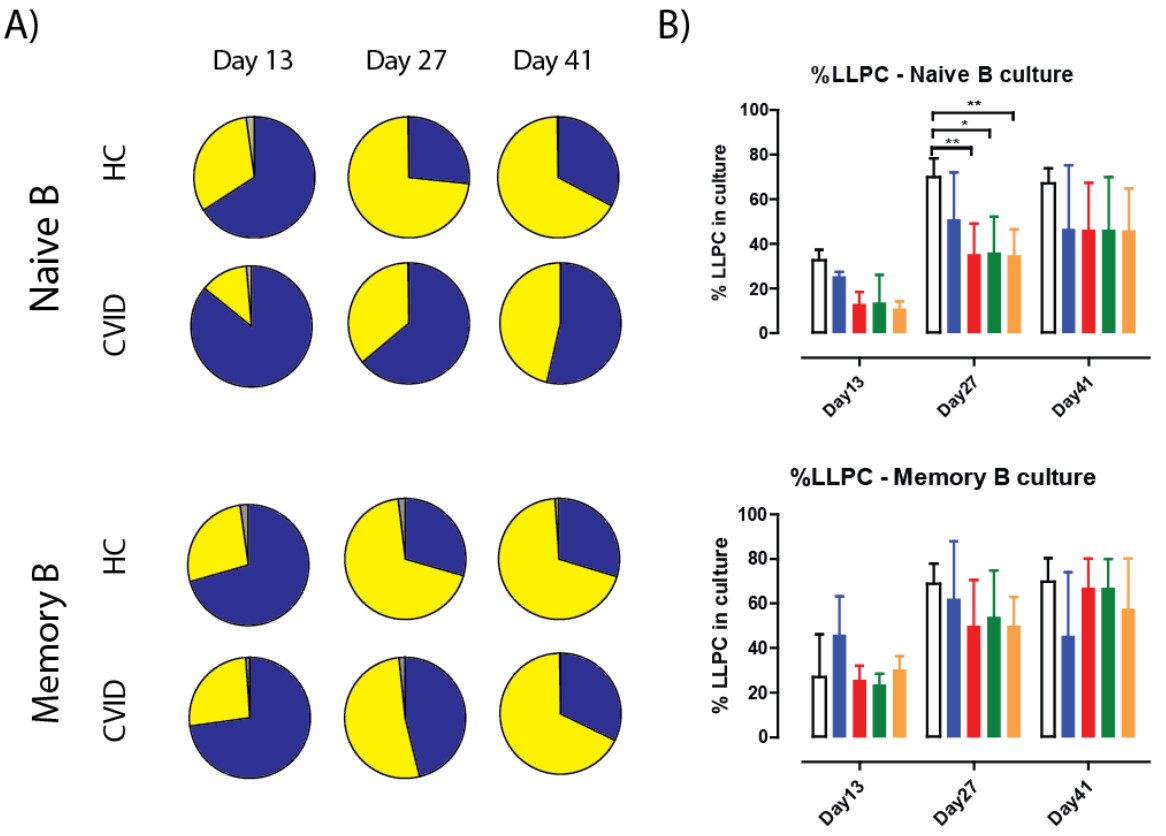

Figure 32. Maturation from CD138^{-ve} to CD138^{+ve} plasma cells.

(A) The proportion of SLPC (Blue) and LLPC (Yellow) within naïve and memory cultures at Day 13, Day 27 and Day 41 are shown in a series of piecharts. (B) The proportion of LLPC in cultures from naïve and memory cultures at Day 13, Day 27 and Day 41 of healthy donors (n=10-6), disease controls (n=4-2), CVID (n=14-8), Group1 patients (n=7-5) and Group2 patients (n=7-3) are depicted. Some cultures died out before Day 41 and the minimum (n) is reflected by the latter number. Statistical differences are highlighted by *, ** or *** (two tailed Mann-Whitney U test).

4.3.2 Surviving LLPCs demonstrated normal immunoglobulin production, gene expression and survivability.

Unlike many other primary antibody deficiencies, both clinical and *in vitro* data suggest that the failure of antibody production is only partial in CVID. Hence, the subpopulation of phenotypically normal LLPCs seen in the previous experiment could be functionally normal, preventing the complete collapse of the antibody producing machinery. To characterise this LLPC-like subpopulation, their survivability, immunoglobulin production and the expression of key B-cell transcription factors were further examined.

4.3.2.1 Survivability of plasma cells

Survivability was measured by the proportional change in SLPCs and LLPCs over the three time points (Day 13, Day 27 and Day 41). The cell counts on Day 13 were used as starting counts (100%). Equivocal proportional decline in SLPCs and LLPCs were noted in all groups (Figure 33). The proportional increase in memory-derived LLPCs in healthy controls was transiently higher at Day 27, possibly secondary to more efficient conversion from the initial plasmablast pool or continued upregulation of CD138 expression during this period. However, no statistical significance was observed (2-way ANOVA). Overall, the small proportion of CVID B-cells that had successfully upregulated the cardinal phenotypes of plasma cell appeared to retain normal survivability.

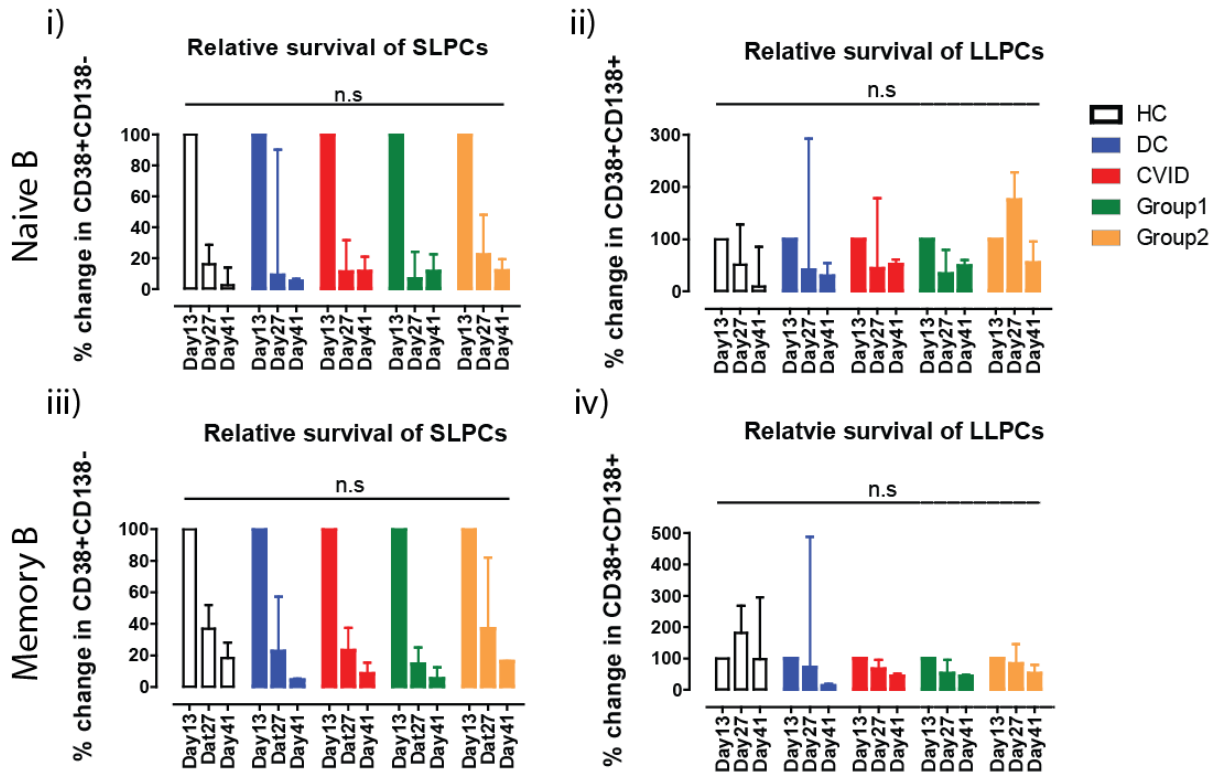

Figure 33. Survivability of plasma cells over 6 weeks.

SLPC (7-AAD$^-$CD20$^-$CD27$^+$CD38$^+$CD138$^-$) and LLPC (7-AAD$^-$CD20$^-$CD27$^+$CD38$^+$CD138$^+$) counts within naïve and memory cultures on Day 13, Day 27 and Day 41 were determined on flow cytometry using counting beads. Survivability was determined by the percentage changes in cell counts over the three time points. Medians and interquartile ranges are shown (2-way ANOVA).

4.3.2.2 Immunoglobulin production of plasma cells

Immunoglobulin production was measured from supernatant harvested from the bottom transwell chambers of the plasma cell cultures using sandwich ELISA between Day 6 and Day 41. IgM outputs by differentiated naïve and memory B-cells were similar between healthy controls and patients. Conversely, IgG and IgA production by both differentiated naïve and memory B-cells were significantly lower in patients (Figure 34). Given that there were large numerical discrepancies of surviving cells within each culture potentially confounding the results, IgM, IgA and IgG output were

further corrected to the total number of PCs (SLPCs + LLPCs) within the corresponding cultures on Day 13, Day 27 and Day 41. The difference in IgG production between healthy controls and patients was normalised by correcting to the number of plasma cells within the cultures; indicating that the reduction in IgG largely reflects a decrease in plasma cell number, rather than a true functional deficit in secretion amongst plasma cells . However, the reduction in IgA production was not attributed to the falling cell count, suggesting IgA deficiency may be deep-rooted in CVID (Figure 35). The intrinsic deficiency in IgA production continue to support that selective IgA deficiency (sIgAD) and CVID are related disorders [318].

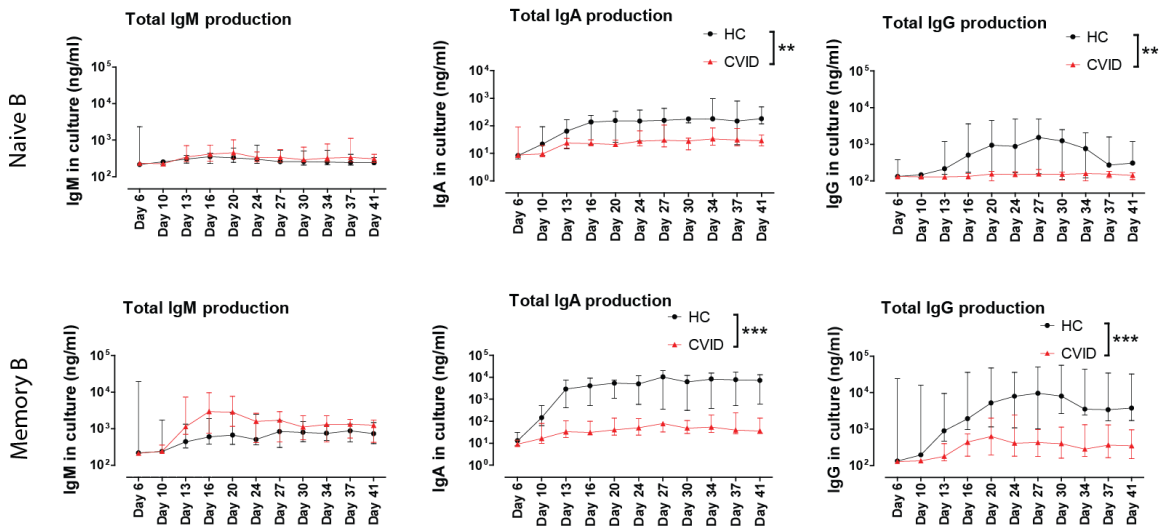

Figure 34. Immunoglobulin production by 6-week plasma cell culture.

Supernatant was collected from the bottom transwell chamber of plasma cell cultures between Day 6 to Day41, every 3.5 days. Sandwiched ELISA was used to measure the total amounts of IgM (left), IgA (middle) and IgG (right) in the naïve and memory cultures according to a reference serum (HC, n=10-6; CVID, n=14-8). Statistical differences between groups were calculated by 2-way ANOVA. Medians and interquartile ranges are shown. Statistical significance are indicated as *p<0.05, **p<0.01, ***p<0.001.

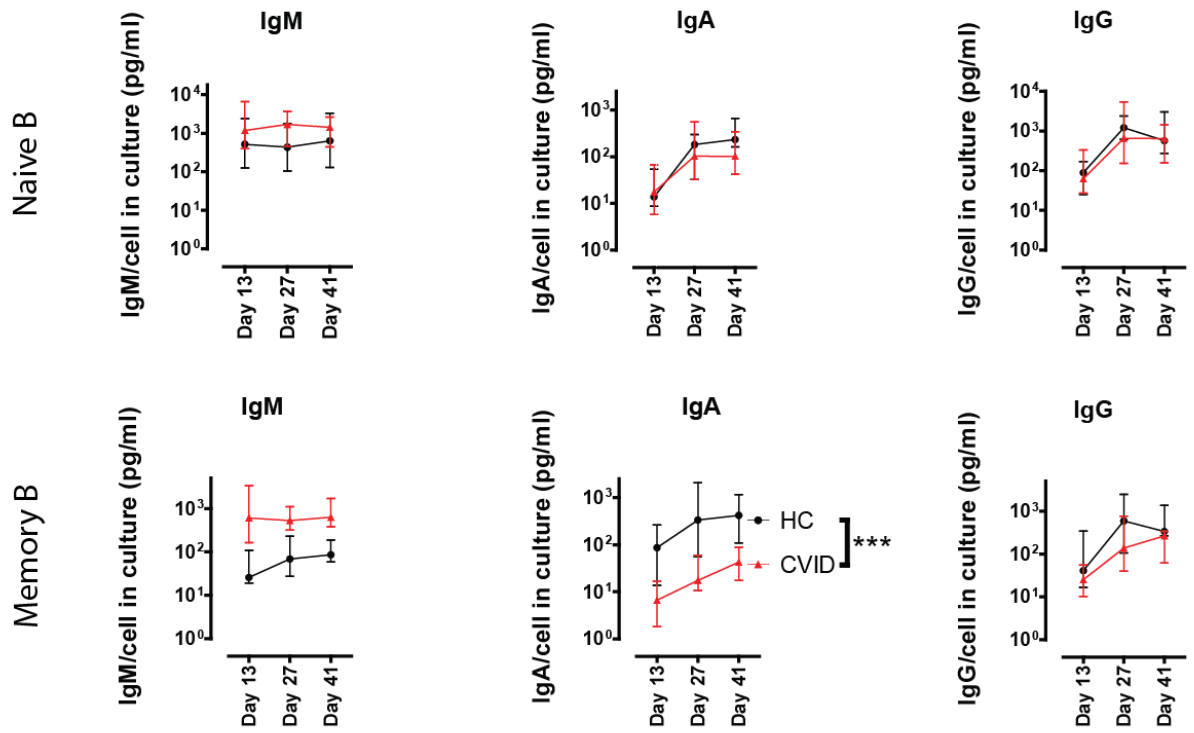

Figure 35. Immunoglobulin production per plasma cell.

IgM, IgA and IgG were corrected to the total of SLPCs and LLPCs in cultures on Day 13, Day 27 and Day 41 (HC, n=10-6; CVID, n=14-8). Statistical differences between groups were calculated by 2-way ANOVA. Medians and interquartile ranges are shown. Statistical significance are indicated as *p<0.05, **p<0.01, ***p<0.001.

4.3.2.3 Gene expression of plasma cells

For key B-cell transcription factors, mRNA from memory B-cell cultures was harvested at Day 13 for qPCR gene expression studies. Regretfully, insufficient material could be retrieved from the naïve cultures for this part of the analysis. Consistent with normal plasma cell differentiation, we observed significant up-regulations of *BLIMP1*, *XBP1* and *IRF4* and down-regulations of *PAX5* and *BCL6* under our experimental conditions. However, equivocal expression of *BLIMP1*, *XBP1*, *IRF4*, *PAX5* or *BCL6* was noted between healthy controls and patients (Figure 36). Despite being much less abundant,

our data suggest that the subpopulation of phenotypically normal LLPCs in CVID have normal survivability, gene expression and IgG production. Together with the acquisition of an appropriate phenotype and retained IgG secretion capacity argues that much of the capacity to initiate and execute the plasma cell programme is retained.

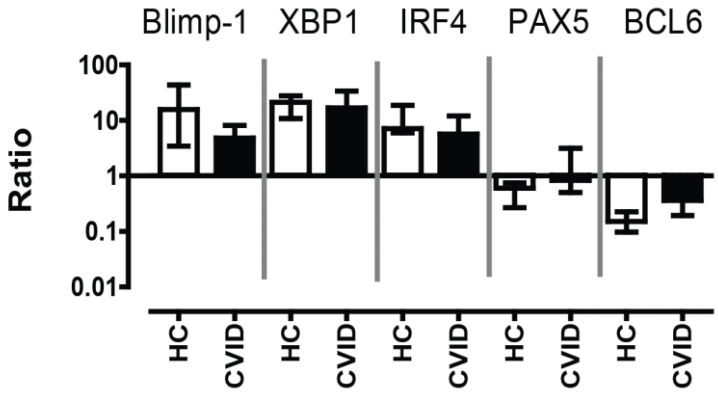

Figure 36. Cultured plasma cell gene expression in healthy donors and CVID patients.

Memory-derived plasma cell cultures were harvested on Day 13 for qPCR. Gene expression ratio ($2^{\Delta\Delta CT}$) of *BLIMP-1*, *XBP1*, *IRF4*, *PAX5* and *BCL6* were calculated using endogenous (average of beta-Actin and GAPDH) and undifferentiated controls (Day 0 Naïve B-cells), HC: n=5 and CVID: n=5. Medians and interquartile ranges are depicted. Statistical differences are highlighted by *, ** or *** (two tailed Mann-Whitney U test).

4.4 Discussion:

This chapter examines the B-cell terminal differentiation potential and long term plasma cell survival in CVID. By inducing the cardinal phenotype for long-lived plasma cell (LLPC), this experiment represents a better model for baseline antibody level than short term activation of B-cells. Despite being the majority population in CVID, the data show that only a fraction of CVID naïve B-cells could be activated and successfully differentiated into LLPCs. By contrast, despite low frequency in peripheral blood, reactivation of memory B-cells was only moderately affected with better preserved gene expressions, phenotype adaptation and antibody production observed. In keeping with the majority of the published data, the findings of this chapter continue to support that sIgAD and CVID are related disorders [318].

Together with the results from the T-cell experiments in Chapter 3, an arrest in or aberrant lymphogenesis is supported. Although KREC was not directly examined in this study, the data would be consistent with previous work that the maintenance of the naïve B-cell population in CVID would rely more heavily on homeostatic proliferation, subjecting B-cells to a multitude of failure including terminal differentiation.

One of the potential limitations of the current experimental design was that class-switched and non-switched memory B-cells were not independently examined. Murine and human studies had demonstrated their distinct functions and differentiation potentials [319]. Although not statistical significant, slightly inferior PC generation in Group2 CVID patients was observed. Group2 closer resembles the features of the Freiburg 1a classification with patients having lower frequencies of class-switched memory B-cells, providing a plausible explanation of their inferior ability to generate PC. However no correlations between this B-cell subset with LLPC and immunoglobulin outputs was found. Nevertheless, it would be extremely difficult to obtain enough material to culture class-switched and non-switched memory B-cells separately in order to address this question.

Although memory B-cells from CVID patients demonstrated less profound deficiencies *in vitro*, the numerical reduction in class-switched and non-switched memory B-cells in peripheral blood poses as a significant paradox to the current conjecture. Ample immunophenotypic data in the literature reported the reduction of class-switched memory B-cells in peripheral blood, which is currently considered to be the most important B-cell finding for CVID [19, 174, 177]. The data currently do not provide any insights if the suspected attenuated naïve B-cell population could effectively develop into memory B-cells. Meanwhile, the maintenance and *in vivo* half-life of memory B-cells is highly complex; a matter under debate of whether re-encounter of antigens is necessary for the long term survival of these cells [320]. Further work is required to address this question.

Histological reports have previously demonstrated a block between the plasmablast stage and the LLPC stage in CVID patients [220]. Although the origin of these intermediate cell types was not clear, it is possible that they represent those partially differentiated naïve B-cells shown in this chapter. Regretfully, insufficient material could be retrieved from the naïve B-cell cultures to accurately determine their gene expression, in particularly for *BLIMP1,* but further transcriptome analysis should help in confirming this. For memory B-cells, the acquisition of an appropriate phenotype and retained IgG secretion capacity argues that much of the capacity to initiate and execute the PC programme is retained.

Overall, the data hinted that some naïve and most memory circulating B-cells were able to differentiate into fully functional LLPCs, highlighting the possibility of a mixture of healthy and attenuated cells within the B-cell pool. The presence of a minority healthy population would explain for the residual baseline antibody level we observed clinically. This observation is consistent with the majority of functional B-cell studies in CVID, demonstrating partial deficiencies. While clonality may explain mosaicism in the population, it contradicts with the polyclonal nature of B-cells in CVID which has been widely reported [321]. Yet, clonality may occur at various levels during lymphogenesis and events occurred prior to the process of VDJ-rearrangement would not be reflected in IgH profiling, an area that warrant further investigations.

4.5 Summary and conclusion

Similarly to other parameters of B-cell function, this chapter demonstrated a terminal differentiation defect in CVID naïve B-cells for which many were unable to reach or survive as LLPCs. Despite normal peripheral blood count, naïve B-cells were more severely affected than memory B-cells. The combination of reduction in thymic output and abnormal B-cell function appoints to a possible defect in a common progenitor. While a germline genetic defect often affects the entire haematopoietic system, we observed *in vitro* preservation of normal functions in a proportion of lymphocytes, in particular memory cells. To explain the observed T-cell and B-cell deficits, I further hypothesised that a clonal defect occurred in a common lymphoid progenitor stem cell, leading to downstream failure to respond to *de novo* antigens in CVID.

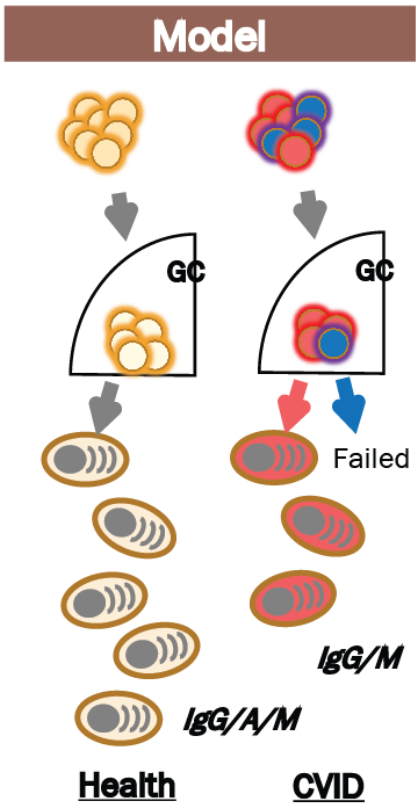

Figure 37. Model of Pre-VDJ clonality in CVID.

Chapter 5

5. Clonal haematopoiesis identified in patients with Common Variable Immunodeficiency.

So far, the studies of T-cells and B-cells of CVID patients are pointing toward a defect before or at the common progenitor level. An acquired arrest in normal lymphogenesis is possible given that the majority of patients presented in adulthood. Within the haematopoietic system, the acquisition of a significant aberrant population is often a result of clonal expansion of a pre-malignant or malignant cell and parallel comparison may be drawn with myelodysplasia, leukaemia and lymphoma [322]. Although the previous experiments were not dissected down to the single cell level, the concept of haematopoietic clonality provides a plausible explanation for many of clinical and experimental findings in CVID, particularly when heterozygosity or partial attenuations were seen, warranting further investigations.

5.1 Abnormal haematopoiesis and clonal haematopoiesis

Clonality within the haematopoietic system is frequently referred to the antigen receptor level (TCR/IgH) [292]. Experimental data, including data from Chapter 3, have shown that T-cells or B-cells are largely polyclonal or oligoclonal in CVID [252, 321]. However, clonality prior to the level of VDJ-rearrangement would not be reflected by TCR or IgH profiling and would be more consistent with an early progenitor defect affecting both lineages. Conforming to the hypothesis of an early

defect, abnormal functions in other lineages such as impaired differentiation, maturation antigen presentation and cytokine profile by dendritic cells and monocytes were shown previously [323-325]. Although autoimmune cytopenia is commonly associated with CVID, both autoimmune haemolytic anaemia and idiopathic thrombocytopenia purpura are mediated through autoantibodies, accelerating the destructions of target cells [326, 327]. An autoantibody mediated disorder however contradicts with the essence of an antibody deficiency, warranting an alternative explanation such as the general failure in bone marrow output.

Direct studies of bone marrow of CVID patients are limited. By examining mononuclear cells from bone marrow biopsies of 11 CVID patients, Isgro *et al* demonstrated a reduction in $CD34^{+}CD38^{-}DR^{+}$ cells, an altered stromal cell composition and abnormal cytokine production (high TNFα and low IL-2) [273]. Mast cells, basophils and eosinophils have yet to attract any major research interests in CVID and their roles remain to be determined. Overall, an early progenitor defect has long been postulated (Figure 38).

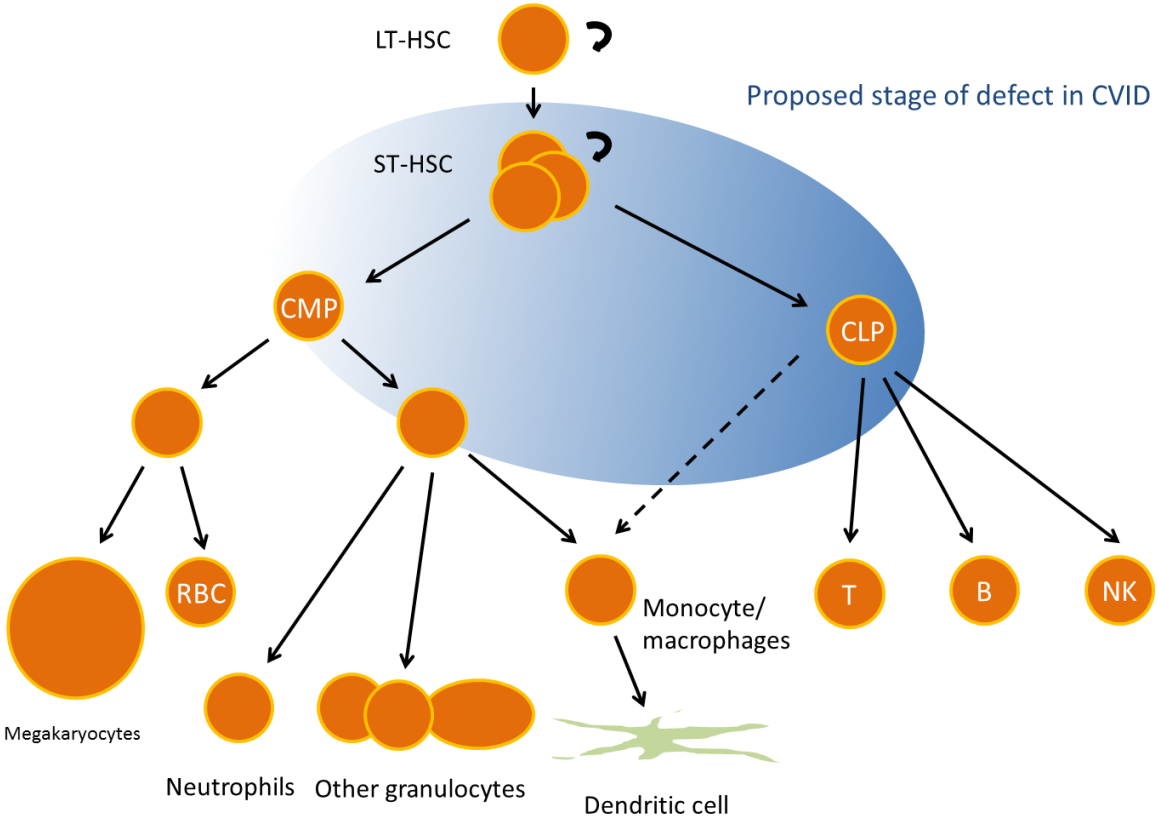

Figure 38. Human haematopoiesis and proposed area of defect in CVID.

The blue zone represents the proposed area of defect with darker shade indicating higher likelihood. CLP = common lymphoid progenitor, CMP = common myeloid progenitor, LT-HSC = long term haematopoietic stem cell, ST-HSC = short term haematopoietic stem.

Clonality at the early progenitor level is best described by the process of clonal haematopoiesis. Similar to monoclonal gammopathy of uncertain significance (MGUS) and monoclonal B-cell lymphocytosis, clonal haematopoiesis is a natural phenomenon within the haematopoietic system. A significant survival advantage over the other progenitors is acquired via somatic mutation by a single haematopoietic stem cell or early progenitor, allowing it to eventually dominate the bone marrow and all of its progenies. This process is relatively rare below the age of 55 but becomes exponentially more common with advancing age. Genomics studies across both sides of the Atlantic have recently estimated that close to 20% of age >90 years may demonstrate clonal haematopoiesis. The initial

driver mutations (DNMT3A, TET2, and ASXL1 etc) often results in more aggressive proliferation and anti-apoptotic activities, leading to acceleration in physiological mutation rate within the haematopoietic compartment [328]. Although majority of the individuals are symptomatic, this process has been linked to increased risk of myelodysplasia, haematological malignancies, acquired aplastic anaemia and paroxysmal nocturnal haemaglobulinaemia [329-331]. Could clonal haematopoiesis also predispose patients to develop CVID and explain its subsequent increased risk of B-cell lymphoma?

Thus now, we have largely discussed how clonality could result in the loss of function, but the reverse may also occur. Revertant mutation has been reported in a number of germline genetic diseases, such as epidermolysis bullosa and leukocyte adhesion deficiency type 1, leading to mosaicism and partially restoring normal functions [332, 333]. This would theoretically allow CVID patients with germline genetic mutations to regain a fraction of their humoral and cellular functions (Figure 39). However revertant mutation is exceedingly rare and is difficult to reconcile its occurrence in the majority of CVID patients as shown in Chapter 4.

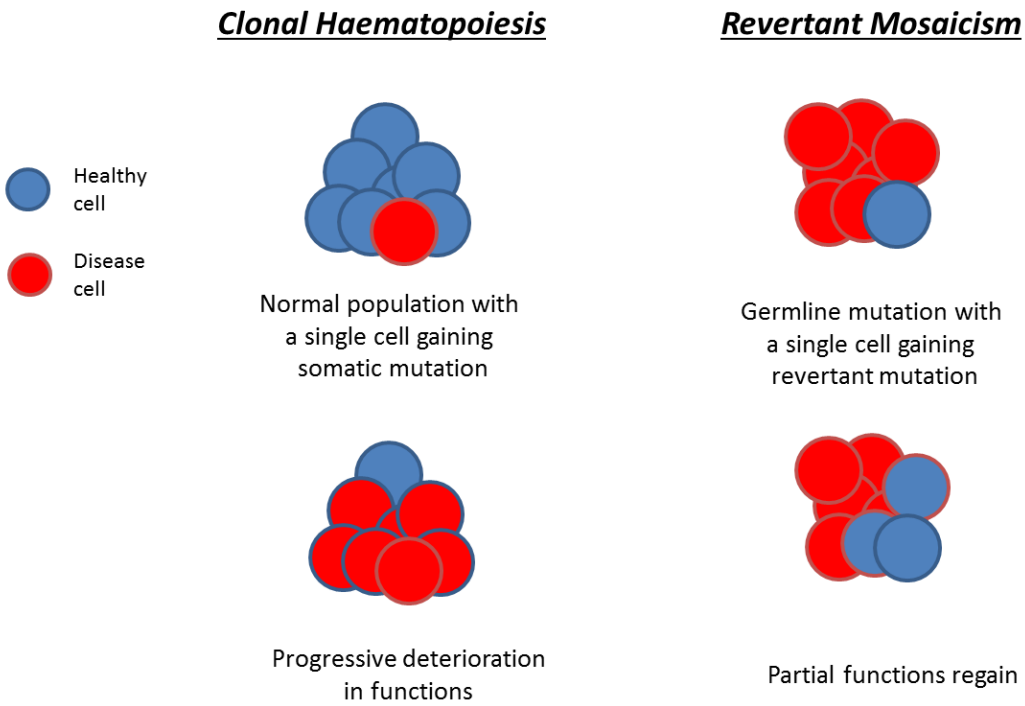

Figure 39. Clonal haematopoiesis v Revertant mosaicism.

This final part of the thesis will test if clonality at the earlier progenitor level could be demonstrated in CVID and whether the process of clonal haematopoiesis could predispose the development of disease.

5.2 Epigenetic anaylsis via X-chromosome inactivation

5.2.1 HUMARA assay: a screening test for early clonality

To balance gene expression on the X-chromosomes in female, one X-chromosome is inactivated via DNA methylation during early embryogenesis. This process exclusively occurs in female since male only carry one X-chromosome. An individual cell at that stage may inactivate either one of the X-chromosomes randomly and this epigenetic phenomenon is retained by its descendants. Hence, all progenies of that cell will have the same X-chromosome inactivated [334]. A number of assays have exploited this unique property to measure clonality targeting highly polymorphic genes (e.g. phosphoglycerate kinase, hypoxanthine phosphoribosyltransferase, DXS255 and androgen receptor) located on the X-chromosome which can be differentiated and quantified by fluorescent based capillary reaction. Since the process of methylation protects DNA from being digested by restriction enzymes, the incubation with a restriction enzyme will allow downstream PCR and capillary reaction to detect only the inactivated allele (Figure 40). Of all assays, the HUMARA assay (androgen receptor) has gained the most popularity and is being integrated into routine clinical testing for myeloid leukaemia. According to large data sets, X-chromosome skewing is distributed in a Gaussian fashion in the general population, peaking at 50%:50%, though extreme skewing may be found in a small proportion of elderly females [335]. Abnormal skewing ratio detected by the HUMARA assay has been shown as a useful screening tool for solid and haematological tumour clonality, marking the

abnormal proliferative events [336]. The HUMARA assay does have limitations with reports showing problems with incomplete enzyme digestion, uneven PCR amplification of different alleles, discordance with other loci on the X-chromosome and its inability to measure clonality in male [334, 337].

Recently, other methods have been developed to measure bone marrow clonality such as quantitative transcriptional assay (qTCA) based on determination of allele-specific ratios of a number of X-chromosome genes and variant allele fraction calculation using whole exome sequencing [330, 338]. These methods are more definitive but are significantly more costly. Although not definitive, the HUMARA assay remains a simple and quick screening tool for clonality.

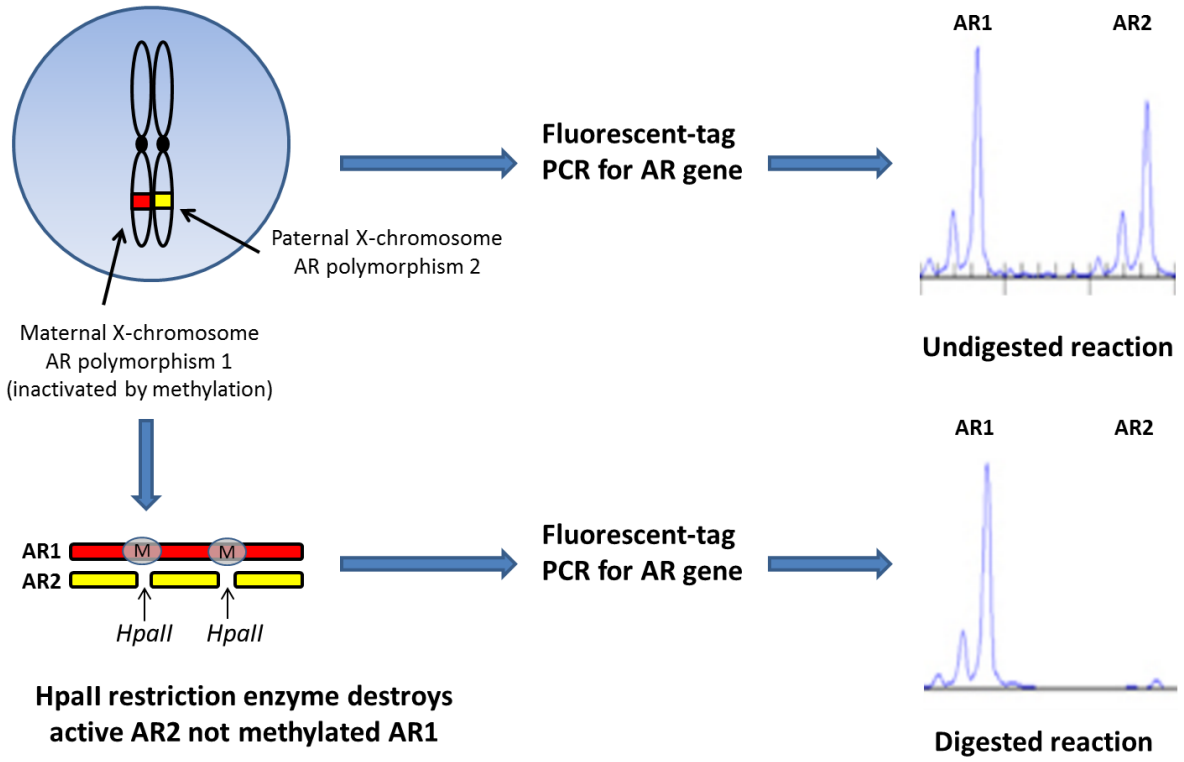

Figure 40. Schema for HUMARA assay.

The assay takes advantage of the high polymorphic CAG repeat region of the androgen receptor allowing the maternal and paternal alleles to be detected at separate positions during capillary reaction. The application of HpaII restriction enzyme destroys the active allele leaving only the methylated inactive allele for PCR amplification and detection. Result is compared with an undigested PCR reaction demonstrating equal expression of both alleles is used in order to estimate the level of skewing. Example of a highly skewed sample with complete dominance of the paternal allele is illustrated.

5.2.2 Precision and stability of HUMARA assay.

Given the potential limitation of the HUMARA assay, the reproducibility of the in-house assay was tested. The inter-run variability was examined by replicate testing of a DNA sample extracted

from whole blood of a healthy donor. All five results demonstrated very similar degree of X-skewing suggesting the assay is highly reproducible. Similarly, DNA samples of 7 individuals were taken 6 weeks apart to determine the stability of X-skewing. No significant changes in X-skewing ratios were seen in any of the donors (Figure 41). Although the accuracy and other intrinsic limitation cannot be addressed, these data provide reassurance that the HUMARA assay is suitable for screening clonality does not generate random results.

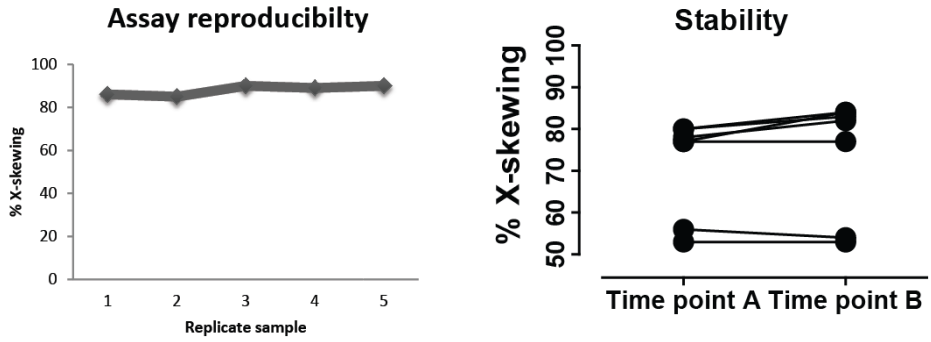

Figure 41. Reproducibility and stability of HUMARA assay.

(Left) Replicate testing of a whole blood DNA sample was conducted to demonstrate assay reproducibility. (Right) Paired whole blood DNA samples were collected 6 weeks apart to demonstrate assay stability (n=7).

5.3 X-inactivation in CVID.

5.3.1 Abnormal X-chromosome skewing by HUMARA assay indicates clonality before VDJ rearrangement in CVID.

Whole blood DNA was extracted from age-matched healthy females and female CVID patients as X-skewing was reported to increase with age (mean age/SEM; HC = 46.75+/-2.51, CVID = 49.72+/-3.15, Group1 = 54+/-4.57 and Group2 = 43.9+/-3.93). X-skewing ratios were determined by the HUMARA assay and corrected using paired undigested controls. Analysis of 22 healthy donors and 23 CVID patients showed marked skewing in CVID patients (mean dominant allelic frequency/SEM; HC = 66.25 +/- 2.35%, CVID = 76.26 +/-3.16%, p = .0253). Consistent with the literature, skewing was only seen in minority of health donors 2/22 (9.1%) but 11/23 CVID patients (47.8%) exhibited moderate to high skewing (>80%). Interestingly, exaggerated skewing was predominately seen in Group1 patients while X-skewing in Group2 patients did not significantly differ from healthy donors (Group1 = 81.98 +/- 3.64%, p = .0016; Group2 = 70.02 +/- 4.74%, p = .6884). A few patients within Group2 did demonstrate extreme skewing suggesting that the differentiation by clinical phenotype may be imperfect. Despite being age-matched, the greater tendency of CVID patients expressing high X-skewing towards 100% supports the presence of clonality prior to VDJ-rearrangement (Figure 42).

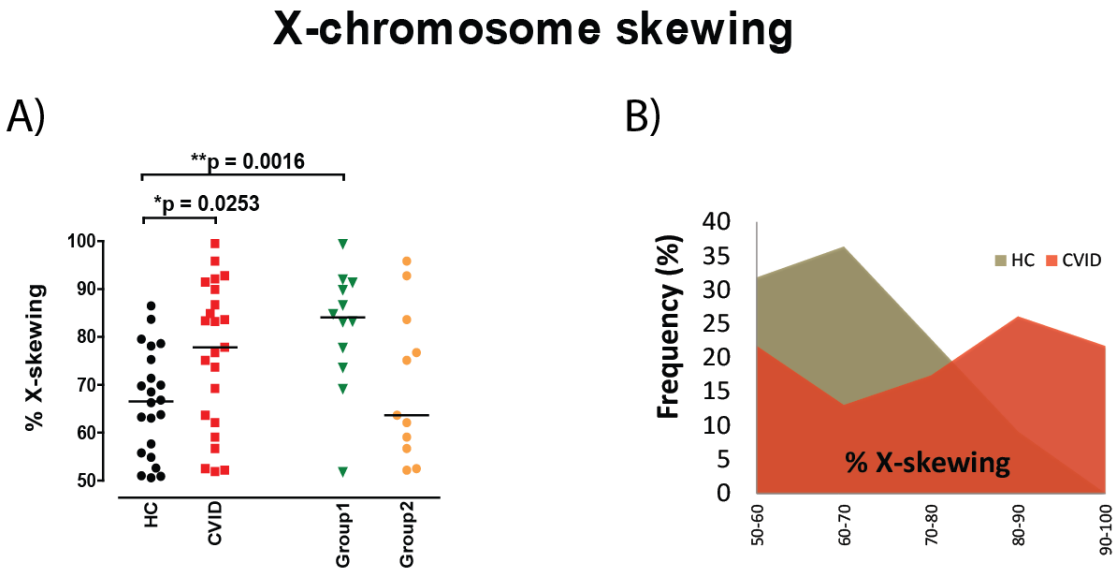

Figure 42. Exaggerated X-chromosome skewing in CVID.

X-chromosome skewing of whole blood DNA was determined using the HUMARA assay. (A) X-skewing was corrected by the matching undigested control. Results of HC (black: n=22), CVID (red: n=23), Group1 patients (green: n=12) and Group2 patients orange: n=11) females are shown. Medians and interquartile ranges are depicted. Statistical differences are highlighted as *, ** or *** (two-tailed Mann-Witney U test). (B) The frequencies of X-skewing of HC (grey) and CVID (red) are shown in a histogram with CVID demonstrating greater tendency towards 100% skewing.

5.3.2 Partial plasma cell generation and IgG production retained by patients with exaggerated X-skewing.

To determine a possible relationship between X-skewing and the failure of humoral immunity, pre-treatment baseline antibody levels and plasma cell generating ability of patients were further examined. Patients were sub-divided into skewed (≥80%) or non-skewed (<80%) groups. The data show that higher levels of baseline IgG and IgA can be seen in skewed patients, whilst equivocal IgM production was noted between the two groups. To further support this, naïve ($CD27^-$) and memory

($CD27^+$) B-cells of patients with ≥80% skewing demonstrated greater ability in generating $CD20^-$ $CD27^+CD38^+CD138^+$ long-lived plasma cells with the greatest difference was seen from the naïve culture on Day 13 ($p = 0.0357$). Although the remaining results did not achieve statistical significance, biological differences were detected (Figure 43).

Hence, the data suggest those patients with exaggerated X-skewing are likely to retain a degree of plasma cell function and clinically present with a partial failure of antibody production and recurrent infections. Furthermore, this observation is consistent with the presence of an aberrant clonal population preventing full humoral functions. By contrast, gross failure of the antibody producing machinery is seen in patients with normal X-chromosome ratios and higher incidence of immune dysregulation, representing a separate group with global intrinsic defect within all lymphocytes.

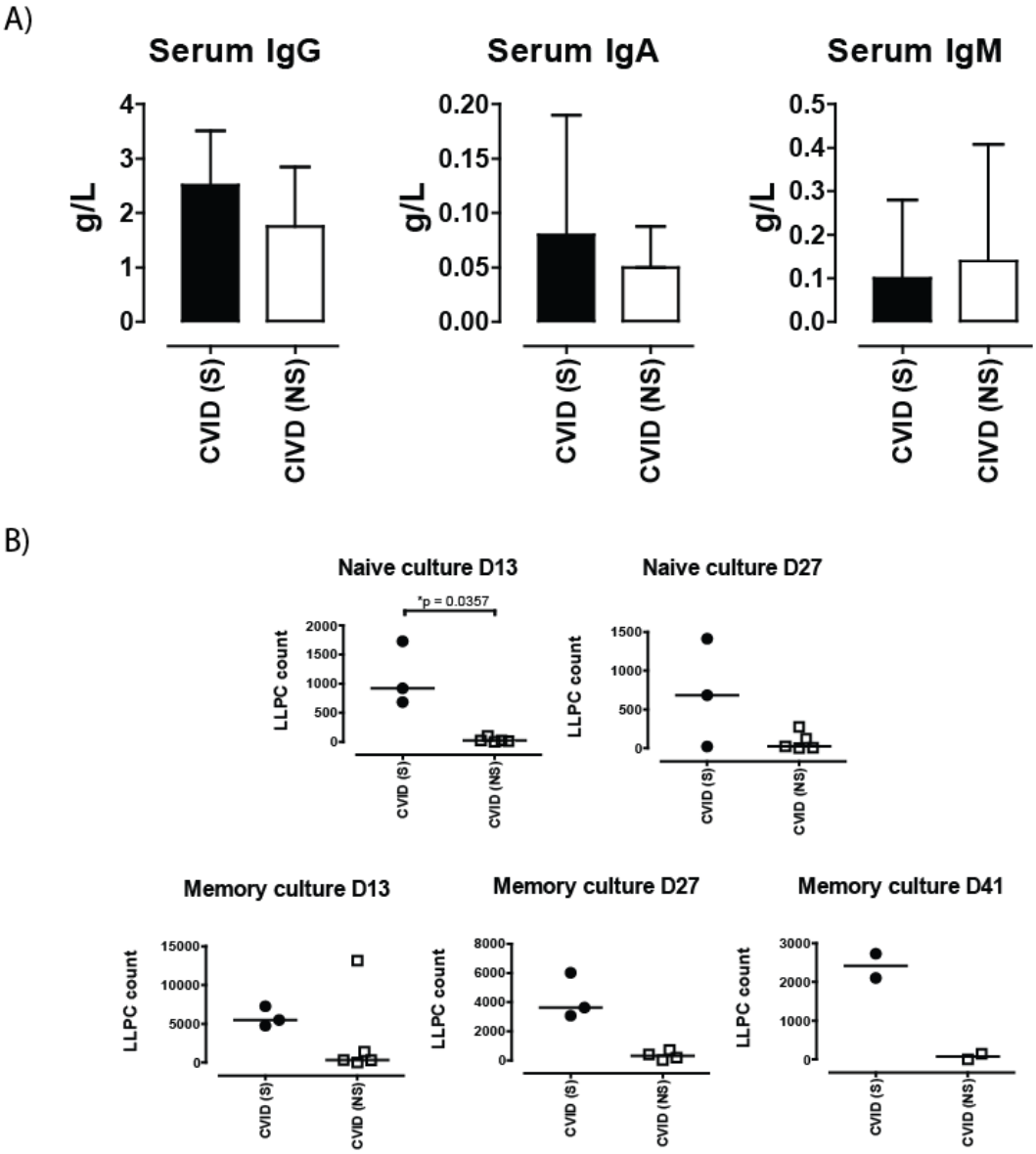

Figure 43. X-skewing and antibody production.

(A) Pre-immunoglobulin replacement therapy baseline serum IgM, IgA and IgG of skewed (S:≥80% skewing, black, n=10) and non-skewed CVID patients (NS:<80% skewing, white, n=11) are shown. (B) Long-lived plasma cells (LLPC: $CD20^{-}CD27^{+}CD38^{+}CD138^{+}$) are generated from isolated naïve or memory B-cell from skewed and non-skewed CVID patients as previously described. LLPC counts within the naïve and memory B-cell cultures on Day 13, Day27 and Day 41 are shown. Medians and interquartile ranges are depicted. Statistical differences are highlighted as *, ** or *** (two-tailed Mann-Witney U test).

5.4 Dissecting the origin of X-skewing in CVID

5.4.1 Exaggerated X-skewing in CVID originates from the early progenitor to stem cell level.

Given the diversity within the haematopoietic system, various haematopoietic linages were examined independently in order to pinpoint the origin of the observed X-skewing. First, whole blood was separated into lymphoid and myeloid lineages using density gradient centrifugation. PBMCs above the Ficoll layer were collected to represent the lymphoid lineage while granulocytes immediately above the red cell layer were collected to represent the myeloid lineage.

Consistent with our hypothesis of an early progenitor defect, similar skewing ratios from both the myeloid and lymphoid compartments were seen within each individual and largely reflected skewing observed in whole blood analysis of Group1 and Group2 CVID patients ($r^2 = 0.7701$) (Figure 44). This suggests that clonality occurs before the lymphoid progenitor stage and is imprinted at the level of the short lived to long-lived haematopoietic stem cell (HSC) stages prior to differentiation into distinct lineages; clonal haematopoiesis. Moreover, we noted that skewing was greater in the myeloid compartments and this imbalance was largely observed in Group1 patients. While HSCs are responsible for the continuous output of all immune cells, the lymphoid compartment has a longer half-life and may retain memory cells from decades ago. By contrast, cells in the myeloid compartment represent relatively recent outputs from the bone morrow and have a rapid turnaround time. Thus, the imbalance of myeloid versus lymphoid skewing hinted on the timing of the onset of the clonal event.

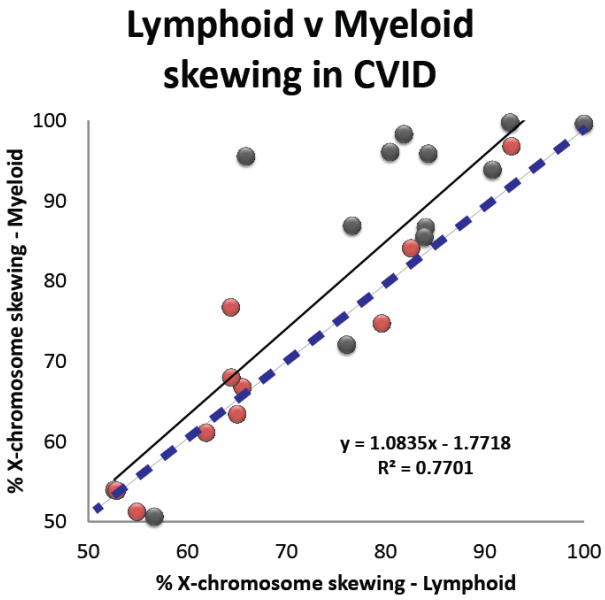

Figure 44. X-skewing of myeloid and lymphoid compartments of CVID patients.

X-chromosome skewing of granulocytes and PBMCs of CVID were analysed separately and depicted accordingly patients (n=23; Group1, n=12, grey; Group2, n=11, red). Each dot presents the myeloid and lymphoid skewing of a patient. Linear regression (black line) and r^2 are shown; whilst the blue dashed line represents a theoretical 1:1 ratio.

5.4.2 Clonality isolated within the haematopoietic system but not in non-blood tissues.

So far, our data suggest that clonality in CVID may be detectable as early as the common progenitor level. To test if this clonal signature is unique to the haematopoietic compartment, buccal samples were used as surrogate germline (non-blood) tissue for comparison. Matching buccal and blood samples from 5 healthy donors and 10 patients demonstrating higher degree of X-skewing were analysed. The skewing ratios in the blood were corrected to the expected ratios observed in the buccal sample (Figure 45). Interestingly, all 5 healthy donors exhibited very similar level of X-skewings in the blood and buccal tissue, suggesting their X-skewings were inscribed during early embryonesis as a result of random X-inactivation; primary X-chromosome skewing. By contrast, 50% of CVID patients

demonstrated discrepancy in blood vs buccal X-skewing with much higher skewing observed in blood. Correcting the blood X-skewing ratios by the expected buccal ratios showed that the dominant allele might be as high as 7 times of its expected frequency. Altogether, our data suggest that the epigenetic signature of X-skewing was unique within the haematopoietic system in some CVID patients and that the defect was unlikely to occur at the germline level. This new piece of evidence supports that some CVID are acquired though genetic or epigenetic changes during life.

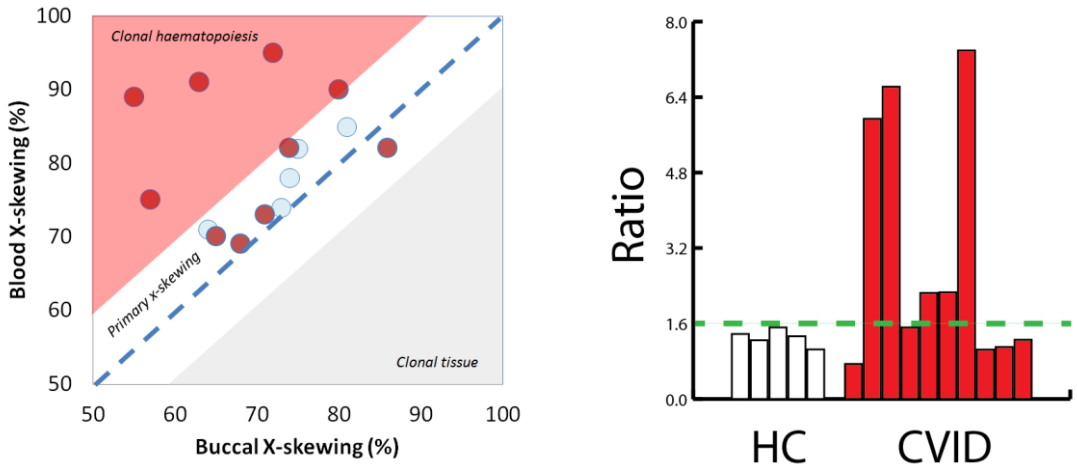

Figure 45. Clonal haematopoiesis in CVID but primary X-chromsome skewing in healthy donors.

(Left) X-skewing by the HUMARA assay was compared between matching blood and buccal samples of healthy donors (n=5, light blue circles) and CVID patients (n=10, red circles) who had previously demonstrated high level of X-skewing in their whole blood analysis. The dotted blue line represents a theoretical 1:1 ratio. Dots in the white zone are considered to have primary X-chromosome skewing while dots in the pink zone are considered to have clonal haematopoiesis. (Right) The X-skewing ratios in the blood were corrected to the expected ratios observed in the buccal sample and depicted as a barchart (HC=white, CVID=red). A ratio of >1.6 (green line) was considered to be highly abnormal.

5.4.3 Higher level of clonality demonstrated with lineages associating with more recent bone marrow egress.

If clonal proliferation of an early progenitor occurred during life in CVID, I further hypothesise that clonality would vary between immune sub-populations with more ancient populations being less affected. To test this, peripheral blood was separated into granulocytes, PBMCs, naïve B-cells and memory B-cells to represent various immunological time points. The X-chromosome skewing of granulocytes, PBMCs, naïve B-cells and memory B-cells were corrected according to the matching buccal sample (Figure 46A). Surprisingly, little changes in skewing ratio were seen in all leukocyte subsets of healthy donors when compared to the baseline buccal skewing. However, a completely difference picture was observed in CVID patients. In CVID, clonality was not uniformly distributed across all leukocyte subsets and the greatest effect was seen amongst granulocytes that represent the most recent bone marrow emigrants. Furthermore, clonality decreases in a step-wise fashion with more ancient populations (Figure 46B). Interestingly, despite presenting in low frequency in the peripheries in CVID, memory B-cells were almost unaffected, suggesting that they were predominantly derived from progenitors prior to the event that caused skewing in the common progenitor. The data, hence, indicate that the process of clonal haematopoiesis might have driven the failure of humoral immunity over time. Similar clinical presentation can be seen in patients demonstrating clonal haematopoiesis, with most patients having stable hypogammaglobulinaemia over a number of years, normal B-cell counts (Table 6).

Overall, this data supports that the possibility of a clonal acquired defect occurring in a progenitor in CVID, that would be invisible to low-depth genomics approach. Moreover, the variable degree of clonality across the haematopoietic system argues that a residual healthy polyclonal population continue to factor in various immune compartments.

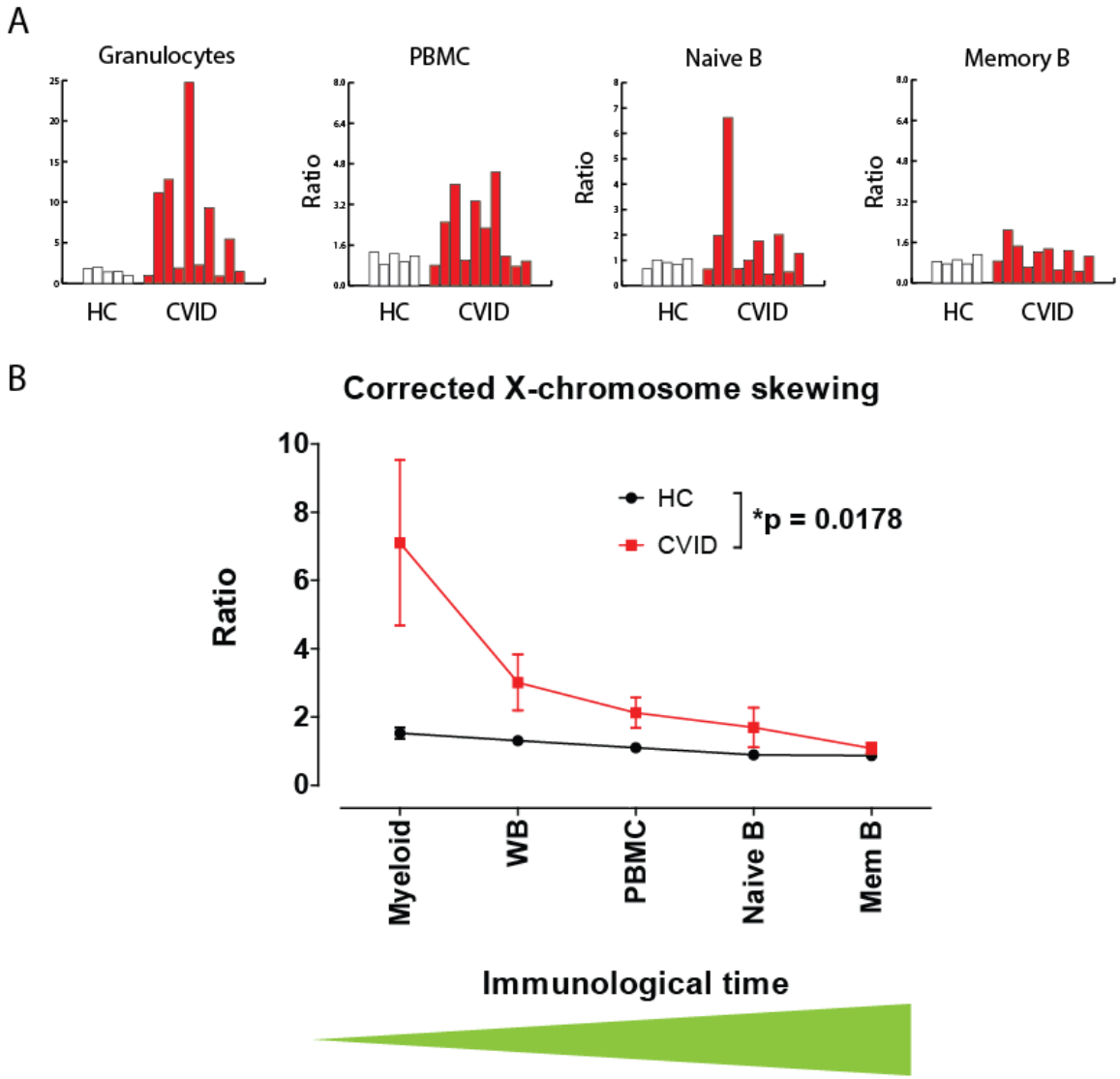

Figure 46. Clonal haematopoiesis and X-skewing through immunological time.

(A) Using buccal X-skewing as baseline, the ratio of allele 1 and allele 2 in granulocytes, PBMC, naïve B-cells ($CD27^-$) and memory B-cells ($CD27^+$) were corrected by the expected value obtained from the matching buccal tissue (HC, n=5, white; CVID, n=10, red). (B) Corrected X-skewing ratios are plotted against immunological time with granulocytes representing the most recent outputs from bone marrow and memory B-cells representing most ancient outputs. Mean and SEM are shown and statistical significance highlighted by *, ** or *** (HC, n=5; CVID, n=10; 2-way ANOVA).

Patient no.	Age of presentation	IgM g/L	IgA g/L	IgG g/L	Bronchiectasis	Massive splenomegaly, lymphadenopathy	Autoimmune, inflammatory complications	Hb g/L
C1	43	0.59	<0.05	Historical	Mild	N	N	132
C2	59	<0.10	<0.05	1.06	Mild	N	N	165
C3	37	0.25	<0.05	3.28	Mild	N	N	128
C4	29	0.69	0.08	2.48	Mild	N	N (Coeliac)	128
C5	13	0.31	<0.05	5.13	Mild	N	N	123
	WBC 10^9/L	**Neutrophils 10^9/L**	**Platelet 10^9/L**	**CD3 cells/mm^3**	**CD4 cells/mm^3**	**CD8 cells/mm^3**	**CD19 cells/mm^3**	**NK cells/mm^3**
C1	4.47	3.15	217	596	452	108	123	241
C2	9.41	6.89	524	1000	607	321	317	317
C3	5.13	3.38	381	658	446	193	147	301
C4	8.43	5.16	359	1008	577	453	377	19
C5	6.75	3.64	318	1517	598	848	245	337

Table 6. Clinical presentation of patients demonstrating clonal haematopoiesis by X-inactivation.

5.5 Discussion:

By dissecting haematopoietic clonality using X-inactivation as a surrogate marker, this chapter demonstrates that clonal skewing in a common lymphoid and myeloid progenitor is closely associated with CVID and may even play a key role in driving the development of disease. The confinement of a clonal epigenetic signature to the haematopoietic compartment argues for CVID as an acquired disorder as opposed to the current dogma of a heterogeneous group of germline genetic disorders [166]. A defect at the stem cell or early progenitor level is supported by the combined deficit observed in both the myeloid and the lymphoid compartments. Using various leukocyte subpopulations to reflect immunological time, the data indicate that immunological space was initially occupied by the unaltered population and was gradually replaced or infiltrated by the diseased population overtime. Hence, neutrophils and other granulocytes, with an estimated circulating half-lives of 6-8 hours [339], exhibited the greatest level of clonality as they are being rapidly replaced by recent bone marrow emigrants.

In CVID, changes within the early progenitor have long been proposed. Derived from their T-cell data Aiuti *et al* hinted that the reduction in thymic output might possibly be due to inadequate thymic input [242]. Previous work by the same group also indicated that altered cytokine output from bone marrow cultures such as IL2, IL-7 and TNFα correlated with the decreased in $CD31^+$ naïve T-cells [273]. The process of clonal haematopoiesis provides a plausible explanation for a single altered progenitor to come to dominate haematopoiesis, exerting the functional deficits and three patients were previously reported in the literature [340]. A recent study examining the DNA methylation changes in one CVID patient showed alteration in a number of candidate genes within the B-cell activation pathway, supporting the hypothesis that the defect lies beyond the germline genetic level [341]. However, further work is needed to pinpoint the molecular level at where the alteration in the early progenitor occurred. Although clonal haematopoiesis is commonly linked to AML, its discovery in myelodysplasia and acquired aplastic anaemia suggests that it could have a much wider implication in other haematological pathologies [328, 329]. Nonetheless, this data challenge the conventional concept of a global impairment in B-cell activation, but instead proposes the presence of mosaicism within the B-cell pool filtered down from the early progenitor level. It is likely that the residual healthy ancient population continues to contribute the baseline antibody level, thus, hypogammaglobulinaemia. Consistent with this, we observed partial retention of plasma cell generating ability in patients demonstrating X-skewing but not in the non-skewed group. The concept of mosaicism also provides a good explanation for the arrays of partial and variable *in vivo* functional deficits observed in CVID patients such as somatic hypermutation, class switching and Ca^{2+} influx. Finally, the variable histological appearance within a single lymph node of a CVID patient further supports this hypothesis [88].

Although heterogeneity will continue to exist under the diagnostic umbrella of CVID, this data show that clonal haematopoiesis occurs in a defined subpopulation of CVID patients. This data currently suggest that patients with recurrent infections, hypogammaglobulinaemia and bronchiectasis without inflammatory complications are more likely to have clonal haematopoiesis. However, a much larger effort involving multiple international cohorts is needed to characterise this subgroup and

accurately determine its true prevalence. Consistent with a survival advantage gained in the myeloid compartment, our previous work has shown that splenomegaly in CVID was predominantly driven by expansion in the red pulp as opposed to lymphoid hyperplasia or granulomata [23]. Despite the close association of clonal haematopoiesis with myelodysplastic syndromes, massive splenomegaly and cytopenias did not feature in our cohort of CVID patients with clonal haematopoiesis. This key paradox cannot be explained by the current data and will require further investigation.

One of the limitations of the current experimental approach is the intrinsic limitations of the HUMARA assay. Both over and under estimation of X-skewing were reported in this technique [338]. Nonetheless, the significant difference from the healthy donor population strongly indicates a biological difference between the two groups. The correction to baseline tissue also offered an additional safely net in demonstrating more reliable shifting in the expected ratio of X-skewing. Our experimental design could be improved by using additional methylated loci on the X-chromosome such as, ZDHHC15, SLITRK4, and PCSK1N, in order to strengthen our conclusion [342]. Regardless, X-chromosome inactivation could only demonstrate clonality in female. Although the process of clonal haematopoiesis is also likely to occur in male patients, supportive evidence by alternative means is needed.

5.6 Summary and conclusion

Collectively, the data are consistent with the hypothesis that clonal/oligoclonal haematopoiesis may predispose to adult-onset antibody deficiency. In contrast to previous discoveries, this phenomenon provides a putative mechanism for the development of sporadic cases of CVID within a general cohort. Moreover, our findings challenge the current molecular dogma and explain for the polygenic nature of CVID. Further work should focus on using a more definitive test to consolidate this hypothesis and accurately characterise the cohort of patients demonstrating this phenomenon.

Chapter 6

6 Discussion

6.1 An acquired blood disorder?

Most cases of CVID are not explained by inherited genetic disorders. This study provides evidence for X-chromosome skewing in the blood consistent with an acquired blood disorder. The arrest in thymic output in combination with the failure of B-cells indicated a defect in the early progenitors and subsequently led to the discovery of clonality before the stage of VDJ-rearrangement (clonal haematopoiesis) in a number of CVID patients and suggests that at least in some CVID patients, the disorder could be due to acquired deleterious mutations in a common progenitor that has a selective advantage over normal haematopoiesis. This phenomenon was demonstrated by deep sequencing approach in other acquired blood disorders such as paroxysmal nocturnal haemoglobulinuria [343], highlighting the importance to alter our current molecular and bioinformatics approaches toward the identification of deleterious somatic mutations and epigenetic changes within the haematopoietic system, such that Rodríguez-Cortez and colleagues have piloted in CVID [341]. Importantly, the development of immunodeficiency via the process of clonal haematopoiesis provides a mechanistic explanation for sporadic cases of CVID, expanding our aetiological understanding beyond paediatric cases from consanguineous background.

Clonal haematopoiesis is an acquired phenomenon when a driver mutation is gained by a single early progenitor/stem cell, allowing its progenies to dominate haematopoiesis. While the failure of humoral immunity marks the most central feature of CVID, defects in T-cell, NK cells, monocytes, dendritic cells as well as many myeloid lineages support a global failure in haematopoiesis. This study

suggests that the failure of haematopoiesis occurred gradually overtime. In keeping with that, data from CVID patients showed a greater declined in naïve CD4 cells and B-cells with advancing age when compared to the expected physiologic rate [233].

In CVID, the occurrence of clonal haematopoiesis could possibly accelerate mutagenesis leading to the acquisition of further somatic mutations responsible for immunodeficiency, and in particular the failure of antibody production. Consistent with this, many of the patients in the whole genome study demonstrated multiple mutations, often within a single gene, that are predictive of antibody failure [166]. Although Good's syndrome is considered to be a different clinical entity, a case of double missense BAFF-R mutation was described [155]. While it is difficult to reconcile that these multiple mutation events were accumulated through generations at the germline level by chances, somatic mutations within an individual life time offer a much better explanation for these changes. Hence, somatic mutations within individuals may be progressive with the initial clonal population continue to evolve overtime and leading to multiple phylogenetically related sub-clonal populations filtering through various lineages; a process that is commonly observed in the clonal evolution of cancer and other pre-malignant conditions [344, 345]. Furthermore, this mechanism also explains for the polygenic nature of CVID with limited sharing in non-driver mutations [166]. The presence of multiple sub-clonal populations together with the pre-existing healthy population could have given rise to the partial and variable nature of CVID, as supported by experimental and clinical evidence generate over the past 60 years. Consistent with that, combined data from the HUMARA assay and plasma cell generation suggest that patients with clonal haematopoiesis have retained a subpopulation of B-cells that could effectively differentiated in functionally normal long-lived plasma cells, as defined by their expression of cardinal surface markers, transcript expression, and immunoglobulin output, maintaining a suboptimal level of baseline serum antibody level. Consistent with the acquired arrest in normal lymphogenesis, naïve B-cells of CVID patients have increased homeostatic proliferation to take up the available immunological space [212] which is reflected by the reduction in naïve B-cell repertoire diversity shown by deep IgH sequencing [346]. Homeostatic proliferation of B-cell is also likely to contribute to the increased risk of B-NHL in CVID.

The study of T-cells also revealed significant abnormalities in the naïve compartment whilst a well-preserved memory compartment protects patients from the development of a severe T-cell immunodeficiency. Together with the findings of the B-cell study, the collapse of thymic output is likely to be secondary to a decrease in or defective input of thymocytes into the thymus. This is in line with radiological evidence showing greater degree of thymic involution in CVID patients in comparison to age-matched published controls. While heavier emphasis is placed on the humoral failure clinically, the most striking and consistent *in vitro* abnormality is marked by the near-complete collapse in thymic output. This study does not currently provide any insights of why naïve B-cells, but not naïve T-cells are generated. The imbalance between the two lineages might be related to the greater scrutiny that T-cells have to go through during its development but more concrete data is needed to support this hypothesis [287].

Age-matched cohort studies have shown that clonal haematopoiesis greatly increases the risk of haematological malignancy [347]. Though the majority of individuals remain healthy, it represents a key transition state toward the development of a premalignant condition such as myelodysplasia. It is estimated that transformation into haematological malignancy occurs in 15% of clonal haematopoiesis compared to 1% in individuals without evidence of clonal haematopoiesis [328]. Large CVID cohort studies suggested that there is a 12 fold increase in haematological malignancy, with B-cell non-Hodgkin's lymphoma (B-NHL) dominating the scene [82]. If clonal haematopoiesis is proven to be true in CVID, a stepwise transition between various states, from clonal haematopoiesis to CVID to B-NHL could be further hypothesised. Additionally, it raises the question if selective IgA deficiency is linked to CVID via a similar process, in particular amongst sIgAD/CVID family cohorts. Although rarely reported, it will be of interest to see if clonal haematopoiesis could be demonstrated in those patients that have evolved from sIgAD into CVID.

6.2 Unanswered questions

Despite the great promise of clonal haematopoiesis explaining for a number of observations in CVID, many unanswered questions remain. While aberrant haematopoiesis could lead to the failure of naïve lymphocytes with memory cells keeping pre-encountered pathogens in check in the T-cell compartment, it is evident that memory is not maintained in the B-cell compartment. The severe reduction in memory B-cells has been a central observation to CVID and is now a new criterion in the revised ESID diagnostic guideline [12]. It was suggested that up to 60% of CVID patients may demonstrate a <0.4% circulating switched memory B-cells in peripheral blood [19]. Humoral immunity is understood to be maintained by a combination of memory B-cells and non-proliferative long-lived plasma cells [319, 348]. In human, the long term fate of memory B-cells following their generation from germinal centres is not fully understood, but murine model suggested that class-switched memory B-cells may have a shorter life span than non-switched IgM^+ memory B-cells [349]. Anyhow, the current study cannot explain the disappearance of memory B-cells in CVID.

In keeping with the lack of self-renewing ability from the bone marrow, rituximab (anti-CD20 antibody) has been reported to trigger the onset of CVID or lead to irreversible B-lymphopenia in existing CVID patients [350, 351]. Bone marrow resident long-lived plasma cell population is dictated by a finite amount of already pre-occupied niche environment which theoretically is unlikely to be affected by an arrest in B-lymphogenesis. Arguably, the arrest in B-lymphogenesis might actually ease the competitive pressure for existing plasma cells, allowing them greater chances of long term survival. However, the dependency from stromal cells and granulocytes to maintain their survival niches makes plasma cells vulnerable to changes in the bone marrow [352]. Hence, it will be of interest to examine for any potential changes brought on by clonal haematopoiesis in the bone marrow; an area that warrant further investigations.

Despite the involvement of the myeloid lineages being consistent with clonal haematopoiesis, it is unclear why well-documented associated diseases such as myelodysplasia and acute myeloid

leukaemia (AML) were rarely reported amongst CVID patients. One could argue that features of myelodysplasia, such as refractory cytopenia, may be found in some CVID patients [353] and is under investigated by a bone marrow biopsy. Of note, this study currently offers no explanation for the development of granulomata; another common histological findings.

Although we identified clonal haematopoiesis mostly in patients with Group1 disease, this clinical phenotype association is far from perfect. In particular, massive splenomegaly did not feature amongst our clonal patients while reduction in thymic output was more severe with Group2 patients. The low sensitivity and specificity of the HUMARA assay also forbid clear delineation of patients with clonal haematopoiesis from the remaining group. Therefore, until a more definitive test is applied to multiple cohorts via international collaboration, it will remain difficult to identify at risk patient by clinical presentation.

Clonal assessment via ultra-deep next generation sequencing has been the method of choice for solid and other haematological malignancies [328, 354]. Combining the power of 500-1000 fold sequencing with variant allele fraction (VAF) bioinformatics analysis, the frequency of a mutated clonal population can be more accurate defined in both male and female. In addition, the resolution of this approach will also allow the detection of specific somatic driver mutations using a carefully designed targeted sequencing panel, resolving the uncertainties we have with the HUMARA assay. Finally, it has the potential to reveal how somatic mutations are filtered through to various myeloid and lymphoid lineages as well as defining the clonal evolution within an individual.

This study has revealed a number of interesting findings relating to the aetiology and pathophysiology of CVID. However, the current hypothesis of clonal haematopoiesis driving CVID is still built upon a number of fragmented observations and lacks of mechanistic demonstration. To further support this hypothesis, future work must focus on addressing these weaknesses and gather direct *in vivo* and *in vitro* evidence.

On another note, the discovery of unique TCRβ clonotypes in CVID opened a new arena for future investigations. Defining the antigenic targets and specificity of these unique T-cells will have an

enormous impact on our understanding of the development of disease complications in CVID. While promising data were shown, high background signals generated from whole blood DNA hindered our analysis. Improved experimental design such as targeting HLA matched patients with a specific clinical complication, the use of tissue specific separated (CD4/CD8) T-cells and pair-wised single cell alpha and beta chains sequencing [355], will have a greater chance of achieving such goals.

6.3 Implication on clinical practice

While more work is still required to test if clonal haematopoiesis could drive the development of CVID, the concept calls for a review of our therapeutic approach in these patients. Current strategy focuses on immunoglobulin replacement therapy and does not tackle on the underlying aetiology. Although it is well-tolerated and has been enormously successful in the past 50 years, immunoglobulin remains as a donated plasma product with finite global supply. Logically, bone marrow transplantation (BMT) appears to be a suitable treatment option for abnormal clonal haematopoiesis. A recent multi-centred retrospective study involving 25 patients of various clinical presentations, mostly for refractory immune dysregulation and lymphoma, showed that endogenous immunoglobulin production can be revived with some patients no longer requiring IVIG years after a bone marrow transplant [356]. However, the procedure carries a significant morbidity and mortality rate, much exceed that of paediatric immunodeficiency BMT [357], with many patients still remained on IVIG afterward; questioning its application in the more general cohort of CVID patients.

Secondly, a high index of clinical suspicion for haematological malignancies is needed for CVID patient given its potential association with an underlying pre-malignant state. While lymphoma is being actively screened for in most centres, the findings of this study suggest that the myeloid compartment should also be considered. As such, a bone marrow biopsy might be indicated for patients with long standing refractory cytopenia and massive splenomegaly.

Thirdly, the poor regenerative capacity of the lymphoid compartment demands more careful consideration before the use for immunosuppressive therapies in these patients. Anecdotal experience has reminded us that the heavy use of these therapies may be fatal (personal communication). Although rituximab has been successfully used in refractory ITP in CVID [23, 358], data on post therapy immune reconstitution is lacking. Similarly, the outcomes on the use of azathioprine, cyclosporine, etc are unclear. A national or international audit on the outcome and immune reconstitution of these patients would be of enormous interest.

Finally, the findings of this study imply that some cases of CVID/adult onset hypogammaglobulinaemia may represent a precursor state for lymphoma, a very principle that might exclude them the definition of CVID according to the revised ESID 2014 diagnostic criteria. Similarly the reduction in naïve T-cells might exclude many of the patients from being labelled as CVID under the new criteria. These two points call for a new nomenclature to accommodate this significant subgroup of patients. Although still at an early stage, the development of a simple and robust diagnostic test for clonal haematopoiesis related antibody deficiency would be of value in the future.

6.4 Beyond Common Variable Immunodeficiency

The discovery of clonal haematopoiesis in CVID patients was unexpected. CVID segregates itself from the majority of primary immunodeficiencies with an onset in adulthood. The findings of this study raise the question if other adult onset immunodeficiencies could be triggered by the same process, especially if somatic mutations could occur at any location across the genome. Consistent with this hypothesis, extreme X-skewing has been reported in carriers of X-linked CGD and X-linked hyper IgM patients, manifesting disease later in life [359, 360]. Similarly, some adult onset GATA2 deficient patients also demonstrated extreme X-skewing [361]. Considering other rarer haematological conditions, is polyclonal B-cell lymphocytosis truly polyclonal?

6.5 Future work

Given the current findings, work has begun in refining the clonal status of CVID patients by ultra-deep sequencing and a second cohort is being sought. The aim is to identify common driver mutations in both male and female patients as well as to understand clonal evolution of the disease by examining various lymphocyte subsets. Future work will also aim to mechanistically demonstrate that the development of clonal haematopoiesis with carefully designed *in vivo* and *in vitro* experiments, whilst in parallel gather collaborative multi-centre clinical data for the outcome of immunosuppressve therapies in CVID. Finally, the unbiased examination of the longitudinal outcome of individuals with clonal haematopoiesis, perhaps via collaboration with the local blood bank, would help us understand the extent of this phenomenon in health and disease.

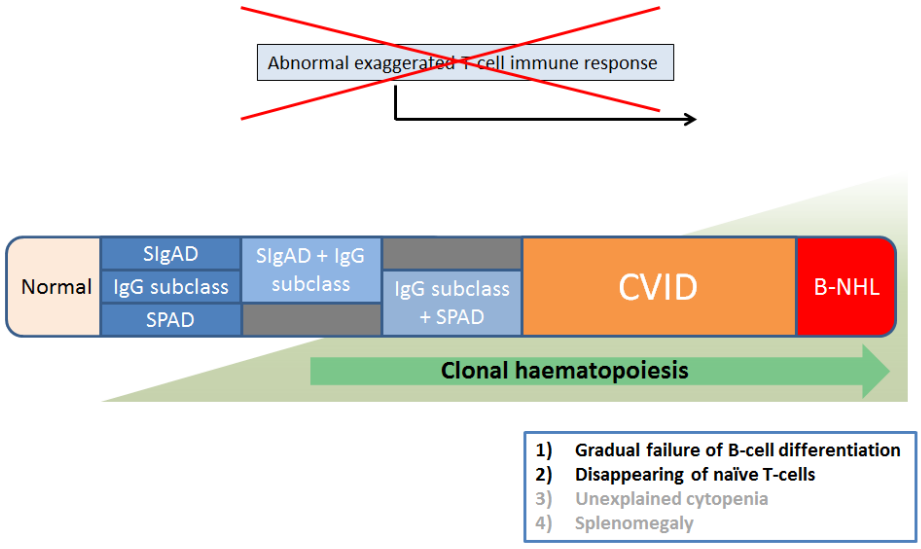

Figure 47. Revised hypothesis of the aetiology of Common Variable Immunodeficiency.

Appendix A

Pan-American/ESID diagnostic criteria for CVID (1999)

"Probable CVID"

Male or female patient who has a marked decrease of IgG (at least 2 SD below the mean for age) and a marked decrease in at least one of the isotypes IgM or IgA, and fulfills all of the following criteria:

1) Onset of immunodeficiency at greater than 2 years of age

2) Absent isohemagglutinins and/or poor response to vaccines

3) Defined causes of hypogammaglobulinemia have been excluded (see 'Differential Diagnosis of Hypogammaglobulinemia')

"Possible CVID"

Male or female patient who has a marked decrease (at least 2 SD below the mean for age) in at least one of the major isotypes (IgM, IgG and IgA) and fulfills all of the following criteria:

1) Onset of immunodeficiency at greater than 2 years of age

2) Absent isohemagglutinins and/or poor response to vaccines

3) Defined causes of hypogammaglobulinemia have been excluded (see 'Differential Diagnosis of Hypogammaglobulinemia')

Spectrum of disease

Most patients with CVI are recognized to have immunodeficiency in the second, third or fourth decade of life, after they have had several pneumonias; however children and older adults may be affected. Viral, fungal and parasitic infections as well as bacterial infections may be problematic. The serum concentration of IgM is normal in about half of the patients. Abnormalities in T cell numbers or function are common. The majority of patients have normal numbers of B cells; however, some have low or absent B cells. Approximately 50% of patients have autoimmune manifestations. There is an increased risk of malignancy.

(Obtained from www.esid.org)

Appendix B

ESID revised diagnostic criteria for CVID (2014)

At least one of the following:

- Increase susceptibility to infection
- Autoimmune manifestations
- Granulomatous disease
- Unexplained polyclonal lymphoproliferation
- Affected family member with antibody deficiency

AND marked decrease of IgG and IgA with or without low IgM levels (measured at least twice; <2SD of the normal levels for their age);

AND at least one of the following:

- Poor antibody response to vaccines (and/or absent isohaemagglutinins); i.e. absence of protective levels despite vaccination where defined
- Low switched memory B cells (<70% of age-related normal value)

AND secondary causes of hypogammaglobulinaemia have been excluded (e.g. drug induced, infectious diseases, protein loss, hypercatabolism, infectious diseases, malignancy, chromosomal anomalies other primary immunodeficiency)

AND diagnosis is established after the 4th year of life (but symptoms may be present before)

AND no evidence of profound T-cell deficiency, defined as 2 out of the following (y=year of life):

- CD4 number/microliter: 2-6y <300, 6-12y <250, >12y <200
- %naive CD4: 2-6y <25%, 6-16y <20%, >16y <10%
- T-cell proliferation absent

(Obtained from www.esid.org)

Appendix C

Patient summary:

Patient number	Age	Gender	Age of diagnosis	IgG	IgA	IgM	†Disease complications	Freiburg Group	‡%smB	¶%CD21^{lo}	TCR repertoire	Naïve T-cell	Plasma cell generation	X-inactivation
CVID02	41	F	38	1.87	<0.05	0.19	Bronchiectasis, transverse myelitis, ILD	II	0.49	6.3	Oligoclonal	Reduced	--	--
CVID03	20	F	18	4.36	0.16	0.19	Mild alopecia areata	II	0.69	2.3	Clonal	--	--	Skewed
CVID04	62	M	38	NK	NK	NK	Bronchiectasis	II	0.56	0.5	Polyclonal	--	--	--
CVID07	41	M	18	NK	NK	NK	Bronchiectasis	Ib	0.09	0.5	Polyclonal	--	--	--
CVID08	60	F	48	2.11	<0.07	0.05	Bronchiectasis, deranged LFTs, hypothyroidism, enteropathy	Ia	0	23.9	Clonal	--	--	Normal
CVID09	40	M	36	<0.1	0.07	<0.1	Bronchiectasis, splenomegaly, lymphadenopathy, AIC, ILD, enteropathy	B<1%	NA	NA	Oligoclonal	Reduced	--	--
CVID10	40	F	33	0.13	<0.05	0.1	Bronchiectasis, splenomegaly, lymphadenopathy, deranged LFTs, AIC, ILD	Ib	0	18.7	Oligoclonal	--	Severely reduced	Normal
CVID11	65	F	59	0.87	<0.1	<0.1	Bronchiectasis, sarcoiliitis, deranged LFTs	B<1%	NA	NA	Polyclonal	--	--	Skewed
CVID13	22	M	20	3.91	0.42	1.44	Bronchiectasis	II	1.03	0.5	Polyclonal	--	Partially reduced	--
CVID16	45	M	44	1.59	<0.05	0.11	Bronchiectasis, autoimmune diabetes, gastric cancer	II	1.68	9.9	Polyclonal	--	Partially reduced	--
CVID175	61	F	58	1.08	<0.05	<0.10	Multiple Sclerosis	Ia	0.19252	42.9	--	--	--	Normal
CVID179	30	F	26	2.99	<0.05	<0.10	Splenomegaly, IBS	Ib	0.075871	1.7	--	--	--	Normal
CVID18	60	F	43	2.94	0.08	0.31	B12 deficiency	Ib	0.12	5.1	Oligoclonal	--	--	Skewed
CVID20	50	F	42	NK	NK	NK	Splenomegaly, lymphadenopathy, polyarteritis, deranged LFTs, AIC, ILD	NK	NK	NK	Polyclonal	--	--	--
CVID21	64	F	51	NK	NK	NK	Bronchiectasis, lymphadenopathy, derranged LFTs	Ib	0.166275	17.9	--	--	--	Skewed
CVID23	45	M	44	3.46	0.48	0.44	Lymphadenopathy, ILD	II	0.76	9.8	Clonal	Reduced	Partially reduced	--
CVID25	50	F	36	3.81	0.14	0.35	Bronchiectasis, splenomegaly, lymphadenopathy, deranged LFTs, AIC, ILD	Ib	0.01	9.3	Polyclonal	--	Severely reduced	Normal
CVID27	27	F	23	3.09	<0.05	<0.10	None	II	0.43	34.8	Oligoclonal	--	--	--
CVID29	64	F	59	1.06	<0.05	<0.10	Bronchiectasis	II	0.60	21.2	--	--	Normal	Skewed
CVID30	67	F	60	2.55	<0.30	<0.10	Breast cancer	II	0.51	15.1	Polyclonal	--	--	Skewed

CVID32	44	M	34	0.06	<0.05	0.06	Bronchiectasis	Ib	0.01	4.4	--	--	Severely reduced	--
CVID33	38	F	30	3.1	4.77	1.23	Bronchiectasis	II	0.66	21	Clonal	--	--	--
CVID34	50	M	49	3.92	0.06	0.16	Bronchiectasis	II	1.67	11.2	Polyclonal	Reduced	--	--
CVID35	50	M	48	0.43	0.39	0.13	Bronchiectasis	Ib	0.3	5.1	Polyclonal	Reduced	--	--
CVID36	45	F	42	2.91	<0.10	0.18	Splenomegaly, AIC	Ia	0	33.8	Polyclonal	--	--	--
CVID39	61	F	11	2.56	<0.05	<0.10	Bronchiectasis	II	3.69	7.9	--	--	Severely reduced	Normal
CVID40	48	F	28	~3.28	<0.05	~0.25	Bronchiectasis	Ia	0.01	53.1	--	--	Partially reduced	Skewed
CVID41	28	F	24	1.65	0.17	0.18	None	II	0.76	2.6	Oligoclonal	--	Severely reduced	Normal
CVID43	57	M	50	NK	NK	NK	Bronchiectasis, splenomegaly, lymphadenopathy, optic neuritis	II	0.48	63.6	Clonal	Reduced	--	--
CVID44	60	M	46	NK	NK	NK	Bronchiectasis, splenomegaly, lymphadenopathy, nodular regenerating hyperplasia (liver), AIC, enteropathy	B<1%	NA	NA	Oligoclonal	--	--	--
CVID47	65	M	55	4.27	1.64	0.26	Bronchiectasis	Ib	0.03	1.1	Clonal	Reduced	--	--
CVID50	33	M	19	5.29	<0.05	<0.03	None	Ia	0.36	31.3	Polyclonal	--	--	--
CVID51	45	F	40	1.75	<0.1	<0.1	Bronchiectasis, autoimmune diabetes, enteropathy	II	2.37	6.8	Polyclonal	Reduced	Severely reduced	Normal
CVID52	45	M	NK	NK	NK	NK	Mild lymphadenopathy	Ia	0.01	62.3	Polyclonal	--	--	--
CVID53	40	F	38	0.4	<0.10	<0.10	Bronchiectasis, splenomegaly, AIC	II	1.3	66.9	Polyclonal	--	--	--
CVID54	17	F	8	1.84	<0.05	<0.06	Borderline splenomegaly	Ib	0.14	8.1	Polyclonal	--	--	--
CVID55	45	F	NK	NK	NK	NK	Bronchiectasis, splenomegaly, Nodular regenerative hyperplasia (liver), AIC, ILD, enteropathy	NK	NK	NK	Oligoclonal	Reduced	--	--
CVID56	24	F	23	0.11	<0.05	<0.10	Bronchiectasis	Ib	0.04	5.5	Oligoclonal	Low normal	--	--
CVID58	28	M	28	2.83	0.1	0.29	Splenomegaly, lymphadenopathy, AIC, ILD	Ia	0.08	42.2	Polyclonal	--	--	--
CVID60	63	M	53	2.71	0.06	0.46	Bronchiectasis, Sjorgren's, AIC, enteropathy	Ia	0.01	28.7	Polyclonal	--	--	--
CVID62	45	F	34	2.85	<0.05	<0.10	Bronchiectasis, splenomegaly, deranged LFTs, ILD	B<1%	NA	NA	Clonal	--	--	Normal
CVID63	60	M	21	NK	NK	NK	Bronchiectasis, splenomegaly, lymphadenopathy, uveitis, AIC, enteropathy, renal cell carcinoma	B<1%	NA	NA	Polyclonal	--	--	--
CVID64	60	M	42	4.35	0.27	0.29	Mild deranged LFTs	B<1%	NA	NA	Polyclonal	--	--	--
CVID65	50	M	NK	NK	NK	NK	Splenomegaly, AIC, ILD	Ia	0.02	89.3	Polyclonal	Reduced	--	--
CVID66	32	F	28	0.55	<0.05	0.2	Bronchiectasis, lymphadenopathy, ILD	B<1%	NA	NA	Polyclonal	--	--	--
CVID67	33	M	29	<0.10	<0.05	<0.10	None	II	0.74	12.9	Clonal	--	Partially reduced	--

CVID68	56	F	38	NK	NK	NK	Enteropathy, nodular prurigo	II	1.321879	16.8	--	--	--	Skewed
CVID69	23	M	14	0.35	<0.10	0.1	Bronchiectasis	II	3.11	9.8	Clonal	--	--	--
CVID71	20	F	20	2.39	0.19	0.09	Splenomegaly, lymphadenopathy, iritis, ILD, enteropathy	Ib	0.05	10.6	Polyclonal	--	--	Skewed
CVID72	65	M	NK	NK	NK	NK	Bronchiectasis, ILD	NK	NK	NK	Polyclonal	--	--	--
CVID74	55	F	47	<0.10	<0.05	<0.10	Bronchiectasis	Ib	0.010804	2.4	--	--	--	Skewed
CVID75	56	F	50	2.65	0.18	0.7	Nodular prurigo, vitiligo	II	0.89	16	--	--	Partially reduced	Normal
CVID77	28	F	10	Unknown	Unknown	Unknown	Bronchiectasis	NK	NK	NK	--	--	--	Normal
CVID78	66	F	NK	NK	NK	NK	Bronchiectasis	NK	NK	NK	--	--	--	Skewed
CVID79	50	F	46	<0.10	<0.05	<0.10	Bronchiectasis, enteropathy	Ib	0.10	19.3	--	--	Partially reduced	--
CVID80	39	F	30	1.53	<0.05	0.44	Bronchiectasis, lymphadenopathy, AIC, ILD. Enteropathy	NK	NK	NK	--	--	--	Normal

†Liver function test (LFT), autoimmune cytopenia (AIC) & interstitial lung disease (ILD) are abbreviated.

‡%sm = frequency of class-switched memory B-cells of total peripheral blood lymphocytes.

¶%CD21^{lo} = frequency of CD21^{lo} B-cells of total B-cells.

References

1. Henderson, D.A., et al., *Smallpox as a biological weapon: medical and public health management. Working Group on Civilian Biodefense.* JAMA, 1999. **281**(22): p. 2127-37.
2. Daileader, P. and Teaching Company., *The late Middle Ages*, in *The great courses*. 2007, Teaching Co.,: Chantilly, VA.
3. *From the Centers for Disease Control and Prevention. Achievements in public health, 1900-1999: fluoridation of drinking water to prevent dental caries.* JAMA, 2000. **283**(10): p. 1283-6.
4. Fenner, F., *A successful eradication campaign. Global eradication of smallpox.* Rev Infect Dis, 1982. **4**(5): p. 916-30.
5. Bruton, O.C., *Agammaglobulinemia.* Pediatrics, 1952. **9**(6): p. 722-8.
6. Tsukada, S., et al., *Deficient expression of a B cell cytoplasmic tyrosine kinase in human X-linked agammaglobulinemia.* Cell, 1993. **72**(2): p. 279-90.
7. Vetrie, D., et al., *The gene involved in X-linked agammaglobulinaemia is a member of the src family of protein-tyrosine kinases.* Nature, 1993. **361**(6409): p. 226-33.
8. Al-Herz, W., et al., *Primary immunodeficiency diseases: an update on the classification from the international union of immunological societies expert committee for primary immunodeficiency.* Front Immunol, 2014. **5**: p. 162.
9. Janeway, C.A., L. Apt, and D. Gitlin, *Agammaglobulinemia.* Trans Assoc Am Physicians, 1953. **66**: p. 200-2.
10. Chapel, H., et al., *Common variable immunodeficiency disorders: division into distinct clinical phenotypes.* Blood, 2008. **112**(2): p. 277-86.
11. Conley, M.E., L.D. Notarangelo, and A. Etzioni, *Diagnostic criteria for primary immunodeficiencies. Representing PAGID (Pan-American Group for Immunodeficiency) and ESID (European Society for Immunodeficiencies).* Clin Immunol, 1999. **93**(3): p. 190-7.
12. Ameratunga, R., et al., *Comparison of diagnostic criteria for common variable immunodeficiency disorder.* Front Immunol, 2014. **5**: p. 415.
13. Xiao, X., et al., *Common variable immunodeficiency and autoimmunity--an inconvenient truth.* Autoimmun Rev, 2014. **13**(8): p. 858-64.
14. Resnick, E.S., et al., *Morbidity and mortality in common variable immune deficiency over 4 decades.* Blood, 2012. **119**(7): p. 1650-7.
15. *Primary immunodeficiency diseases. Report of an IUIS Scientific Committee. International Union of Immunological Societies.* Clin Exp Immunol, 1999. **118 Suppl 1**: p. 1-28.
16. Bonilla, F.A., et al., *Practice parameter for the diagnosis and management of primary immunodeficiency.* Ann Allergy Asthma Immunol, 2005. **94**(5 Suppl 1): p. S1-63.
17. Cunningham-Rundles, C., *Clinical and immunologic analyses of 103 patients with common variable immunodeficiency.* J Clin Immunol, 1989. **9**(1): p. 22-33.
18. Hermaszewski, R.A. and A.D. Webster, *Primary hypogammaglobulinaemia: a survey of clinical manifestations and complications.* Q J Med, 1993. **86**(1): p. 31-42.
19. Wehr, C., et al., *The EUROclass trial: defining subgroups in common variable immunodeficiency.* Blood, 2008. **111**(1): p. 77-85.
20. Mouillot, G., et al., *B-cell and T-cell phenotypes in CVID patients correlate with the clinical phenotype of the disease.* J Clin Immunol, 2010. **30**(5): p. 746-55.
21. Boileau, J., et al., *Autoimmunity in common variable immunodeficiency: correlation with lymphocyte phenotype in the French DEFI study.* J Autoimmun, 2011. **36**(1): p. 25-32.

22. Cunningham-Rundles, C. and C. Bodian, *Common variable immunodeficiency: clinical and immunological features of 248 patients.* Clin Immunol, 1999. **92**(1): p. 34-48.
23. Wong, G.K., et al., *Outcomes of splenectomy in patients with common variable immunodeficiency (CVID): a survey of 45 patients.* Clin Exp Immunol, 2013. **172**(1): p. 63-72.
24. Chapel, H., et al., *Confirmation and improvement of criteria for clinical phenotyping in common variable immunodeficiency disorders in replicate cohorts.* J Allergy Clin Immunol, 2012. **130**(5): p. 1197-1198 e9.
25. Schembri, M.A., D. Dalsgaard, and P. Klemm, *Capsule shields the function of short bacterial adhesins.* J Bacteriol, 2004. **186**(5): p. 1249-57.
26. Lucas, M., et al., *Infection outcomes in patients with common variable immunodeficiency disorders: relationship to immunoglobulin therapy over 22 years.* J Allergy Clin Immunol, 2010. **125**(6): p. 1354-1360 e4.
27. Oksenhendler, E., et al., *Infections in 252 patients with common variable immunodeficiency.* Clin Infect Dis, 2008. **46**(10): p. 1547-54.
28. McHeyzer-Williams, M., et al., *Molecular programming of B cell memory.* Nat Rev Immunol, 2012. **12**(1): p. 24-34.
29. Sun, C.C. and D.A. Thorley-Lawson, *Plasma cell-specific transcription factor XBP-1s binds to and transactivates the Epstein-Barr virus BZLF1 promoter.* J Virol, 2007. **81**(24): p. 13566-77.
30. MacLennan, I.C., *Germinal centers.* Annu. Rev. Immunol., 1994. **12**: p. 117-139.
31. Yoshida, T., et al., *Memory B and memory plasma cells.* Immunological Reviews, 2010. **237**(1): p. 117-139.
32. Radbruch, A., et al., *Competence and competition: the challenge of becoming a long-lived plasma cell.* Nat Rev Immunol, 2006. **6**(10): p. 741-750.
33. Bataille, R., et al., *The phenotype of normal, reactive and malignant plasma cells. Identification of "many and multiple myelomas" and of new targets for myeloma therapy.* Haematologica, 2006. **91**(9): p. 1234-1240.
34. Hideshima, T., et al., *Understanding multiple myeloma pathogenesis in the bone marrow to identify new therapeutic targets.* Nat Rev Cancer, 2007. **7**(8): p. 585-598.
35. Sprynski, A.C., et al., *The role of IGF-1 as a major growth factor for myeloma cell lines and the prognostic relevance of the expression of its receptor.* Blood, 2009. **113**(19): p. 4614-4626.
36. Matsui, W., et al., *Anti-tumour activity of interferon-alpha in multiple myeloma: role of interleukin 6 and tumor cell differentiation.* British Journal of Haematology, 2003. **121**(2): p. 251-258.
37. Winter, O., E. Mohr, and R.A. Manz, *Alternative cell types form a Multi-Component-Plasma-Cell-Niche.* Immunology Letters, 2011. **141**(1): p. 145-146.
38. Huard, B., et al., *APRIL secreted by neutrophils binds to heparan sulfate proteoglycans to create plasma cell niches in human mucosa.* The Journal of Clinical Investigation, 2010. **120**(4): p. 1362-1362.
39. Winter, O., et al., *Pathogenic Long-Lived Plasma Cells and Their Survival Niches in Autoimmunity, Malignancy, and Allergy.* The Journal of Immunology, 2012. **189**(11): p. 5105-5111.
40. Cerutti, A., M. Cols, and I. Puga, *Marginal zone B cells: virtues of innate-like antibody-producing lymphocytes.* Nat Rev Immunol, 2013. **13**(2): p. 118-132.
41. Silverman, G.J. and C.S. Goodyear, *Confounding B-cell defences: lessons from a staphylococcal superantigen.* Nat Rev Immunol, 2006. **6**(6): p. 465-75.
42. Yel, L., *Selective IgA deficiency.* J Clin Immunol, 2010. **30**(1): p. 10-6.
43. Gustafson, R., et al., *Prophylactic therapy for selective IgA deficiency.* Lancet, 1997. **350**(9081): p. 865.
44. Oen, K., R.E. Petty, and M.L. Schroeder, *Immunoglobulin A deficiency: genetic studies.* Tissue Antigens, 1982. **19**(3): p. 174-82.

45. Chandran, S., et al., *Low prevalence of IgA deficiency in north Indian population.* Indian J Med Res, 2006. **123**(5): p. 653-6.
46. Conley, M.E. and M.D. Cooper, *Immature IgA B cells in IgA-deficient patients.* N Engl J Med, 1981. **305**(9): p. 495-7.
47. Horton, R.E. and G. Vidarsson, *Antibodies and their receptors: different potential roles in mucosal defense.* Front Immunol, 2013. **4**: p. 200.
48. Jorgensen, G.H., et al., *Health-related quality of life (HRQL) in immunodeficient adults with selective IgA deficiency compared with age- and gender-matched controls and identification of risk factors for poor HRQL.* Qual Life Res, 2014. **23**(2): p. 645-58.
49. Edwards, E., S. Razvi, and C. Cunningham-Rundles, *IgA deficiency: clinical correlates and responses to pneumococcal vaccine.* Clin Immunol, 2004. **111**(1): p. 93-7.
50. Oxelius, V.A., et al., *IgG subclasses in selective IgA deficiency: importance of IgG2-IgA deficiency.* N Engl J Med, 1981. **304**(24): p. 1476-7.
51. Koistinen, J., *Familial clustering of selective IgA deficiency.* Vox Sang, 1976. **30**(3): p. 181-90.
52. Vorechovsky, I., et al., *Family and linkage study of selective IgA deficiency and common variable immunodeficiency.* Clin Immunol Immunopathol, 1995. **77**(2): p. 185-92.
53. Schroeder, H.W., Jr., H.W. Schroeder, 3rd, and S.M. Sheikh, *The complex genetics of common variable immunodeficiency.* J Investig Med, 2004. **52**(2): p. 90-103.
54. Aghamohammadi, A., et al., *Progression of selective IgA deficiency to common variable immunodeficiency.* Int Arch Allergy Immunol, 2008. **147**(2): p. 87-92.
55. Schaffer, F.M., et al., *Individuals with IgA deficiency and common variable immunodeficiency share polymorphisms of major histocompatibility complex class III genes.* Proc Natl Acad Sci U S A, 1989. **86**(20): p. 8015-9.
56. Olerup, O., et al., *Shared HLA class II-associated genetic susceptibility and resistance, related to the HLA-DQB1 gene, in IgA deficiency and common variable immunodeficiency.* Proc Natl Acad Sci U S A, 1992. **89**(22): p. 10653-7.
57. Howe, H.S., et al., *Common variable immunodeficiency is associated with polymorphic markers in the human major histocompatibility complex.* Clin Exp Immunol, 1991. **83**(3): p. 387-90.
58. Vorechovsky, I., et al., *A putative susceptibility locus on chromosome 18 is not a major contributor to human selective IgA deficiency: evidence from meiotic mapping of 83 multiple-case families.* J Immunol, 1999. **163**(4): p. 2236-42.
59. Kralovicova, J., et al., *Fine-scale mapping at IGAD1 and genome-wide genetic linkage analysis implicate HLA-DQ/DR as a major susceptibility locus in selective IgA deficiency and common variable immunodeficiency.* J Immunol, 2003. **170**(5): p. 2765-75.
60. Braig, D.U., et al., *Linkage of autosomal dominant common variable immunodeficiency to chromosome 5p and evidence for locus heterogeneity.* Hum Genet, 2003. **112**(4): p. 369-78.
61. Finck, A., et al., *Linkage of autosomal-dominant common variable immunodeficiency to chromosome 4q.* Eur J Hum Genet, 2006. **14**(7): p. 867-75.
62. Schaffer, A.A., et al., *Analysis of families with common variable immunodeficiency (CVID) and IgA deficiency suggests linkage of CVID to chromosome 16q.* Hum Genet, 2006. **118**(6): p. 725-9.
63. Ferreira, R.C., et al., *Association of IFIH1 and other autoimmunity risk alleles with selective IgA deficiency.* Nat Genet, 2010. **42**(9): p. 777-80.
64. Li, J., et al., *Association of CLEC16A with human common variable immunodeficiency disorder and role in murine B cells.* Nat Commun, 2015. **6**: p. 6804.
65. Smyth, D.J., et al., *A genome-wide association study of nonsynonymous SNPs identifies a type 1 diabetes locus in the interferon-induced helicase (IFIH1) region.* Nat Genet, 2006. **38**(6): p. 617-9.
66. Gateva, V., et al., *A large-scale replication study identifies TNIP1, PRDM1, JAZF1, UHRF1BP1 and IL10 as risk loci for systemic lupus erythematosus.* Nat Genet, 2009. **41**(11): p. 1228-33.

67. Sakurai, D., et al., *TACI regulates IgA production by APRIL in collaboration with HSPG.* Blood, 2007. **109**(7): p. 2961-7.
68. Salzer, U., et al., *Mutations in TNFRSF13B encoding TACI are associated with common variable immunodeficiency in humans.* Nat Genet, 2005. **37**(8): p. 820-8.
69. Castigli, E., et al., *TACI is mutant in common variable immunodeficiency and IgA deficiency.* Nature Genetics, 2005. **37**(8): p. 829-834.
70. Castigli, E., et al., *Reexamining the role of TACI coding variants in common variable immunodeficiency and selective IgA deficiency.* Nat Genet, 2007. **39**(4): p. 430-1.
71. Pan-Hammarstrom, Q., et al., *Reexamining the role of TACI coding variants in common variable immunodeficiency and selective IgA deficiency.* Nat Genet, 2007. **39**(4): p. 429-30.
72. Warnatz, K., et al., *B-cell activating factor receptor deficiency is associated with an adult-onset antibody deficiency syndrome in humans.* Proc Natl Acad Sci U S A, 2009. **106**(33): p. 13945-50.
73. Cataldo, F., et al., *Prevalence and clinical features of selective immunoglobulin A deficiency in coeliac disease: an Italian multicentre study. Italian Society of Paediatric Gastroenterology and Hepatology (SIGEP) and "Club del Tenue" Working Groups on Coeliac Disease.* Gut, 1998. **42**(3): p. 362-5.
74. Agarwal, S., et al., *Characterization of immunologic defects in patients with common variable immunodeficiency (CVID) with intestinal disease.* Inflamm Bowel Dis, 2011. **17**(1): p. 251-9.
75. Gough, S.C., L.S. Walker, and D.M. Sansom, *CTLA4 gene polymorphism and autoimmunity.* Immunol Rev, 2005. **204**: p. 102-15.
76. Haimila, K., et al., *The shared CTLA4-ICOS risk locus in celiac disease, IgA deficiency and common variable immunodeficiency.* Genes Immun, 2009. **10**(2): p. 151-61.
77. Schubert, D., et al., *Autosomal dominant immune dysregulation syndrome in humans with CTLA4 mutations.* Nat Med, 2014. **20**(12): p. 1410-6.
78. Grimbacher, B., et al., *Homozygous loss of ICOS is associated with adult-onset common variable immunodeficiency.* Nat Immunol, 2003. **4**(3): p. 261-8.
79. Rogena, E.A., et al., *A review of the pattern of AIDS defining, HIV associated neoplasms and premalignant lesions diagnosed from 2000-2011 at Kenyatta National Hospital, Kenya.* Infect Agent Cancer, 2015. **10**: p. 28.
80. Swann, J.B. and M.J. Smyth, *Immune surveillance of tumors.* J Clin Invest, 2007. **117**(5): p. 1137-46.
81. Batlevi, C.L., et al., *Novel immunotherapies in lymphoid malignancies.* Nat Rev Clin Oncol, 2015.
82. Vajdic, C.M., et al., *Are antibody deficiency disorders associated with a narrower range of cancers than other forms of immunodeficiency?* Blood, 2010. **116**(8): p. 1228-34.
83. Kinlen, L.J., et al., *Prospective study of cancer in patients with hypogammaglobulinaemia.* Lancet, 1985. **1**(8423): p. 263-6.
84. Cunningham-Rundles, C., et al., *Incidence of cancer in 98 patients with common varied immunodeficiency.* J Clin Immunol, 1987. **7**(4): p. 294-9.
85. Mellemkjaer, L., et al., *Cancer risk among patients with IgA deficiency or common variable immunodeficiency and their relatives: a combined Danish and Swedish study.* Clin Exp Immunol, 2002. **130**(3): p. 495-500.
86. Quinti, I., et al., *Long-term follow-up and outcome of a large cohort of patients with common variable immunodeficiency.* J Clin Immunol, 2007. **27**(3): p. 308-16.
87. Cunningham-Rundles, C., et al., *Selective IgA deficiency and neoplasia.* Vox Sang, 1980. **38**(2): p. 61-7.
88. Unger, S., et al., *Ill-defined germinal centers and severely reduced plasma cells are histological hallmarks of lymphadenopathy in patients with common variable immunodeficiency.* J Clin Immunol, 2014. **34**(6): p. 615-26.

89. Gompels, M.M., et al., *Lymphoproliferative disease in antibody deficiency: a multi-centre study.* Clin Exp Immunol, 2003. **134**(2): p. 314-20.
90. Dargent, J.L., et al., *Atypical hyperplasia of the marginal zone of B follicles in a polymorphic Epstein-Barr virus-associated lymphoproliferative disorder occurring in an adolescent with human immunodeficiency virus infection.* Pediatr Dev Pathol, 2009. **12**(1): p. 59-62.
91. Schulte, K.M. and N. Talat, *Castleman's disease--a two compartment model of HHV8 infection.* Nat Rev Clin Oncol, 2010. **7**(9): p. 533-43.
92. Victora, G.D. and M.C. Nussenzweig, *Germinal centers.* Annu Rev Immunol, 2012. **30**: p. 429-57.
93. Basso, K. and R. Dalla-Favera, *Germinal centres and B cell lymphomagenesis.* Nat Rev Immunol, 2015. **15**(3): p. 172-84.
94. Aghamohammadi, A., et al., *Lymphoma of mucosa-associated lymphoid tissue in common variable immunodeficiency.* Leuk Lymphoma, 2006. **47**(2): p. 343-6.
95. Desar, I.M., et al., *Extranodal marginal zone (MALT) lymphoma in common variable immunodeficiency.* Neth J Med, 2006. **64**(5): p. 136-40.
96. Papa, A., et al., *Helicobacter pylori eradication and remission of low-grade gastric mucosa-associated lymphoid tissue lymphoma: a long-term follow-up study.* J Clin Gastroenterol, 2000. **31**(2): p. 169-71.
97. Thiede, C., et al., *Eradication of Helicobacter pylori and stability of remissions in low-grade gastric B-cell lymphomas of the mucosa-associated lymphoid tissue: results of an ongoing multicenter trial.* Recent Results Cancer Res, 2000. **156**: p. 125-33.
98. Rickert, R.C., J. Jellusova, and A.V. Miletic, *Signaling by the tumor necrosis factor receptor superfamily in B-cell biology and disease.* Immunol Rev, 2011. **244**(1): p. 115-33.
99. Seshasayee, D., et al., *Loss of TACI causes fatal lymphoproliferation and autoimmunity, establishing TACI as an inhibitory BLyS receptor.* Immunity, 2003. **18**(2): p. 279-88.
100. Batten, M., et al., *TNF deficiency fails to protect BAFF transgenic mice against autoimmunity and reveals a predisposition to B cell lymphoma.* J Immunol, 2004. **172**(2): p. 812-22.
101. Guadagnoli, M., et al., *Development and characterization of APRIL antagonistic monoclonal antibodies for treatment of B-cell lymphomas.* Blood, 2011. **117**(25): p. 6856-65.
102. Martinez-Gallo, M., et al., *TACI mutations and impaired B-cell function in subjects with CVID and healthy heterozygotes.* J Allergy Clin Immunol, 2013. **131**(2): p. 468-76.
103. Bacchelli, C., et al., *The C76R transmembrane activator and calcium modulator cyclophilin ligand interactor mutation disrupts antibody production and B-cell homeostasis in heterozygous and homozygous mice.* J Allergy Clin Immunol, 2011. **127**(5): p. 1253-9 e13.
104. Knight, A.K., et al., *High serum levels of BAFF, APRIL, and TACI in common variable immunodeficiency.* Clin Immunol, 2007. **124**(2): p. 182-9.
105. Mackay, F. and S.G. Tangye, *The role of the BAFF/APRIL system in B cell homeostasis and lymphoid cancers.* Curr Opin Pharmacol, 2004. **4**(4): p. 347-54.
106. Salzer, U., et al., *ICOS deficiency in patients with common variable immunodeficiency.* Clin Immunol, 2004. **113**(3): p. 234-40.
107. Takahashi, N., et al., *Impaired CD4 and CD8 effector function and decreased memory T cell populations in ICOS-deficient patients.* J Immunol, 2009. **182**(9): p. 5515-27.
108. Hutloff, A., et al., *ICOS is an inducible T-cell co-stimulator structurally and functionally related to CD28.* Nature, 1999. **397**(6716): p. 263-6.
109. Witsch, E.J., et al., *ICOS and CD28 reversely regulate IL-10 on re-activation of human effector T cells with mature dendritic cells.* Eur J Immunol, 2002. **32**(9): p. 2680-6.
110. Mak, T.W., et al., *Costimulation through the inducible costimulator ligand is essential for both T helper and B cell functions in T cell-dependent B cell responses.* Nat Immunol, 2003. **4**(8): p. 765-72.
111. Wong, S.C., et al., *Impaired germinal center formation and recall T-cell-dependent immune responses in mice lacking the costimulatory ligand B7-H2.* Blood, 2003. **102**(4): p. 1381-8.

112. Deng, X., S. Yan, and W. Wei, *IL-21 acts as a promising therapeutic target in systemic lupus erythematosus by regulating plasma cell differentiation.* Cell Mol Immunol, 2015. **12**(1): p. 31-39.
113. Greve, B., et al., *The diabetes susceptibility locus Idd5.1 on mouse chromosome 1 regulates ICOS expression and modulates murine experimental autoimmune encephalomyelitis.* J Immunol, 2004. **173**(1): p. 157-63.
114. Wicker, L.S., et al., *Fine mapping, gene content, comparative sequencing, and expression analyses support Ctla4 and Nramp1 as candidates for Idd5.1 and Idd5.2 in the nonobese diabetic mouse.* J Immunol, 2004. **173**(1): p. 164-73.
115. Nurieva, R.I., et al., *Inducible costimulator is essential for collagen-induced arthritis.* J Clin Invest, 2003. **111**(5): p. 701-6.
116. Scott, B.G., et al., *ICOS is essential for the development of experimental autoimmune myasthenia gravis.* J Neuroimmunol, 2004. **153**(1-2): p. 16-25.
117. Warnatz, K., et al., *Human ICOS deficiency abrogates the germinal center reaction and provides a monogenic model for common variable immunodeficiency.* Blood, 2006. **107**(8): p. 3045-52.
118. Bossaller, L., et al., *ICOS deficiency is associated with a severe reduction of CXCR5+CD4 germinal center Th cells.* J Immunol, 2006. **177**(7): p. 4927-32.
119. Ohm-Laursen, L., et al., *Normal ICOS, ICOSL and AID alleles in Danish patients with common variable immunodeficiency.* Scand J Immunol, 2005. **61**(6): p. 566-74.
120. Lee, W.I., et al., *Molecular analysis of a large cohort of patients with the hyper immunoglobulin M (IgM) syndrome.* Blood, 2005. **105**(5): p. 1881-90.
121. Fearon, D.T. and M.C. Carroll, *Regulation of B lymphocyte responses to foreign and self-antigens by the CD19/CD21 complex.* Annu Rev Immunol, 2000. **18**: p. 393-422.
122. Mongini, P.K., et al., *The affinity threshold for human B cell activation via the antigen receptor complex is reduced upon co-ligation of the antigen receptor with CD21 (CR2).* J Immunol, 1997. **159**(8): p. 3782-91.
123. Chen, Z., et al., *Humoral immune responses in Cr2-/- mice: enhanced affinity maturation but impaired antibody persistence.* J Immunol, 2000. **164**(9): p. 4522-32.
124. van Zelm, M.C., et al., *An antibody-deficiency syndrome due to mutations in the CD19 gene.* N Engl J Med, 2006. **354**(18): p. 1901-12.
125. Kanegane, H., et al., *Novel mutations in a Japanese patient with CD19 deficiency.* Genes Immun, 2007. **8**(8): p. 663-70.
126. Gardby, E. and N.Y. Lycke, *CD19-deficient mice exhibit poor responsiveness to oral immunization despite evidence of unaltered total IgA levels, germinal centers and IgA-isotype switching in Peyer's patches.* Eur J Immunol, 2000. **30**(7): p. 1861-71.
127. You, Y., et al., *Cutting edge: Primary and secondary effects of CD19 deficiency on cells of the marginal zone.* J Immunol, 2009. **182**(12): p. 7343-7.
128. Gardby, E., X.J. Chen, and N.Y. Lycke, *Impaired CD40-signalling in CD19-deficient mice selectively affects Th2-dependent isotype switching.* Scand J Immunol, 2001. **53**(1): p. 13-23.
129. Maecker, H.T. and S. Levy, *Normal lymphocyte development but delayed humoral immune response in CD81-null mice.* J Exp Med, 1997. **185**(8): p. 1505-10.
130. Tsitsikov, E.N., J.C. Gutierrez-Ramos, and R.S. Geha, *Impaired CD19 expression and signaling, enhanced antibody response to type II T independent antigen and reduction of B-1 cells in CD81-deficient mice.* Proc Natl Acad Sci U S A, 1997. **94**(20): p. 10844-9.
131. Bradbury, L.E., V.S. Goldmacher, and T.F. Tedder, *The CD19 signal transduction complex of B lymphocytes. Deletion of the CD19 cytoplasmic domain alters signal transduction but not complex formation with TAPA-1 and Leu 13.* J Immunol, 1993. **151**(6): p. 2915-27.
132. van Zelm, M.C., et al., *CD81 gene defect in humans disrupts CD19 complex formation and leads to antibody deficiency.* J Clin Invest, 2010. **120**(4): p. 1265-74.

133. Thiel, J., et al., *Genetic CD21 deficiency is associated with hypogammaglobulinemia.* J Allergy Clin Immunol, 2012. **129**(3): p. 801-810 e6.
134. Kamal, A. and M. Khamashta, *The efficacy of novel B cell biologics as the future of SLE treatment: a review.* Autoimmun Rev, 2014. **13**(11): p. 1094-101.
135. Kuijpers, T.W., et al., *CD20 deficiency in humans results in impaired T cell-independent antibody responses.* J Clin Invest, 2010. **120**(1): p. 214-22.
136. Hultin, L.E., et al., *CD20 (pan-B cell) antigen is expressed at a low level on a subpopulation of human T lymphocytes.* Cytometry, 1993. **14**(2): p. 196-204.
137. Mackay, F. and P. Schneider, *Cracking the BAFF code.* Nat Rev Immunol, 2009. **9**(7): p. 491-502.
138. Meyer-Bahlburg, A., et al., *Characterization of a late transitional B cell population highly sensitive to BAFF-mediated homeostatic proliferation.* J Exp Med, 2008. **205**(1): p. 155-68.
139. Hymowitz, S.G., et al., *Structures of APRIL-receptor complexes: like BCMA, TACI employs only a single cysteine-rich domain for high affinity ligand binding.* J Biol Chem, 2005. **280**(8): p. 7218-27.
140. Ng, L.G., et al., *B cell-activating factor belonging to the TNF family (BAFF)-R is the principal BAFF receptor facilitating BAFF costimulation of circulating T and B cells.* J Immunol, 2004. **173**(2): p. 807-17.
141. Darce, J.R., et al., *Regulated expression of BAFF-binding receptors during human B cell differentiation.* J Immunol, 2007. **179**(11): p. 7276-86.
142. Benson, M.J., et al., *Cutting edge: the dependence of plasma cells and independence of memory B cells on BAFF and APRIL.* J Immunol, 2008. **180**(6): p. 3655-9.
143. O'Connor, B.P., et al., *BCMA is essential for the survival of long-lived bone marrow plasma cells.* J Exp Med, 2004. **199**(1): p. 91-8.
144. Mackay, F. and P. Schneider, *TACI, an enigmatic BAFF/APRIL receptor, with new unappreciated biochemical and biological properties.* Cytokine Growth Factor Rev, 2008. **19**(3-4): p. 263-76.
145. von Bulow, G.U., J.M. van Deursen, and R.J. Bram, *Regulation of the T-independent humoral response by TACI.* Immunity, 2001. **14**(5): p. 573-82.
146. Yan, M., et al., *Activation and accumulation of B cells in TACI-deficient mice.* Nat Immunol, 2001. **2**(7): p. 638-43.
147. Litinskiy, M.B., et al., *DCs induce CD40-independent immunoglobulin class switching through BLyS and APRIL.* Nat Immunol, 2002. **3**(9): p. 822-9.
148. Castigli, E., et al., *TACI and BAFF-R mediate isotype switching in B cells.* J Exp Med, 2005. **201**(1): p. 35-9.
149. Castigli, E., et al., *Transmembrane activator and calcium modulator and cyclophilin ligand interactor enhances CD40-driven plasma cell differentiation.* J Allergy Clin Immunol, 2007. **120**(4): p. 885-91.
150. Sakurai, D., et al., *TACI attenuates antibody production costimulated by BAFF-R and CD40.* Eur J Immunol, 2007. **37**(1): p. 110-8.
151. Zhang, L., et al., *Transmembrane activator and calcium-modulating cyclophilin ligand interactor mutations in common variable immunodeficiency: clinical and immunologic outcomes in heterozygotes.* J Allergy Clin Immunol, 2007. **120**(5): p. 1178-85.
152. Salzer, U., et al., *Relevance of biallelic versus monoallelic TNFRSF13B mutations in distinguishing disease-causing from risk-increasing TNFRSF13B variants in antibody deficiency syndromes.* Blood, 2009. **113**(9): p. 1967-76.
153. Orange, J.S., et al., *Genome-wide association identifies diverse causes of common variable immunodeficiency.* J Allergy Clin Immunol, 2011. **127**(6): p. 1360-7 e6.
154. Losi, C.G., et al., *Mutational analysis of human BAFF receptor TNFRSF13C (BAFF-R) in patients with common variable immunodeficiency.* J Clin Immunol, 2005. **25**(5): p. 496-502.

155. Lougaris, V., et al., *BAFF-R mutations in Good's syndrome.* Clin Immunol, 2014. **153**(1): p. 91-3.
156. Kolfschoten, G.A., et al., *TWE-PRIL; a fusion protein of TWEAK and APRIL.* Biochemical Pharmacology, 2003. **66**(8): p. 1427-1432.
157. Wang, H.Y., et al., *Antibody deficiency associated with an inherited autosomal dominant mutation in TWEAK.* Proc Natl Acad Sci U S A, 2013. **110**(13): p. 5127-32.
158. Poveda, J., et al., *TWEAK/Fn14 and Non-Canonical NF-kappaB Signaling in Kidney Disease.* Front Immunol, 2013. **4**: p. 447.
159. Chen, K., et al., *Germline mutations in NFKB2 implicate the noncanonical NF-kappaB pathway in the pathogenesis of common variable immunodeficiency.* Am J Hum Genet, 2013. **93**(5): p. 812-24.
160. Liu, Y., et al., *Novel NFKB2 mutation in early-onset CVID.* J Clin Immunol, 2014. **34**(6): p. 686-90.
161. Tucker, E., et al., *A novel mutation in the Nfkb2 gene generates an NF-kappa B2 "super repressor".* J Immunol, 2007. **179**(11): p. 7514-22.
162. van Luijn, M.M., et al., *Multiple sclerosis-associated CLEC16A controls HLA class II expression via late endosome biogenesis.* Brain, 2015. **138**(Pt 6): p. 1531-47.
163. Muhali, F.S., et al., *Polymorphisms of CLEC16A region and autoimmune thyroid diseases.* G3 (Bethesda), 2014. **4**(6): p. 973-7.
164. Lopez-Herrera, G., et al., *Deleterious mutations in LRBA are associated with a syndrome of immune deficiency and autoimmunity.* Am J Hum Genet, 2012. **90**(6): p. 986-1001.
165. Ombrello, M.J., et al., *Cold urticaria, immunodeficiency, and autoimmunity related to PLCG2 deletions.* N Engl J Med, 2012. **366**(4): p. 330-8.
166. van Schouwenburg, P.A., et al., *Application of whole genome and RNA sequencing to investigate the genomic landscape of common variable immunodeficiency.* Clin Immunol, 2015.
167. Castigli, E., et al., *TACI is mutant in common variable immunodeficiency and IgA deficiency.* Nat Genet, 2005. **37**(8): p. 829-34.
168. Kuehn, H.S., et al., *Immune dysregulation in human subjects with heterozygous germline mutations in CTLA4.* Science, 2014. **345**(6204): p. 1623-7.
169. Zhou, Q., et al., *A hypermorphic missense mutation in PLCG2, encoding phospholipase Cgamma2, causes a dominantly inherited autoinflammatory disease with immunodeficiency.* Am J Hum Genet, 2012. **91**(4): p. 713-20.
170. Ahn, S. and C. Cunningham-Rundles, *Role of B cells in common variable immune deficiency.* Expert Rev Clin Immunol, 2009. **5**(5): p. 557-64.
171. Denz, A., et al., *Impaired up-regulation of CD86 in B cells of "type A" common variable immunodeficiency patients.* Eur J Immunol, 2000. **30**(4): p. 1069-77.
172. Groth, C., et al., *Impaired up-regulation of CD70 and CD86 in naive (CD27-) B cells from patients with common variable immunodeficiency (CVID).* Clin Exp Immunol, 2002. **129**(1): p. 133-9.
173. Saxon, A., et al., *B cells from a distinct subset of patients with common variable immunodeficiency (CVID) have increased CD95 (Apo-1/fas), diminished CD38 expression, and undergo enhanced apoptosis.* Clin Exp Immunol, 1995. **102**(1): p. 17-25.
174. Brouet, J.C., et al., *Study of the B cell memory compartment in common variable immunodeficiency.* Eur J Immunol, 2000. **30**(9): p. 2516-20.
175. Wu, Y.C., D. Kipling, and D.K. Dunn-Walters, *The relationship between CD27 negative and positive B cell populations in human peripheral blood.* Front Immunol, 2011. **2**: p. 81.
176. Warnatz, K., et al., *Severe deficiency of switched memory B cells (CD27(+)IgM(-)IgD(-)) in subgroups of patients with common variable immunodeficiency: a new approach to classify a heterogeneous disease.* Blood, 2002. **99**(5): p. 1544-51.

177. Piqueras, B., et al., *Common variable immunodeficiency patient classification based on impaired B cell memory differentiation correlates with clinical aspects.* J Clin Immunol, 2003. **23**(5): p. 385-400.
178. Alachkar, H., et al., *Memory switched B cell percentage and not serum immunoglobulin concentration is associated with clinical complications in children and adults with specific antibody deficiency and common variable immunodeficiency.* Clin Immunol, 2006. **120**(3): p. 310-8.
179. Carsetti, R., et al., *The loss of IgM memory B cells correlates with clinical disease in common variable immunodeficiency.* J Allergy Clin Immunol, 2005. **115**(2): p. 412-7.
180. Morbach, H., et al., *Reference values for B cell subpopulations from infancy to adulthood.* Clin Exp Immunol, 2010. **162**(2): p. 271-9.
181. Kruetzmann, S., et al., *Human immunoglobulin M memory B cells controlling Streptococcus pneumoniae infections are generated in the spleen.* J Exp Med, 2003. **197**(7): p. 939-45.
182. Seifert, M., et al., *Functional capacities of human IgM memory B cells in early inflammatory responses and secondary germinal center reactions.* Proc Natl Acad Sci U S A, 2015. **112**(6): p. E546-55.
183. Rodriguez-Bayona, B., et al., *Decreased frequency and activated phenotype of blood CD27 IgD IgM B lymphocytes is a permanent abnormality in systemic lupus erythematosus patients.* Arthritis Res Ther, 2010. **12**(3): p. R108.
184. Hansen, A., C. Daridon, and T. Dorner, *What do we know about memory B cells in primary Sjogren's syndrome?* Autoimmun Rev, 2010. **9**(9): p. 600-3.
185. Culton, D.A., et al., *Similar CD19 dysregulation in two autoantibody-associated autoimmune diseases suggests a shared mechanism of B-cell tolerance loss.* J Clin Immunol, 2007. **27**(1): p. 53-68.
186. Wei, C., et al., *A new population of cells lacking expression of CD27 represents a notable component of the B cell memory compartment in systemic lupus erythematosus.* J Immunol, 2007. **178**(10): p. 6624-33.
187. Malbran, A., et al., *Loss of circulating CD27+ memory B cells and CCR4+ T cells occurring in association with elevated EBV loads in XLP patients surviving primary EBV infection.* Blood, 2004. **103**(5): p. 1625-31.
188. Bright, P., et al., *Changes in B cell immunophenotype in common variable immunodeficiency: cause or effect - is bronchiectasis indicative of undiagnosed immunodeficiency?* Clin Exp Immunol, 2013. **171**(2): p. 195-200.
189. Toellner, K.M., et al., *Low-level hypermutation in T cell-independent germinal centers compared with high mutation rates associated with T cell-dependent germinal centers.* J Exp Med, 2002. **195**(3): p. 383-9.
190. Nonoyama, S., et al., *Activated B cells from patients with common variable immunodeficiency proliferate and synthesize immunoglobulin.* J Clin Invest, 1993. **92**(3): p. 1282-7.
191. Borte, S., et al., *Interleukin-21 restores immunoglobulin production ex vivo in patients with common variable immunodeficiency and selective IgA deficiency.* Blood, 2009. **114**(19): p. 4089-98.
192. Punnonen, J., et al., *IL-4 synergizes with IL-10 and anti-CD40 MoAbs to induce B-cell differentiation in patients with common variable immunodeficiency.* Scand J Immunol, 1997. **45**(2): p. 203-12.
193. Eisenstein, E.M., K. Chua, and W. Strober, *B cell differentiation defects in common variable immunodeficiency are ameliorated after stimulation with anti-CD40 antibody and IL-10.* J Immunol, 1994. **152**(12): p. 5957-68.
194. Branda, R.F., et al., *B-cell proliferation and differentiation in common variable immunodeficiency patients produced by an antisense oligomer to the rev gene of HIV-1.* Clin Immunol Immunopathol, 1996. **79**(2): p. 115-21.

195. Cunningham-Rundles, C., et al., *TLR9 activation is defective in common variable immune deficiency.* J Immunol, 2006. **176**(3): p. 1978-87.
196. Yu, J.E., et al., *Toll-like receptor 7 and 9 defects in common variable immunodeficiency.* J Allergy Clin Immunol, 2009. **124**(2): p. 349-56, 356 e1-3.
197. Rosel, A.L., et al., *Classification of common variable immunodeficiencies using flow cytometry and a memory B-cell functionality assay.* J Allergy Clin Immunol, 2015. **135**(1): p. 198-208.
198. Scharenberg, A.M., L.A. Humphries, and D.J. Rawlings, *Calcium signalling and cell-fate choice in B cells.* Nat Rev Immunol, 2007. **7**(10): p. 778-89.
199. Foerster, C., et al., *B cell receptor-mediated calcium signaling is impaired in B lymphocytes of type Ia patients with common variable immunodeficiency.* J Immunol, 2010. **184**(12): p. 7305-13.
200. Visentini, M., et al., *Dysregulated extracellular signal-regulated kinase signaling associated with impaired B-cell receptor endocytosis in patients with common variable immunodeficiency.* J Allergy Clin Immunol, 2014. **134**(2): p. 401-10.
201. van de Ven, A.A., et al., *Defective calcium signaling and disrupted CD20-B-cell receptor dissociation in patients with common variable immunodeficiency disorders.* J Allergy Clin Immunol, 2012. **129**(3): p. 755-761 e7.
202. Mitrevski, M., et al., *Intravenous Immunoglobulin and Immunomodulation of B-Cell - in vitro and in vivo Effects.* Front Immunol, 2015. **6**: p. 4.
203. Bryant, A., et al., *Classification of patients with common variable immunodeficiency by B cell secretion of IgM and IgG in response to anti-IgM and interleukin-2.* Clin Immunol Immunopathol, 1990. **56**(2): p. 239-48.
204. Davies, E.G. and A.J. Thrasher, *Update on the hyper immunoglobulin M syndromes.* Br J Haematol, 2010. **149**(2): p. 167-80.
205. Salek Farrokhi, A., et al., *Evaluation of class switch recombination in B lymphocytes of patients with common variable immunodeficiency.* J Immunol Methods, 2013. **394**(1-2): p. 94-9.
206. Schena, F., et al., *Dependence of immunoglobulin class switch recombination in B cells on vesicular release of ATP and CD73 ectonucleotidase activity.* Cell Rep, 2013. **3**(6): p. 1824-31.
207. Levy, Y., et al., *Defect in IgV gene somatic hypermutation in common variable immuno-deficiency syndrome.* Proc Natl Acad Sci U S A, 1998. **95**(22): p. 13135-40.
208. Bonhomme, D., et al., *Impaired antibody affinity maturation process characterizes a subset of patients with common variable immunodeficiency.* J Immunol, 2000. **165**(8): p. 4725-30.
209. Andersen, P., et al., *Deficiency of somatic hypermutation of the antibody light chain is associated with increased frequency of severe respiratory tract infection in common variable immunodeficiency.* Blood, 2005. **105**(2): p. 511-7.
210. Schejbel, L., et al., *Deficiency of somatic hypermutation of immunoglobulin G transcripts is a better predictor of severe respiratory tract infections than lack of memory B cells in common variable immunodeficiency.* J Clin Immunol, 2005. **25**(4): p. 392-403.
211. Duvvuri, B., et al., *Altered spectrum of somatic hypermutation in common variable immunodeficiency disease characteristic of defective repair of mutations.* Immunogenetics, 2011. **63**(1): p. 1-11.
212. Driessen, G.J., et al., *B-cell replication history and somatic hypermutation status identify distinct pathophysiologic backgrounds in common variable immunodeficiency.* Blood, 2011. **118**(26): p. 6814-23.
213. Slifka, M.K., et al., *Humoral immunity due to long-lived plasma cells.* Immunity, 1998. **8**(3): p. 363-72.
214. van Laar, J.M., et al., *Sustained secretion of immunoglobulin by long-lived human tonsil plasma cells.* Am J Pathol, 2007. **171**(3): p. 917-27.
215. Mesin, L., et al., *Long-lived plasma cells from human small intestine biopsies secrete immunoglobulins for many weeks in vitro.* J Immunol, 2011. **187**(6): p. 2867-74.

216. Herbst, E.W., et al., *Intestinal B cell defects in common variable immunodeficiency.* Clin Exp Immunol, 1994. **95**(2): p. 215-21.
217. Washington, K., et al., *Gastrointestinal pathology in patients with common variable immunodeficiency and X-linked agammaglobulinemia.* Am J Surg Pathol, 1996. **20**(10): p. 1240-52.
218. Khodadad, A., et al., *Gastrointestinal manifestations in patients with common variable immunodeficiency.* Dig Dis Sci, 2007. **52**(11): p. 2977-83.
219. Daniels, J.A., et al., *Gastrointestinal tract pathology in patients with common variable immunodeficiency (CVID): a clinicopathologic study and review.* Am J Surg Pathol, 2007. **31**(12): p. 1800-12.
220. Taubenheim, N., et al., *Defined blocks in terminal plasma cell differentiation of common variable immunodeficiency patients.* J Immunol, 2005. **175**(8): p. 5498-503.
221. Ochtrop, M.L., et al., *T and B lymphocyte abnormalities in bone marrow biopsies of common variable immunodeficiency.* Blood, 2011. **118**(2): p. 309-18.
222. MacLennan, I.C., et al., *Extrafollicular antibody responses.* Immunol Rev, 2003. **194**: p. 8-18.
223. Farrant, J., et al., *Study of B and T cell phenotypes in blood from patients with common variable immunodeficiency (CVID).* Immunodeficiency, 1994. **5**(2): p. 159-69.
224. Baumert, E., et al., *Immunophenotypical alterations in a subset of patients with common variable immunodeficiency (CVID).* Clin Exp Immunol, 1992. **90**(1): p. 25-30.
225. Bateman, E.A., et al., *T cell phenotypes in patients with common variable immunodeficiency disorders: associations with clinical phenotypes in comparison with other groups with recurrent infections.* Clin Exp Immunol, 2012. **170**(2): p. 202-11.
226. Varzaneh, F.N., et al., *Cytokines in common variable immunodeficiency as signs of immune dysregulation and potential therapeutic targets - a review of the current knowledge.* J Clin Immunol, 2014. **34**(5): p. 524-43.
227. Eisenstein, E.M., J.S. Jaffe, and W. Strober, *Reduced interleukin-2 (IL-2) production in common variable immunodeficiency is due to a primary abnormality of CD4+ T cell differentiation.* J Clin Immunol, 1993. **13**(4): p. 247-58.
228. Holm, A.M., et al., *Impaired secretion of IL-10 by T cells from patients with common variable immunodeficiency--involvement of protein kinase A type I.* J Immunol, 2003. **170**(11): p. 5772-7.
229. Yi, J.S., M.A. Cox, and A.J. Zajac, *T-cell exhaustion: characteristics, causes and conversion.* Immunology, 2010. **129**(4): p. 474-81.
230. Wherry, E.J. and M. Kurachi, *Molecular and cellular insights into T cell exhaustion.* Nat Rev Immunol, 2015. **15**(8): p. 486-99.
231. Lanio, N., et al., *Immunophenotypic profile of T cells in common variable immunodeficiency: is there an association with different clinical findings?* Allergol Immunopathol (Madr), 2009. **37**(1): p. 14-20.
232. Viallard, J.F., et al., *CD8+HLA-DR+ T lymphocytes are increased in common variable immunodeficiency patients with impaired memory B-cell differentiation.* Clin Immunol, 2006. **119**(1): p. 51-8.
233. Vlkova, M., et al., *Age dependency and mutual relations in T and B lymphocyte abnormalities in common variable immunodeficiency patients.* Clin Exp Immunol, 2006. **143**(2): p. 373-9.
234. Perreau, M., et al., *Exhaustion of bacteria-specific CD4 T cells and microbial translocation in common variable immunodeficiency disorders.* J Exp Med, 2014. **211**(10): p. 2033-45.
235. Ye, J., et al., *TLR8 signaling enhances tumor immunity by preventing tumor-induced T-cell senescence.* EMBO Mol Med, 2014. **6**(10): p. 1294-311.
236. Chou, J.P., et al., *Prostaglandin E2 promotes features of replicative senescence in chronically activated human CD8+ T cells.* PLoS One, 2014. **9**(6): p. e99432.
237. Fischer, M.B., et al., *A defect in the early phase of T-cell receptor-mediated T-cell activation in patients with common variable immunodeficiency.* Blood, 1994. **84**(12): p. 4234-41.

238. Aukrust, P., et al., *Increased activation of protein kinase A type I contributes to the T cell deficiency in common variable immunodeficiency.* J Immunol, 1999. **162**(2): p. 1178-85.
239. West, E.E., et al., *PD-L1 blockade synergizes with IL-2 therapy in reinvigorating exhausted T cells.* J Clin Invest, 2013. **123**(6): p. 2604-15.
240. Cunningham-Rundles, C., et al., *Long-term low-dose IL-2 enhances immune function in common variable immunodeficiency.* Clin Immunol, 2001. **100**(2): p. 181-90.
241. Rump, J.A., et al., *A double-blind, placebo-controlled, crossover therapy study with natural human IL-2 (nhuIL-2) in combination with regular intravenous gammaglobulin (IVIG) infusions in 10 patients with common variable immunodeficiency (CVID).* Clin Exp Immunol, 1997. **110**(2): p. 167-73.
242. Giovannetti, A., et al., *Unravelling the complexity of T cell abnormalities in common variable immunodeficiency.* J Immunol, 2007. **178**(6): p. 3932-43.
243. Lin, S.J., et al., *Effect of interleukin 15 and interleukin 2 on anti-CD3-induced T-cell activation and apoptosis in children with common variable immunodeficiency.* Ann Allergy Asthma Immunol, 2003. **91**(1): p. 65-70.
244. Goldberg, A.C., et al., *Exogenous leptin restores in vitro T cell proliferation and cytokine synthesis in patients with common variable immunodeficiency syndrome.* Clin Immunol, 2005. **114**(2): p. 147-53.
245. Serrano, D., et al., *Characterization of the T cell receptor repertoire in patients with common variable immunodeficiency: oligoclonal expansion of CD8(+) T cells.* Clin Immunol, 2000. **97**(3): p. 248-58.
246. Viallard, J.F., et al., *Perturbations of the CD8(+) T-cell repertoire in CVID patients with complications.* Results Immunol, 2013. **3**: p. 122-8.
247. Duchmann, R., et al., *Differential usage of T-cell receptor V beta gene families by CD4+ and CD8+ T cells in patients with CD8hi common variable immunodeficiency: evidence of a post-thymic effect.* Immunology, 1996. **87**(1): p. 99-107.
248. Marashi, S.M., et al., *Inflammation in common variable immunodeficiency is associated with a distinct CD8(+) response to cytomegalovirus.* J Allergy Clin Immunol, 2011. **127**(6): p. 1385-93 e4.
249. Marashi, S.M., et al., *Influence of cytomegalovirus infection on immune cell phenotypes in patients with common variable immunodeficiency.* J Allergy Clin Immunol, 2012. **129**(5): p. 1349-1356 e3.
250. Bates, C.A., et al., *Granulomatous-lymphocytic lung disease shortens survival in common variable immunodeficiency.* J Allergy Clin Immunol, 2004. **114**(2): p. 415-21.
251. Maglione, P.J., et al., *Tertiary lymphoid neogenesis is a component of pulmonary lymphoid hyperplasia in patients with common variable immunodeficiency.* J Allergy Clin Immunol, 2014. **133**(2): p. 535-42.
252. Ramesh, M., et al., *Clonal and constricted T cell repertoire in Common Variable Immune Deficiency.* Clin Immunol, 2015.
253. Dejaco, C., et al., *Imbalance of regulatory T cells in human autoimmune diseases.* Immunology, 2006. **117**(3): p. 289-300.
254. Fevang, B., et al., *Low numbers of regulatory T cells in common variable immunodeficiency: association with chronic inflammation in vivo.* Clin Exp Immunol, 2007. **147**(3): p. 521-5.
255. Yu, G.P., et al., *Regulatory T cell dysfunction in subjects with common variable immunodeficiency complicated by autoimmune disease.* Clin Immunol, 2009. **131**(2): p. 240-53.
256. Genre, J., et al., *Reduced frequency of CD4(+)CD25(HIGH)FOXP3(+) cells and diminished FOXP3 expression in patients with Common Variable Immunodeficiency: a link to autoimmunity?* Clin Immunol, 2009. **132**(2): p. 215-21.

257. Arumugakani, G., P.M. Wood, and C.R. Carter, *Frequency of Treg cells is reduced in CVID patients with autoimmunity and splenomegaly and is associated with expanded CD21lo B lymphocytes.* J Clin Immunol, 2010. **30**(2): p. 292-300.
258. Horn, J., et al., *Decrease in phenotypic regulatory T cells in subsets of patients with common variable immunodeficiency.* Clin Exp Immunol, 2009. **156**(3): p. 446-54.
259. Carter, C.R., et al., *CVID patients with autoimmunity have elevated T cell expression of granzyme B and HLA-DR and reduced levels of Treg cells.* J Clin Pathol, 2013. **66**(2): p. 146-50.
260. Arandi, N., et al., *Frequency and expression of inhibitory markers of CD4(+) CD25(+) FOXP3(+) regulatory T cells in patients with common variable immunodeficiency.* Scand J Immunol, 2013. **77**(5): p. 405-12.
261. Fulcher, D.A., et al., *Invariant natural killer (iNK) T cell deficiency in patients with common variable immunodeficiency.* Clin Exp Immunol, 2009. **157**(3): p. 365-9.
262. Carvalho, K.I., et al., *Skewed distribution of circulating activated natural killer T (NKT) cells in patients with common variable immunodeficiency disorders (CVID).* PLoS One, 2010. **5**(9).
263. Trujillo, C.M., et al., *Quantitative and functional evaluation of innate immune responses in patients with common variable immunodeficiency.* J Investig Allergol Clin Immunol, 2011. **21**(3): p. 207-15.
264. Gao, Y., et al., *Common variable immunodeficiency is associated with a functional deficiency of invariant natural killer T cells.* J Allergy Clin Immunol, 2014. **133**(5): p. 1420-8, 1428 e1.
265. Cowan, J.E., W.E. Jenkinson, and G. Anderson, *Thymus medulla fosters generation of natural Treg cells, invariant gammadelta T cells, and invariant NKT cells: What we learn from intrathymic migration.* Eur J Immunol, 2015. **45**(3): p. 652-60.
266. Nazzal, D., et al., *Human thymus medullary epithelial cells promote regulatory T-cell generation by stimulating interleukin-2 production via ICOS ligand.* Cell Death Dis, 2014. **5**: p. e1420.
267. Berzins, S.P., et al., *Limited correlation between human thymus and blood NKT cell content revealed by an ontogeny study of paired tissue samples.* Eur J Immunol, 2005. **35**(5): p. 1399-407.
268. Maldonado, A., et al., *Decreased effector memory CD45RA+ CD62L- CD8+ T cells and increased central memory CD45RA- CD62L+ CD8+ T cells in peripheral blood of rheumatoid arthritis patients.* Arthritis Res Ther, 2003. **5**(2): p. R91-6.
269. Fekete, A., et al., *Disturbances in B- and T-cell homeostasis in rheumatoid arthritis: suggested relationships with antigen-driven immune responses.* J Autoimmun, 2007. **29**(2-3): p. 154-63.
270. Hazenberg, M.D., et al., *T cell receptor excision circles as markers for recent thymic emigrants: basic aspects, technical approach, and guidelines for interpretation.* J Mol Med (Berl), 2001. **79**(11): p. 631-40.
271. Guazzi, V., et al., *Assessment of thymic output in common variable immunodeficiency patients by evaluation of T cell receptor excision circles.* Clin Exp Immunol, 2002. **129**(2): p. 346-53.
272. De Vera, M.J., L. Al-Harthi, and A.T. Gewurz, *Assessing thymopoiesis in patients with common variable immunodeficiency as measured by T-cell receptor excision circles.* Ann Allergy Asthma Immunol, 2004. **93**(5): p. 478-84.
273. Isgro, A., et al., *Bone marrow clonogenic capability, cytokine production, and thymic output in patients with common variable immunodeficiency.* J Immunol, 2005. **174**(8): p. 5074-81.
274. Liston, A., A. Enders, and O.M. Siggs, *Unravelling the association of partial T-cell immunodeficiency and immune dysregulation.* Nat Rev Immunol, 2008. **8**(7): p. 545-58.
275. Galli, G., et al., *Invariant NKT cells sustain specific B cell responses and memory.* Proc Natl Acad Sci U S A, 2007. **104**(10): p. 3984-9.
276. Ross, E.A., et al., *Thymic function is maintained during Salmonella-induced atrophy and recovery.* J Immunol, 2012. **189**(9): p. 4266-74.

277. Leyva-Rangel, J.P., et al., *Bacterial clearance reverses a skewed T-cell repertoire induced by Salmonella infection.* Immun Inflamm Dis, 2015. **3**(3): p. 209-23.
278. Savino, W., *The thymus is a common target organ in infectious diseases.* PLoS Pathog, 2006. **2**(6): p. e62.
279. Aw, D. and D.B. Palmer, *The origin and implication of thymic involution.* Aging Dis, 2011. **2**(5): p. 437-43.
280. Singh, Y., et al., *Restricted TCR-alpha CDR3 diversity disadvantages natural regulatory T cell development in the B6.2.16 beta-chain transgenic mouse.* J Immunol, 2010. **185**(6): p. 3408-16.
281. Venturi, V., et al., *Methods for comparing the diversity of samples of the T cell receptor repertoire.* J Immunol Methods, 2007. **321**(1-2): p. 182-95.
282. Cocco, M., et al., *In vitro generation of long-lived human plasma cells.* J Immunol, 2012. **189**(12): p. 5773-85.
283. Lau, A.W., et al., *Skewed X-chromosome inactivation is common in fetuses or newborns associated with confined placental mosaicism.* Am J Hum Genet, 1997. **61**(6): p. 1353-61.
284. Farber, D.L., N.A. Yudanin, and N.P. Restifo, *Human memory T cells: generation, compartmentalization and homeostasis.* Nat Rev Immunol, 2014. **14**(1): p. 24-35.
285. Zarnitsyna, V.I., et al., *Estimating the diversity, completeness, and cross-reactivity of the T cell repertoire.* Front Immunol, 2013. **4**: p. 485.
286. Venturi, V., et al., *The molecular basis for public T-cell responses?* Nat Rev Immunol, 2008. **8**(3): p. 231-8.
287. Anderson, G., P.J. Lane, and E.J. Jenkinson, *Generating intrathymic microenvironments to establish T-cell tolerance.* Nat Rev Immunol, 2007. **7**(12): p. 954-63.
288. Yassai, M.B., et al., *A clonotype nomenclature for T cell receptors.* Immunogenetics, 2009. **61**(7): p. 493-502.
289. Marrack, P., et al., *Evolutionarily conserved amino acids that control TCR-MHC interaction.* Annu Rev Immunol, 2008. **26**: p. 171-203.
290. Thomas, N., et al., *Tracking global changes induced in the CD4 T-cell receptor repertoire by immunization with a complex antigen using short stretches of CDR3 protein sequence.* Bioinformatics, 2014. **30**(22): p. 3181-8.
291. Scifo, C., et al., *Selection of T-cell receptors with a recurrent CDR3beta peptide-contact motif within the repertoire of alloreactive CD8(+) T cells.* Eur J Immunol, 2011. **41**(8): p. 2414-23.
292. Langerak, A.W., et al., *EuroClonality/BIOMED-2 guidelines for interpretation and reporting of Ig/TCR clonality testing in suspected lymphoproliferations.* Leukemia, 2012. **26**(10): p. 2159-71.
293. Robins, H.S., et al., *Comprehensive assessment of T-cell receptor beta-chain diversity in alphabeta T cells.* Blood, 2009. **114**(19): p. 4099-107.
294. Alamyar, E., et al., *IMGT((R)) tools for the nucleotide analysis of immunoglobulin (IG) and T cell receptor (TR) V-(D)-J repertoires, polymorphisms, and IG mutations: IMGT/V-QUEST and IMGT/HighV-QUEST for NGS.* Methods Mol Biol, 2012. **882**: p. 569-604.
295. Mamedov, I.Z., et al., *Preparing unbiased T-cell receptor and antibody cDNA libraries for the deep next generation sequencing profiling.* Front Immunol, 2013. **4**: p. 456.
296. Carlson, C.S., et al., *Using synthetic templates to design an unbiased multiplex PCR assay.* Nat Commun, 2013. **4**: p. 2680.
297. Sufficool, K.E., et al., *T-cell clonality assessment by next-generation sequencing improves detection sensitivity in mycosis fungoides.* J Am Acad Dermatol, 2015. **73**(2): p. 228-236 e2.
298. Venturi, V., et al., *A mechanism for TCR sharing between T cell subsets and individuals revealed by pyrosequencing.* J Immunol, 2011. **186**(7): p. 4285-94.
299. Eugster, A., et al., *High diversity in the TCR repertoire of GAD65 autoantigen-specific human CD4+ T cells.* J Immunol, 2015. **194**(6): p. 2531-8.

300. Jost, L., *Partitioning diversity into independent alpha and beta components.* Ecology, 2007. **88**(10): p. 2427-39.
301. Francis, I.R., et al., *The thymus: reexamination of age-related changes in size and shape.* AJR Am J Roentgenol, 1985. **145**(2): p. 249-54.
302. Serana, F., et al., *Thymic and bone marrow output in patients with common variable immunodeficiency.* J Clin Immunol, 2011. **31**(4): p. 540-9.
303. den Braber, I., et al., *Maintenance of peripheral naive T cells is sustained by thymus output in mice but not humans.* Immunity, 2012. **36**(2): p. 288-97.
304. Waller, E.C., et al., *Differential costimulation through CD137 (4-1BB) restores proliferation of human virus-specific "effector memory" (CD28(-) CD45RA(HI)) CD8(+) T cells.* Blood, 2007. **110**(13): p. 4360-6.
305. Geginat, J., A. Lanzavecchia, and F. Sallusto, *Proliferation and differentiation potential of human CD8+ memory T-cell subsets in response to antigen or homeostatic cytokines.* Blood, 2003. **101**(11): p. 4260-6.
306. Gamadia, L.E., et al., *Primary immune responses to human CMV: a critical role for IFN-gamma-producing CD4+ T cells in protection against CMV disease.* Blood, 2003. **101**(7): p. 2686-92.
307. Northfield, J.W., et al., *Human immunodeficiency virus type 1 (HIV-1)-specific CD8+ T(EMRA) cells in early infection are linked to control of HIV-1 viremia and predict the subsequent viral load set point.* J Virol, 2007. **81**(11): p. 5759-65.
308. Sievers, F., et al., *Fast, scalable generation of high-quality protein multiple sequence alignments using Clustal Omega.* Mol Syst Biol, 2011. **7**: p. 539.
309. Eisenstein, M., *Personalized, sequencing-based immune profiling spurs startups.* Nat Biotechnol, 2013. **31**(3): p. 184-6.
310. Visentini, M., et al., *Telomere-dependent replicative senescence of B and T cells from patients with type 1a common variable immunodeficiency.* Eur J Immunol, 2011. **41**(3): p. 854-62.
311. van Zelm, M.C., et al., *Replication history of B lymphocytes reveals homeostatic proliferation and extensive antigen-induced B cell expansion.* J Exp Med, 2007. **204**(3): p. 645-55.
312. Johnson, K.M., K. Owen, and P.L. Witte, *Aging and developmental transitions in the B cell lineage.* Int Immunol, 2002. **14**(11): p. 1313-23.
313. Rakhmanov, M., et al., *Circulating CD21low B cells in common variable immunodeficiency resemble tissue homing, innate-like B cells.* Proc Natl Acad Sci U S A, 2009. **106**(32): p. 13451-6.
314. Isnardi, I., et al., *Complement receptor 2/CD21- human naive B cells contain mostly autoreactive unresponsive clones.* Blood, 2010. **115**(24): p. 5026-36.
315. Huggins, J., et al., *CpG DNA activation and plasma-cell differentiation of CD27- naive human B cells.* Blood, 2007. **109**(4): p. 1611-9.
316. Ding, B.B., et al., *IL-21 and CD40L synergistically promote plasma cell differentiation through upregulation of Blimp-1 in human B cells.* J Immunol, 2013. **190**(4): p. 1827-36.
317. Jourdan, M., et al., *An in vitro model of differentiation of memory B cells into plasmablasts and plasma cells including detailed phenotypic and molecular characterization.* Blood, 2009. **114**(25): p. 5173-81.
318. Hammarstrom, L., I. Vorechovsky, and D. Webster, *Selective IgA deficiency (SIgAD) and common variable immunodeficiency (CVID).* Clin Exp Immunol, 2000. **120**(2): p. 225-31.
319. Kurosaki, T., K. Kometani, and W. Ise, *Memory B cells.* Nat Rev Immunol, 2015. **15**(3): p. 149-59.
320. Gray, D., *A role for antigen in the maintenance of immunological memory.* Nat Rev Immunol, 2002. **2**(1): p. 60-5.
321. H, I.J., et al., *Strategies for B-cell receptor repertoire analysis in primary immunodeficiencies: from severe combined immunodeficiency to common variable immunodeficiency.* Front Immunol, 2015. **6**: p. 157.

322. Walter, M.J., et al., *Clonal diversity of recurrently mutated genes in myelodysplastic syndromes.* Leukemia, 2013. **27**(6): p. 1275-82.
323. Bayry, J., et al., *Common variable immunodeficiency is associated with defective functions of dendritic cells.* Blood, 2004. **104**(8): p. 2441-3.
324. Barbosa, R.R., et al., *Monocyte activation is a feature of common variable immunodeficiency irrespective of plasma lipopolysaccharide levels.* Clin Exp Immunol, 2012. **169**(3): p. 263-72.
325. Cambronero, R., et al., *Up-regulation of IL-12 in monocytes: a fundamental defect in common variable immunodeficiency.* J Immunol, 2000. **164**(1): p. 488-94.
326. Cines, D.B., et al., *The ITP syndrome: pathogenic and clinical diversity.* Blood, 2009. **113**(26): p. 6511-21.
327. Semple, J.W. and J. Freedman, *Autoimmune pathogenesis and autoimmune hemolytic anemia.* Semin Hematol, 2005. **42**(3): p. 122-30.
328. Steensma, D.P., et al., *Clonal hematopoiesis of indeterminate potential and its distinction from myelodysplastic syndromes.* Blood, 2015.
329. Yoshizato, T., et al., *Somatic Mutations and Clonal Hematopoiesis in Aplastic Anemia.* N Engl J Med, 2015. **373**(1): p. 35-47.
330. Jaiswal, S., et al., *Age-related clonal hematopoiesis associated with adverse outcomes.* N Engl J Med, 2014. **371**(26): p. 2488-98.
331. Genovese, G., et al., *Clonal hematopoiesis and blood-cancer risk inferred from blood DNA sequence.* N Engl J Med, 2014. **371**(26): p. 2477-87.
332. Pasmooij, A.M., et al., *Revertant mosaicism in junctional epidermolysis bullosa due to multiple correcting second-site mutations in LAMB3.* J Clin Invest, 2007. **117**(5): p. 1240-8.
333. Tone, Y., et al., *Somatic revertant mosaicism in a patient with leukocyte adhesion deficiency type 1.* Blood, 2007. **109**(3): p. 1182-4.
334. Augui, S., E.P. Nora, and E. Heard, *Regulation of X-chromosome inactivation by the X-inactivation centre.* Nat Rev Genet, 2011. **12**(6): p. 429-42.
335. Amos-Landgraf, J.M., et al., *X chromosome-inactivation patterns of 1,005 phenotypically unaffected females.* Am J Hum Genet, 2006. **79**(3): p. 493-9.
336. Minks, J., W.P. Robinson, and C.J. Brown, *A skewed view of X chromosome inactivation.* J Clin Invest, 2008. **118**(1): p. 20-3.
337. Chen, G.L. and J.T. Prchal, *X-linked clonality testing: interpretation and limitations.* Blood, 2007. **110**(5): p. 1411-9.
338. Swierczek, S.I., et al., *Methylation of AR locus does not always reflect X chromosome inactivation state.* Blood, 2012. **119**(13): p. e100-9.
339. Summers, C., et al., *Neutrophil kinetics in health and disease.* Trends Immunol, 2010. **31**(8): p. 318-24.
340. Belickova, M., et al., *Clonal hematopoiesis and acquired thalassemia in common variable immunodeficiency.* Mol Med, 1994. **1**(1): p. 56-61.
341. Rodriguez-Cortez, V.C., et al., *Monozygotic twins discordant for common variable immunodeficiency reveal impaired DNA demethylation during naive-to-memory B-cell transition.* Nat Commun, 2015. **6**: p. 7335.
342. Bertelsen, B., Z. Tumer, and K. Ravn, *Three new loci for determining x chromosome inactivation patterns.* J Mol Diagn, 2011. **13**(5): p. 537-40.
343. Shen, W., et al., *Deep sequencing reveals stepwise mutation acquisition in paroxysmal nocturnal hemoglobinuria.* J Clin Invest, 2014. **124**(10): p. 4529-38.
344. Murtaza, M., et al., *Multifocal clonal evolution characterized using circulating tumour DNA in a case of metastatic breast cancer.* Nat Commun, 2015. **6**: p. 8760.
345. Shlush, L.I. and A. Mitchell, *AML evolution from preleukemia to leukemia and relapse.* Best Pract Res Clin Haematol, 2015. **28**(2-3): p. 81-89.
346. Roskin, K.M., et al., *IgH sequences in common variable immune deficiency reveal altered B cell development and selection.* Sci Transl Med, 2015. **7**(302): p. 302ra135.

347. Xie, M., et al., *Age-related mutations associated with clonal hematopoietic expansion and malignancies.* Nat Med, 2014. **20**(12): p. 1472-8.
348. Dorner, T. and A. Radbruch, *Selecting B cells and plasma cells to memory.* J Exp Med, 2005. **201**(4): p. 497-9.
349. Taylor, J.J., M.K. Jenkins, and K.A. Pape, *Heterogeneity in the differentiation and function of memory B cells.* Trends Immunol, 2012. **33**(12): p. 590-7.
350. Diwakar, L., et al., *Does rituximab aggravate pre-existing hypogammaglobulinaemia?* J Clin Pathol, 2010. **63**(3): p. 275-7.
351. Mogensen, T.H., et al., *Common variable immunodeficiency unmasked by treatment of immune thrombocytopenic purpura with Rituximab.* BMC Hematol, 2013. **13**(1): p. 4.
352. Nutt, S.L., et al., *The generation of antibody-secreting plasma cells.* Nat Rev Immunol, 2015. **15**(3): p. 160-71.
353. Tefferi, A. and J.W. Vardiman, *Myelodysplastic syndromes.* N Engl J Med, 2009. **361**(19): p. 1872-85.
354. Han, S.W., et al., *Targeted sequencing of cancer-related genes in colorectal cancer using next-generation sequencing.* PLoS One, 2013. **8**(5): p. e64271.
355. Han, A., et al., *Linking T-cell receptor sequence to functional phenotype at the single-cell level.* Nat Biotechnol, 2014. **32**(7): p. 684-92.
356. Wehr, C., et al., *Multicenter experience in hematopoietic stem cell transplantation for serious complications of common variable immunodeficiency.* J Allergy Clin Immunol, 2015. **135**(4): p. 988-97 e6.
357. Slatter, M.A. and A.R. Gennery, *Advances in hematopoietic stem cell transplantation for primary immunodeficiency.* Expert Rev Clin Immunol, 2013. **9**(10): p. 991-9.
358. Gobert, D., et al., *Efficacy and safety of rituximab in common variable immunodeficiency-associated immune cytopenias: a retrospective multicentre study on 33 patients.* Br J Haematol, 2011. **155**(4): p. 498-508.
359. Battersby, A.C., et al., *Clinical manifestations of disease in X-linked carriers of chronic granulomatous disease.* J Clin Immunol, 2013. **33**(8): p. 1276-84.
360. de Saint Basile, G., et al., *CD40 ligand expression deficiency in a female carrier of the X-linked hyper-IgM syndrome as a result of X chromosome lyonization.* Eur J Immunol, 1999. **29**(1): p. 367-73.
361. Dickinson, R.E., et al., *The evolution of cellular deficiency in GATA2 mutation.* Blood, 2014. **123**(6): p. 863-74.